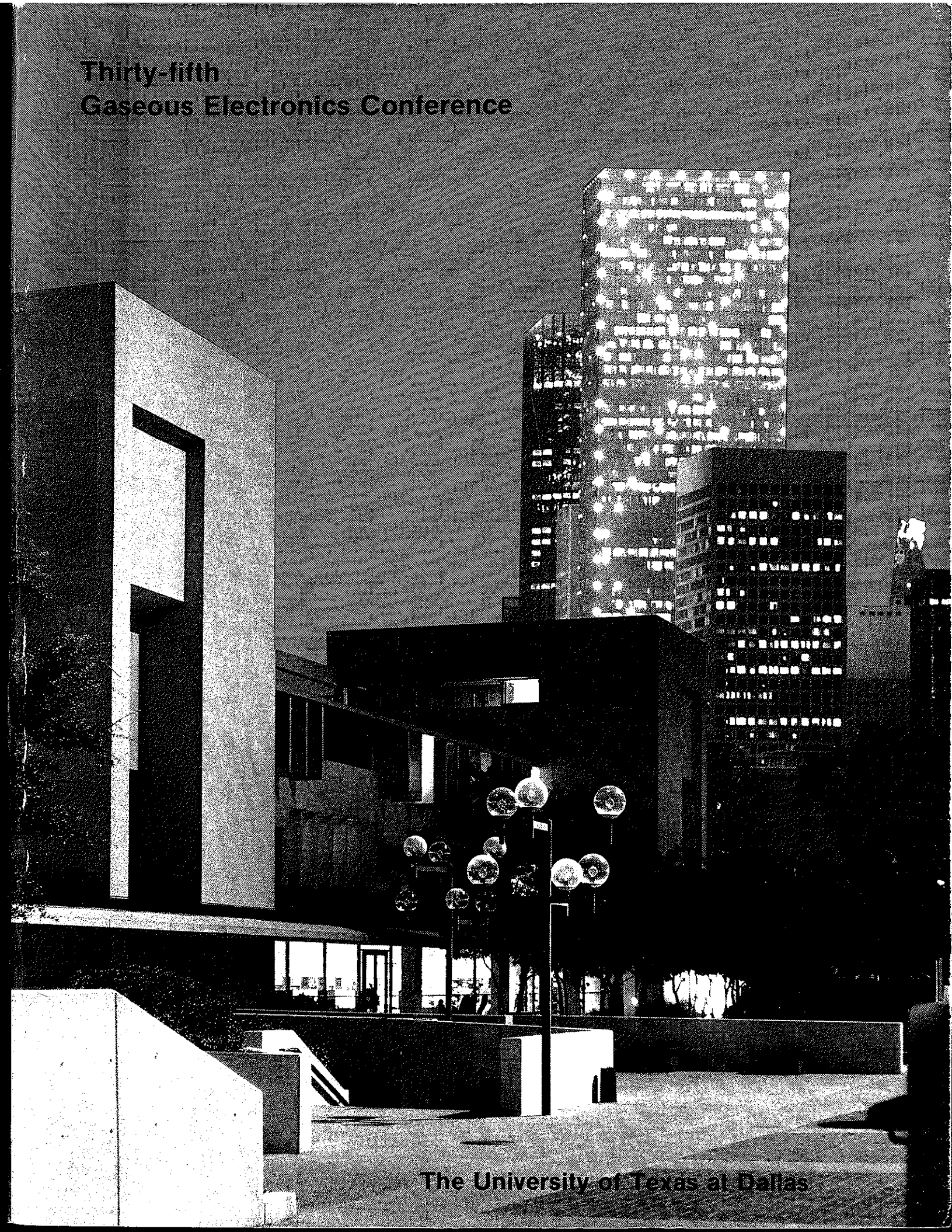# Thirty-fifth
Gaseous Electronics Conference

The University of Texas at Dallas

Thirty-fifth Annual

Gaseous Electronics Conference

October 19–22, 1982

PROGRAM AND ABSTRACTS

SPONSORED BY:
The University of Texas at Dallas
American Physical Society Division of Electron and Atomic Physics

ASSISTED BY:
Air Force Office of Scientific Research
Office of Naval Research
National Science Foundation

EXECUTIVE COMMITTEE

L. P. HARRIS, *Chairman*
General Electric Corporate R& D

W. P. ALLIS, *Honorary Chairman*
Massachusetts Institute of Technology

A. GARSCADDEN, *Chairman Elect*
Air Force Wright Aeronautical Lab

C. B. COLLINS, *Secretary*
The University of Texas at Dallas

W. H. LONG, JR., *Treasurer*
Northrop Research and Technology Center

M. J. BONESS
Avco Everett Research Laboratory, Inc.

G. A. FARRALL
General Electric Corporate R&D

M. R. FLANNERY
Georgia Institute of Technology

R. M. HILL
SRI International

R. JOHNSEN
University of Pittsburgh

LOCAL COMMITTEE

E. BREIG
C. D. CANTRELL
C. B. COLLINS
A. J. CUNNINGHAM

B. JOHNSON
F. W. LEE
L. MELTON

A TOPICAL CONFERENCE OF THE AMERICAN PHYSICAL SOCIETY

ACKNOWLEDGMENTS

CONTENTS

35TH GASEOUS ELECTRONICS CONFERENCE PROGRAM

REGISTRATION AND MIXER (CASH BAR)

RICHARDSON HILTON

OCTOBER 18, 1982

MONDAY EVENING 7:30 - 10:00

A: RECOMBINATION
Chairperson: D. R. Bates, Queens University, Belfast

A-1   SIMPLIFIED MODEL OF COLLISIONAL IONIZATION AND RECOMBINATION FOR HIGHLY
       EXCITED ATOMS   (7 min)
       P. A. Vicharelli and A. V. Phelps

A-2   DISSOCIATIVE-RECOMBINATION OF $e + H_3^+$. AN ANALYSIS OF REACTION PRODUCT
       DISTRIBUTION   (7 min)
       H. H. Michels and R. H. Hobbs

A-3   DISSOCIATIVE RECOMBINATION OF ELECTRONS WITH NO^+ IONS   (7 min)
       J. N. Bardsley

A-4   THEORY OF ELECTRON-ION AND OF ION-ION RECOMBINATION   (7 min)
       M. R. Flannery

A-5   THEORY OF THREE BODY ELECTRON RECOMBINATION IN MOLECULAR GASES   (7 min)
       W. L. Morgan

A-6   MUTUAL NEUTRALIZATION IN RARE GAS HALIDES   (7 min)
       B. L. Whitten, W. L. Morgan and J. N. Bardsley

COFFEE BREAK 10:00 - 10:30

BA: ARCS I
Chairperson: G. A. Farrall, General Electric R&D

10:30 a.m.
Room A

BA-1　ANODIC EROSION IN MULTI-CATHODE-SPOT VACUUM ARCS
S. Shalev, S. Goldsmith and R. L. Boxman　(7 min)

BA-2　ARC CURRENT AND ELECTRIC FIELD MEASUREMENTS IN A TRANSVERSE MAGNETIC FIELD METAL PLASMA ARC SWITCH
C. Scheffler, D. Dettman and R. Dollinger　(7 min)

BA-3　CHARACTERISTICS OF METAL PLASMA ARC SWITCHES
J. Sullivan, C. Scheffler, C. King, D. Dettman and R. Dollinger　(7 min)

BA-4　BOUNCING EXPANSION OF THE CATHODIC PLASMA IN VACUUM ALONG THE TRANSVERSE APPLIED B. FIELD
M. G. Drouet and J. L. Meunier　(7 min)

BA-5　EXPERIMENTAL STUDY OF ARC SPOT MOTION ON A CONICAL CATHODE
H. P. Mercure, R. Rajotte and M. G. Drouet　(7 min)

BA-6　ANODE FALL MEASUREMENTS IN HIGH INTENSITY ARCS
N. Sanders and E. Pfender　(7 min)

BA-7　STUDY OF A FREE-BURNING HIGH INTENSITY ARGON ARC
K. Etemadi, K. C. Hsu and E. Pfender　(7 min)

BA-8　COMMENTS ON APPLICATIONS OF ONE-DIMENSIONAL MODELS TO STEADY-STATE AND DYNAMIC ARC PLASMAS
S. S. Ahmed, D. M. Benenson and D. T. Tuma　(7 min)

BA-9　PHYSICAL MECHANISMS OF SLIDING DISCHARGES AT THE SURFACE OF MOIST POLLUTED INSULATING AND/OR SEMICONDUCTIVE SURFACES
H. P. Mercure　(7 min)

BB: LASERS
Chairperson: J. G. Eden, Univ. Illinois

10:30 a.m.
Room B

BB-1　EFFICIENT DISCHARGE EXCITATIONS OF AN X-RAY PREIONIZED XeCl LASER
D. E. Rothe, J. E. Levatter, T. Petach, C. Wallace and R. Sandstrom　(7 min)

BB-2　MEASUREMENT OF THE THRESHOLD X-RAY FLUX FOR PREIONIZING AN XeCl LASER
C. R. Tallman and I. J. Bigio　(7 min)

BB-3　STIMULATED EMISSION FROM RADIATIVE COLLISIONS IN HE-N_2
L. W. Downes, S. D. Marcum, W. E. Wells, K. Y. Tang and R. A. Tilton　(7 min)

BB-4　ENHANCED HgBr ($B^2\Sigma^+ \rightarrow X^2\Sigma^+$) EMISSION
W. P. Lapatovich, G. R. Gibbs and J. M. Proud　(7 min)

BB-5　KINETIC STUDIES OF THE TRIATOMIC EXCIMER Xe_2Br
R. A. Williams, W. L. Wilson, R. Sauerbrey and F. K. Tittel　(7 min)

BB-6　FLASHLAMP-PUMPED IODINE MONOBROMIDE LASING CHARACTERISTICS
L. E. Zapata and R. J. DeYoung　(7 min)

BB-7　ELECTRON SUPERELASTIC EFFICIENCY LOSS IN TE LASERS
J. Mellis and A. L. S. Smith　(7 min)

BB-8　EFFECTS OF DIFFUSION ON CHARACTERISTICS OF CW CO_2 LASER DISCHARGES
G. L. Rogoff　(10 min)

LUNCH 12:00 - 1:30

CA: ARCS II

1:30 p.m.
Room A

Chairperson: W. M. Keeffe, GTE Sylvania

CA-1 SPECTROSCOPIC DETERMINATION OF OPERATING PRESSURE IN METAL HALIDE ARCS
W. M. Keeffe and H. L. Rothwell　　(7 min)

CA-2 GEOMETRY-DEPENDENT NET EMISSION COEFFICIENTS FOR MODELING HIGH PRESSURE RADIATIVE ARCS
R. J. Zollweg　　(7 min)

CA-3 TIME DEPENDENT BEHAVIOR OF THE CONTRACTION REGION OF HIGH PRESSURE MERCURY LAMPS
R. Schäfer and H. P. Stormberg　　(7 min)

CA-4 THE EFFECT OF WALL TEMPERATURE ON SODIUM D-LINE RADIATION IN THE HIGH PRESSURE SODIUM ARC
R. P. Gilliard and J. H. Ingold　　(7 min)

CA-5 RADIANT EFFICIENCY OF LARGE BORE FLASHLAMPS
L. P. Bradley, A. E. Orel, and H. T. Powell

CA-6 NEODYMIUM PUMPING EFFICIENCY OF LARGE BORE FLASHLAMPS
L. P. Bradley, A. E. Orel and H. T. Powell　　(10 min)

CA-7 LASER INDUCED FLUORESCENCE IMAGING OF ELECTRODE VAPOR IN A SPARK GAP SWITCH
R. A. Dougal, P. F. Williams, and D. C. Pease　　(7 min)

CA-8 PLASMA PROCESSES IN HYDROGEN THYRATRONS
J. A. Kunc, S. Guha, H. Cole and M. A. Gundersen

CB: HEAVY PARTICLE COLLISIONS

1:30 p.m.
Room B

Chairperson: M. R. Flannery, Georgia Tech.

CB-1 ENHANCEMENT OF CHARGE-TRANSFER REACTION RATE CONSTANTS BY ION VIBRATIONAL EXCITATION
M. Durup-Ferguson, H. Böhringer, D. W. Fahey, and E. E. Ferguson　　(20 min)

CB-2 VIBRATIONAL RELAXATION OF MOLECULAR IONS BY LOW ENERGY (<1eV) COLLISIONS
E. E. Ferguson, M. Durup-Ferguson, H. Böhringer, and D. W. Fahey　　(7 min)

CB-3 ELECTRON AND ION COLLISIONS WITH CH_4, C_2H_6 SiH_4, and Si_2H_6
H. Chatham, D. Hils, R. Robertson and A. Gallagher　　(7 min)

CB-4 CHARGE TRANSFER FROM H_2 TO NEAR-THERMAL O_2^+ AND O_3^+ IONS
D. A. Church and H. M. Holzscheiter　　(7 min)

CB-5 CHARGE TRANSFER IN Ne^{8+}-Ne COLLISIONS BETWEEN 1 AND 100 eV IMPACT ENERGY
S. Hagmann, C. L. Cocke, P. Richard, A. Skutlartz, H. Schmidt-Böcking, and R. Schuch　　(7 min)

CB-6 CHEMISTRY OF SOME NEGATIVE CLUSTER IONS OF ATMOSPHERIC INTEREST
H. Böhringer, D. W. Fahey and F. C. Fehsenfeld　　(7 min)

CB-7 COLLISION STUDIES OF O^- IONS WITH H_2 and D_2
R. L. C. Wu, Y. Ichikawa, and T. O. Tiernan　　(7 min)

CB-8 DRIFT TUBE ENERGY TRANSFER PROCESSES OF N_2^+ STUDIED WITH LASER-INDUCED FLUORESCENCE
M. A. Duncan and S. R. Leone　　(7 min)

D: WORKSHOP ON CHEMICAL PROCESSES IN PLANETARY ATMOSPHERES
Chairperson: A. Dalgarno, Harvard University

3:15 p.m.
Room D

    This workshop convenes in the honor and presence of Professor Sir David Bates, F.R.S. His imaginative foresight and pioneering studies laid the foundation of our current understanding of the basic atomic and molecular processes controlling the collisional and radiative economy of the atmospheres of the earth and neighboring planets. The session will provide an overview of the increased understanding of such fundamental atomic processes as a result of the flights of the Voyager, Mariner and Pioneer spacecrafts and the Atmospheric Explorer Mission.

1. PROCESSES OBSERVED AND PROBLEMS ENCOUNTERED IN ATMOSPHERES OF VENUS AND MARS - *A. I. Stewart*

2. UPPER ATMOSPHERE PHYSICS AND CHEMISTRY OF THE OUTER PLANETS - *J. C. McConnell*

3. ESCAPE OF GASES FROM PLANETARY ATMOSPHERES - *M. B. McElroy*

4. PROGRESS IN ATMOSPHERIC CHEMISTRY SINCE THE LAUNCH OF THE ATMOSPHERE EXPLORER SATELLITES - *W. B. Hanson and E. L. Breig*

5. GENERAL DISCUSSION

OCTOBER 20, 1982

EA: PHOTON INTERACTIONS Chairperson: P. Vicharelli, JILA/NBS & U. Colorado	9:00 a.m. Room A	EB: BASIC PROCESSES IN HgBr LASERS Chairperson: J. J. Ewing, Math Sciences NW	9:00 a.m. Room B
EA-1 OPTOGALVANIC SPECTROSCOPY OF A HOLLOW CATHODE DISCHARGE R. Shuker, A. Ben-Amar and G. Erez	(20 min)	EB-1 DISSOCIATIVE EXCITATION OF $HgBr_2$ BY LOW ENERGY ELECTRON IMPACT J. R. Twist and M. L. Lake	(9 min)
EA-2 EXPERIMENTAL AND THEORETICAL INVESTIGATION OF OPTOGALVANIC EFFECTS IN THE NEON POSITIVE COLUMN D. Doughty and J. E. Lawler	(10 min)	EB-2 $HgBr^*(B)$ PRODUCTION BY ELECTRON IMPACT ON $HgBr_2$ C. L. Chen and P. J. Chantry	(9 min)
EA-3 OPTOGALVANIC EFFECTS IN THE OBSTRUCTED GLOW DISCHARGE J. E. Lawler and D. Doughty		EB-3 PSEUDO-OPTICAL ABSORPTION SPECTRA IN $HgCl_2$ AND $HgBr_2$ FROM 4 TO 14 eV D. Spence, R.-G. Wang and M. A. Dillon	(9 min)
EA-4 MULTIPHOTON IONIZATION IN XENON AND XENON-NITROGEN MIXTURES S. K. Dhali and P. F. Williams	(7 min)	EB-4 TOTAL QUENCHING CROSS SECTIONS OF METASTABLE ATOMS AND MOLECULES BY $HgBr_2$ J. L. Daniels and L. D. Schearer	(9 min)
EA-5 PHOTODETACHMENT AS A CONTROL MECHANISM FOR DIFFUSE DISCHARGE SWITCHES G. Schaefer, P. F. Williams, K. H. Schoenbach and J. Moseley	(7 min)	EB-5 RELATIVE FLUORESCENCE EFFICIENCIES FOR MERCURY-HALIDE VAPORS EXCITED BY COLLISIONS WITH $N_2(A^3\Sigma)$ L.D. Schearer	(9 min)
EA-6 LASER IRRADIATION OF SODIUM VAPOR: COMPARISON OF PULSED AND CW EXPERIMENTS V. S. Kushawaha, W. P. Garver, C. E. Burkhardt and J. J. Leventhal	(7 min)	EB-6 REANALYSIS OF THE B→X TRANSITIONS IN THE MERCURY HALIDES J. Tellinghuisen, P. C. Tellinghuisen, J. G. Ashmore and K. S. Viswanathan	(9 min)
EA-7 BRANCHING RATIO MEASUREMENTS RELEVANT TO THE INTERPRETATION OF VOYAGER EUV SPECTRA M. D. Morrison and A. J. Cunningham	(7 min)		

COFFEE BREAK 10:15 - 10:45

FA: ELECTRON COLLISIONS
Chairperson: J. N. Bardsley, Univ. Pittsburgh

10:45 a.m.
Room A

FA-1 CALCULATION OF ELECTRON EXCITATION CROSS-SECTION OF 3P STATE OF SODIUM
Z. Azar and R. Shuker (7 min)

FA-2 ELECTRON-IMPACT EXCITATION OF THE XENON ATOM
J. E. Gastineau, F. A. Sharpton, L. W. Anderson and C. C. Lin (7 min)

FA-3 ROTATIONAL TRANSITIONS IN THE IONIZATION-EXCITATION OF COLD N_2 BEAMS BY ELECTRON IMPACT
J. P. Doering, S. Hernandez and P. J. Dagdigian (20 min)

FA-4 ELECTRON-IMPACT EXCITATION OF THE $D^3\Sigma_u^+$ STATE OF THE NITROGEN MOLECULE
A. R. Filippelli, S. Chung, C. C. Lin and E. T. P. Lee (7 min)

FA-5 PRODUCTION OF ATOMIC OXYGEN EMISSION BY ELECTRON-IMPACT DISSOCIATION OF O_2
F. A. Sharpton, M. R. Pederson, A. R. Filippelli, L. W. Anderson, C. C. Lin and R. E. Murphy (7 min)

FB: MODELING OF HgBr LASERS
Chairperson: W. H. Long, Northrop Research

10:45 a.m.
Room B

FB-1 MERCURY BROMIDE KINETIC MODEL
L. J. Palumbo, R. L. Taylor and H. L. Chen (20 min)

FB-2 HgBr(B→X)/$HgBr_2$ LASER KINETICS
W. L. Nighan, R. T. Brown, J. J. Hinchen, and W. J. Wiegand (10 min)

FB-3 ELECTRON KINETICS ANALYSIS FOR HgBr LASERS USING A MEASURED B STATE EXCITATION CROSS SECTION
L. E. Kline, C. L. Chen, P. J. Chantry and L. J. Denes (10 min)

FB-4 ELECTRON CROSS SECTIONS FOR NEON IN THE RANGE 7 TO 100 eV
L. E. Kline (10 min)

LUNCH 12:00 - 1:30

7

1:30 p.m.
Room C

G: DISTRIBUTION FUNCTIONS AND ELECTRON TRANSPORT
Chairperson: W. F. Bailey, Air Force Institute of Technology – Wright Patterson AFB

G-1 ELECTRON MULTIPLICATION IN GASES: THE STOCHASTIC IONIZATION COEFFICIENT AND THE
E/N LIMIT OF THE TOWNSEND IONIZATION COEFFICIENT
E. E. Kunhardt, Y. Tzeng and J. P. Boeuf
(20 min)

G-2 NON-EQUILIBRIUM DEVELOPMENT OF AN ELECTRON SWARM IN NITROGEN: A MONTE
CARLO STUDY WITH STATISTICAL ENHANCEMENT FOR HIGH ENERGY ELECTRONS
Y. Tzeng, and E. E. Kunhardt
(10 min)

G-3 THE EFFECTS OF SPACE CHARGE ON AVALANCHE DEVELOPMENT: A SELF-CONSISTENT
MICROSCOPIC STUDY USING MONTE CARLO TECHNIQUE
Y. Tzeng and E. E. Kunhardt

G-4 NONLOCAL BOLTZMANN CODE FOR ELECTRON-BEAM-GENERATED PLASMA CHANNELS
S. S. Yu and R. E. Melendez
(7 min)

G-5 ELECTRON CONDUCTIVITY IN A RAPIDLY INCREASING ELECTRIC FIELD
J. N. Bardsley and B. M. Penetrante
(10 min)

G-6 ELECTRON ENERGY DISTRIBUTIONS IN MICROWAVE DISCHARGES
J. N. Bardsley and R. Chakrabarti

G-7 EFFECTS OF VARIOUS SECONDARY ELECTRON ENERGY DISTRIBUTIONS ON ELECTRON
TRANSPORT IN N_2
S. Yoshida, A. V. Phelps and L. C. Pitchford
(7 min)

G-8 CROSS-SECTION DATA FOR HIGH MOBILITY GASES
A. Garscadden and G. L. Duke
(7 min)

G-9 TRANSPORT COEFFICIENTS AND COLLISIONAL CROSS SECTIONS OF SF_6
J. P. Novak and M. Frechette
(7 min)

3:15 p.m.
Room D

H: WORKSHOP ON ATOMIC AND MOLECULAR COLLISION PROCESSES IN DENSE PLASMAS
Chairperson: M. R. Flannery, Georgia Institute of Technology

This workshop will focus on fundamental atomic and molecular processes, such as ion-ion recombination, electron-ion recombination, ion-molecule reactions, bimolecular and termolecular charge transfer and Penning ionization, occurring in plasmas formed in high pressure gases. Theory, experiment and computer simulation of such processes will be discussed. Ample time has been provided for general discussion of these topics.

1. ION-ION RECOMBINATION AND RELATED PROCESSES - D. R. Bates

2. MEASUREMENT AND MODELLING OF ION-MOLECULE REACTIONS AT ATMOSPHERIC PRESSURE - C. B. Collins and F. W. Lee

3. KINETIC PROCESSES IN DENSE HELIUM-NITROGEN AND HELIUM-HYDROGEN PLASMAS - J. Stevefelt

4. COMPUTER EXPERIMENTS AND RECOMBINATION THEORY - W. L. Morgan

5. GENERAL DISCUSSION

DINNER 5:45 - 7:15

OCTOBER 20, 1982

IA: POSTER SESSION

7:15 p.m.
Room S1

IA-1 NEGATIVE ION CONCENTRATIONS, ELECTRON ENERGY DISTRIBUTIONS, AND VIBRATIONAL POPULATION DISTRIBUTIONS IN HYDROGEN DISCHARGES
J. R. Hiskes and A. M. Karo

IA-2 ELECTRON TEMPERATURE DEPENDENCE OF THE RECOMBINATION OF ELECTRONS WITH H_3^+ and H_5^+ IONS
J. A. MacDonald, M. A. Biondi and R. Johnsen

IA-3 BASIC MICROSCOPIC THEORY OF ION-ION RECOMBINATION
M. R. Flannery and E. J. Mansky

IA-4 ULTRAVIOLET PHOTODISSOCIATION OF RARE GAS DIMER IONS (Xe_2^+, Kr_2^+)
A. W. McCown, M. N. Ediger, S. M. Stazak and J. G. Eden

IA-5 IMPROVED ABSOLUTE FREE-FREE EMISSION COEFFICIENTS FOR ELECTRONS IN ARGON
S. J. Buckman and A. V. Phelps

IA-6 TRANSITION PROBABILITY MEASUREMENTS FOR SOME Ar I 4s-4p TRANSITIONS
D. W. Jones, W. L. Wiese and K. Musiol

IA-7 KINETIC PROCESSES IN DENSE HELIUM-HYDROGEN PLASMAS
J. Stevefelt, O. Motret, and A. Bouchoule

IA-8 REACTION RATE COEFFICIENTS FOR C^+, CO^+, AND CO_2^+, O_2^+ N_2^+ Miller, R. E. Wetterskog and
J. F. Paulson

IA-9 TEMPERATURE DEPENDENCE OF 3-BODY ASSOCIATION REACTIONS OF IONS IN NITROGEN
S. Dheandhanoo, R. Johnsen and M. A. Biondi

IB: POSTER SESSION

7:15 p.m.
Room S2

IB-1 NEAR-THRESHOLD VIBRATIONAL EXCITATION IN ELECTRON-CO_2 COLLISIONS--A SIMPLE MODEL
B. L. Whitten and N. F. Lane

IB-2 NON-MAXWELLIAN ELECTRONS IN A LASER PRODUCED SODIUM PLASMA
W. L. Morgan

IB-3 ELECTRON IMPACT COLLISION STRENGTHS FOR EXCITATION FROM THE 2P LEVELS TO ALL LEVELS WITH n = 3, 4 and 5 IN He-LIKE IONS
D. H. Sampson, S. J. Goett, and R. E. H. Clark

IB-4 ELECTRON COLLISIONAL EXCITATION OF Na 3P ATOMS TO THE 3D STATE
B. Stumpf and A. Gallagher

IB-5 PLASMA ELECTRON HEATING IN A DC MULTIDIPOLE PLASMA
M. D. Haworth and R. E. Kribel

IB-6 EFFECTS OF ELECTRON LOSS DUE TO ATTACHMENT ON SWARM PARAMETERS IN SF_6-N_2 MIXTURES
L. C. Pitchford and A. V. Phelps

IB-7 ION RUNAWAY INDUCED BY MODEL ION-ATOM POTENTIALS
I. R. Gatland

IB-8 CHARACTERISTICS OF A MICROWAVE GENERATED SURFACE WAVE PLASMA IN A STANDING WAVES STRUCTURE
J. Marec, E. Bloyet, E. Dervisevic, P. Leprince, M. Pouey, and S. Saada

IB-9 WAVE PROPAGATION DURING IGNITION OF LOW PRESSURE Hg-RARE GAS DISCHARGES
J. F. Lowry and M. D. Nahemow

OCTOBER 21, 1982

9:00 a.m.
Room C

J: BREAKDOWN I
Chairperson: *E. E. Kunhardt, Texas Tech. Univ.*

J-1 RUNAWAY ELECTRONS IN FAST GAS DISCHARGES (9 min)
W. W. Byszewski and G. Reinhold

J-2 ELECTRON SHOCK STRUCTURE IN THE ELECTRICAL BREAKDOWN OF N_2 (9 min)
H. Jurenka and E. Barreto

J-3 DIELECTRIC COLLAPSE IN SMALL HIGH PRESSURE DISCHARGES (9 min)
E. Barreto and H. Jurenka

J-4 STATISTICAL DELAY TIMES AND BREAKDOWN PROBABILITY IN N_2, Ar, H_2, and SF_6 (9 min)
R. V. Hodges, R. N. Varney, and J. F. Riley

J-5 INITIATION OF ELECTRON AVALANCHES BY PHOTODETACHMENT IN IRRADIATED GAPS (9 min)
CONTAINING O_2 or SF_6
R. J. Van Brunt and M. Misakian

COFFEE BREAK 10:00 - 10:30

12

OCTOBER 21, 1982

K: LARGE APERTURE DISCHARGE LASERS
Chairperson: L. F. Champagne, Naval Research Laboratory

10:30 a.m.
Room C

K-1 PERFORMANCE MEASUREMENTS OF AN 8 LITER SELF SUSTAINED DISCHARGE TEA LASER
     M. J. Pechersky and R. J. Spreadbury   (12 min)

K-2 HOOK MEASUREMENTS IN LARGE COPPER LASERS
     B. E. Warner and G. V. Seely   (12 min)

K-3 LARGE BORE COPPER VAPOR LASER DISCHARGE KINETICS
     M. J. Kushner and B. E. Warner   (12 min)

K-4 APERTURE SCALING OF DISCHARGE-PUMPED XeCl LASERS
     B. L. Wexler and R. Burnham   (12 min)

BUSINESS MEETING 11:45 - 12:15   Room C

LUNCH 12:15 - 1:30

13

OCTOBER 21, 1982

LA: NEGATIVE IONS AND ATTACHMENT Chairperson: H. Böhringer, NOAA Aeronomy Lab	1:30 p.m. Room A		LB: CORONA AND BREAKDOWN II Chairperson: H. Jurenka, State U. of N.Y.	1:30 p.m. Room B
LA-1 VOLUME PRODUCTION OF HYDROGEN NEGATIVE IONS IN PLASMAS M. Bacal, A. M. Bruneteau, M. Nachman, M. Péalat, J. P. E. Taran and J. Taillet	(20 min)		LB-1 THEORY OF TRICHEL PULSES IN OXYGEN R. Morrow and J. J. Lowke	(7 min)
LA-2 EFFECT OF ROT-VIBRATIONAL EXCITATION ON DISSOCIATIVE ATTACHMENT OF H_2 J. M. Wadehra	(7 min)		LB-2 TOWARD A FUNDAMENTAL MODEL FOR STEADY POINT-PLANE CORONAS B. L. Henson	(7 min)
LA-3 MEASUREMENT OF ATTACHMENT COEFFICIENTS AT HIGH PRESSURES P. Bletzinger	(7 min)		LB-3 A SIMPLE MODEL OF LASER-TRIGGERED BREAKDOWN P. F. Williams and R. A. Dougal	(7 min)
LA-4 MEASUREMENTS OF ATTACHMENT AND IONIZATION COEFFICIENTS IN CCl_4 D. K. Davies	(7 min)		LB-4 SPECTRAL AND TEMPORAL EVOLUTION OF LASER BREAKDOWN IN SF_6 P. J. Hargis, Jr. LB-5 MULTIFREQUENCY LASER BREAKDOWN IN SF_6 P. J. Hargis, Jr.; L. C. Pitchford, T. A. Green, J. R. Woodworth and R. A. Hamil	(14 min)
LA-5 A SWARM STUDY OF ELECTRON ATTACHMENT TO THE PERFLUOROALKANES S. R. Hunter and L. G. Christophorou	(7 min)		LB-6 A PARAMETRIC STUDY OF LASER TRIGGERING OF A 500-KV GAS-FILLED SWITCH J. R. Woodworth and P. J. Hargis, Jr.	(7 min)
LA-6 FRAGMENTATION OF FLUOROETHERS AND FLUOROSULPHIDES UNDER LOW-ENERGY (≤10 eV) ELECTRON IMPACT S. M. Spyrou and L. G. Christophorou	(7 min)		LB-7 THEORY OF R.F. BREAKDOWN IN NITROGEN R. Morrow	(7 min)
			LB-8 BREAKDOWN OF ROD-PLANE GAPS UNDER HIGH FREQUENCY VOLTAGES M. S. Abou-Seada, H. Anis, and S. M. Salem	(7 min)
			LB-9 TWO DIMENSIONAL DESCRIPTION OF THE DEVELOPMENT OF TRANSIENT GAS DISCHARGES W. W. Byszewski, K. C. Chung, and J. M. Proud	(7 min)

LB-10 SIMULATION OF PROBABILITY DISTRIBUTIONS FOR THE BREAKDOWN VOLTAGE OF SURFACE DISCHARGES
M. J. Kushner   (7 min)

LB-11 ANALYSIS OF DISCHARGE DAMAGE AND BREAKDOWN IN GASEOUS CAVITIES IN INSULATING MATERIALS
A. A. Hossam-Eldin   (7 min)

LABORATORY TOUR *3:00 - 6:00 p.m.*
University of Texas at Dallas
Physics Department
Center for Quantum Electronics
Center for Space Sciences

SOCIAL HOUR *7:00 p.m. Richardson Hilton*

BANQUET *8:00 p.m. Richardson Hilton*

15

MA: METASTABLE COLLISIONS
Chairperson: R. Bieniek, U. Missouri-Rolla — 9:00 a.m. Room A

MA-1 VELOCITY DEPENDENT TOTAL SCATTERING CROSS SECTIONS FOR METASTABLE HELIUM ON He, Ne, Ar, Kr AND Xe
J. W. Sheldon and K. A. Hardy (7 min)

MA-2 TEMPERATURE DEPENDENCE OF DE-EXCITATION RATE CONSTANTS FOR NEON EXCITED ATOMS
C. Akoshile, J. Clark and A. J. Cunningham (7 min)

MA-3 THE IONIZATION COEFFICIENT IN Ar-Hg MIXTURES
A. L. J. Burgmans and A. H. M. Smeets (7 min)

MA-4 OBSERVATION OF ^{5}S NITROGEN METASTABLE STATE IN CHARGE EXCHANGE COLLISIONS
K. B. McAfee, Jr., C. R. Szmanda and R. S. Hozack (7 min)

MA-5 METASTABLES IONS AND THE F-REGION PHOTO-CHEMISTRY OF N_2^+
E. L. Breig, W. B. Hanson, J. H. Hoffman and D. G. Torr (7 min)

MA-6 TIME RESOLVED OBSERVATIONS OF $O(^1D)$ ENERGY TRANSFER
G. A. Germany, G. J. Salamo and R. J. Anderson (7 min)

MA-7 MEASUREMENT OF BIMOLECULAR AND TERMOLECULAR CHARGE EXCHANGE AND PENNING IONIZATION RATE CONSTANTS
L. W. Downes, S. D. Marcum and W. E. Wells

MA-8 ROTATIONAL SPECTRA OF NITROGEN ION TRANSITIONS PRODUCED BY PENNING IONIZATION AT HIGH PRESSURES
L. W. Downes, S. D. Marcum and W. E. Wells

(10 min)

MB: GLOW DISCHARGES I
Chairperson: L. E. Kline, Westinghouse R&D — 9:00 a.m. Room B

MB-1 ELECTRON DENSITY MEASUREMENTS IN A LOW PRESSURE Na-Ne DISCHARGE USING DOPPLER-FREE TWO-PHOTON SPECTROSCOPY
H. J. Cornelissen and A. L. J. Burgmans (7 min)

MB-2 HEATING IN A PULSED NITROGEN DISCHARGE
J. P. Boeuf and E. E. Kunhardt (7 min)

MB-3 MONTE CARLO SIMULATION OF ELECTRON PROPERTIES IN PARALLEL PLATE CAPACITIVELY COUPLED RF DISCHARGES
M. J. Kushner (7 min)

MB-4 MICROWAVE CAPILLARY DISCHARGES
J. Marec, E. Bloyet, E. Dervisevic P. Leprince, M. Pouey, and S. Saada (7 min)

MB-5 RADIATION EFFICIENCY OF THE ARGON-MERCURY DISCHARGE AT HIGH E/N
C. N. Stewart and J. H. Ingold (7 min)

MB-6 AXIAL PARTICLE DENSITY GRADIENT IN DIRECT-CURRENT DISCHARGES
J. H. Ingold and H. J. Oskam (7 min)

MB-7 MODELLING OF He-SiH$_4$-PH$_3$ GAS MIXTURE GLOW DISCHARGE POSITIVE COLUMN PLASMAS
J.-S. Chang, R. M. Hobson and Y. Ichikawa (7 min)

MB-8 PARTICLE BALANCE AND PLASMA PARAMETERS IN OXYGEN GLOW DISCHARGE POSITIVE COLUMN
Y. Ichikawa, R. L. C. Wu, T. O. Tiernan and T. Kaneda (7 min)

MB-9 STUDIES OF A GLOW DISCHARGE ELECTRON BEAM
Z. Yu, J. Meyer, J. Rocca and G. Collins (7 min)

COFFEE BREAK 10:15 - 10:45

OCTOBER 22, 1982

FRIDAY MORNING

N: GLOW DISCHARGES II AND BOUNDARY PHENOMENA

10:45 a.m.

Chairperson: A. Garscadden, Air Force Wright Aeronautical Labs

Room C

N-1 THEORY OF THE BOUNDARY LAYER IN A PARTIALLY IONIZED PLASMA (20 min)
    K.-U. Riemann

N-2 THEORY OF THE ELECTRON DISTRIBUTION FUNCTION IN STRONG INHOMOGENEITIES (7 min)
    A. Schumacher

N-3 ELECTRON WALL CURRENT AND FLOATING POTENTIAL IN A WEAKLY IONIZED PLASMA (7 min)
    A. Schumacher

N-4 BODY FITTED NON-LINEAR ELECTRIC FIELD IN GLOW DISCHARGES (7 min)
    W. M. Moeny, H. J. Happ, and P. J. Roache

N-5 CATHODE SHEATH FORMATION IN A PULSED, HIGH-PRESSURE DISCHARGE (7 min)
    W. H. Long, Jr.

N-6 ANALYSIS OF POSITIVE ION MASS SPECTRA AT THE CATHODE OF A GLOW DISCHARGE (7 min)
    M. C. Siddagangappa and M. S. Naidu

ADJOURN 12:00 NOON

SESSION A
9:00 A.M., TUESDAY, OCTOBER 19, 1982

RECOMBINATION

CHAIRPERSON: D. R. BATES
               QUEENS UNIVERSITY, BELFAST

A-1 Simplified Model of Collisional Ionization and Recombination for Highly Excited Atoms* - P.A. VICHARELLI and A.V. PHELPS, JILA, U. of Colorado and NBS---The simplified model of collisional-radiative recombination of Bates[1] has been extended to include the excitation and deexcitation of highly excited atoms in collisions with neutral atoms and the direct collisional ionization and recombination of each excited state. When only atom collisions are added, ionization and recombination coefficients vary with electron and atom density as found by Collins.[2] Direct collisional ionization and recombination[3] greatly increase the effective ionization coefficient at moderately low fractional ionization but only increase the recombination coefficient slightly.

[1] D.R. Bates, Proc. Roy. Soc. (London) A337, 15 (1974).
[2] C.B. Collins, Phys. Rev. 177, 254 (1969).
[3] L. Vriens and A.H.M. Smeets, Phys. Rev. A22, 940 (1980).

A-2 Dissociative-Recombination of $e + H_3^+$. An Analysis of Reaction Product Distribution - H.H. MICHELS, R.H. HOBBS, United Technologies Research Center*-- Dissociative-recombination (DR) of $e + H_3^+$ is exothermic by ∿9 eV to form $H + H_2$ and endothermic by nearly 6 eV to form the ion pair, $H^- + H_2^+$. The detailed branching of this reaction depends on the shape of the $^2A_1$ and $^2B_2$ hypersurfaces for H_3 for interatomic separations in the vicinity of 2-3Å. Detailed ab initio calculations of these hypersurfaces have been carried out within a CI framework. We find that the reaction path for (DR) begins with electron attachment to form the symmetric $^2A_1$ state of H_3 which is unstable toward asymmetric distortion into the surfaces $^2A_1$ and $^2B_2$. The $^2A_1$ surface connects to $H + H_2^\ddagger$ leaving H_2 with a significant amount of vibrational energy owing to the larger R_e of H_3^+. The branching to $H + H + H$ and the role of Rydberg states will also be discussed.

A-3 <u>Dissociative Recombination of Electrons with NO$^+$ Ions</u> – J. N. BARDSLEY, <u>U. of Pittsburgh</u>* -- Cross sections are calculated for direct dissociative recombination of electrons with NO$^+$ ions in the lowest four vibrational states, using a non-local resonant scattering theory. Contributions from the I $^2\Sigma$, A' $^2\Sigma$, B $^2\Pi$, L $^2\Pi$ and B' $^2\Delta$ are included. For ground state ions the cross section falls from 340 Å^2 at 0.03 eV to 5 Å^2 at 1 eV. The corresponding recombination rate decreases from 4.3×10^{-7} cm^3 s^{-1} at 300 K to 6.2×10^{-8} at 6000 K. For the excited vibrational levels, the cross sections and recombination rates are smaller. The dissociation leads almost entirely to $N(^2D) + O(^3P)$. The consistencies, and inconsistencies, of these results with previous experimental results will be discussed.

A-4 <u>Theory of Electron-Ion and of Ion-Ion Recombination</u> – M. R. FLANNERY, <u>Georgia Institute of Technology</u>*-- A basic microscopic theory of electron-ion collisional recombination in a dense gas is proposed. An expression is derived for the probability of collisions between a neutral gas particle and a negative ion (or electron) with radial separation $R \leq R_0$ from, and moving in a hyperbolic orbit about, a central positive ion. A simple "one channel" treatment of recombination can then be presented. Contact with the more basic "multichannel" theory[1] is established. For electron-ion recombination in a monotonic gas, the low gas density limit is identical with that of Pitaevskii. Results of the simple treatment are provided for (Kr$^+$-F$^-$) and (Xe$^+$-Cl$^-$) as a function of density of various rare gases.

[1]M. R. Flannery, Phil. Trans. Roy. Soc. A <u>304</u>, 447 (1982).

A-5 Theory of Three Body Electron Recombination in Molecular Gases-W.L. MORGAN, Lawrence Livermore Nat. Lab.[*]
The method of molecular dynamics[1](MD) has been used to simulate the electron-molecule recombination process $e + M^+ + M$. The MD calculations were performed for CO_2^+ in CO_2 and CH_4^+ in CH_4. The effects of inelastic electron molecule collisions, which enhance the recombination rate, are included in the calculations using a "null collision" algorithm. For CO_2 the computed rate coefficient increases linearly with pressure and agrees with recent experimental data[2] for $p \lesssim 2$ atm. Above this pressure the calculated rate, in contrast to the measured rate, saturates and then declines for $p > 8$ atm. Reasons for this behavior will be discussed.

[1]W.L. Morgan, J.N. Bardsley, J. Lin, and B.L. Whitten, Phys. Rev. A, to be published.
[2]D.A. Armstrong, E.S. Sennhauser, J.M. Warman, and U. Sowada, Chem. Phys. Letts. 86, 281 (1982).

A-6 Mutual Neutralization in Rare Gas Halides – B. L. WHITTEN, W. L. MORGAN, Lawrence Livermore Natl. Lab., & J. N. BARDSLEY, U. of Pittsburgh*--Previous work has indicated that mutual neutralization (MN)$(X^+ + Y^- \to X^* + Y)$ and three body recombination $(X^+ + Y^- + Z \to XY^* + Z)$ are competing processes and branching between them can significantly affect the formation rate of XY^*. Experimental and theoretical calculations of MN for systems with large crossing points differ by many orders of magnitude. We have performed quantum mechanical calculations of MN for $Ne^+ + F^-$ $(R_x \sim 10$ Å$)$ and $Ar^+ + F^-$ $(R_x \sim 19$ Å$)$. We find that, in both these cases the Landau-Zener model gives an accurate prediction of the quantum cross sections. This indicates that, at atmospheric pressure, MN is the dominant recombination process for $Ne^+ + F^-$, while three body recombination dominates for $Ar^+ + F^-$. We offer an explanation of the discrepancy between our results and others. We also discuss spin-orbit effects in ArF and the competition between MN and three-body recombination in NeF.

SESSION BA
10:30 a.m., Tuesday, October 19, 1982

ARCS I

Chairperson: G. A. Farrall
General Electric R&D

BA-1 Anodic Erosion in Multi-Cathode-Spot
Vacuum Arcs- S. SHALEV, S. GOLDSMITH, and
R.L. BOXMAN, Tel-Aviv U.*-- Anodic erosion in a
multi-cathode-spot vacuum arc between 12-14 mm
diam, 4 mm gap electrodes was studied. Arcs of
30 ms duration and peak currents of 0.4-2.2 kA
were ignited by means of a trigger electrode
recessed in the cathode. Emission of anodic
material lines was observed spectroscopically
even at low currents, but anodic weight loss
was not observed because of the deposition of
cathodic material. For currents exceeding a
threshold value dependant on material, melting
of the anode, usually at the center, was
observed. The threshold current in A for
various cathode-anode pairs follows: Cu-Zn,
500; Al-Zn, 760; Cu-Al, 880; Zn-Zn, 1000;
Al-Al, 1120; Mo-Cu, 2160; Cu-Cu, >2200. In
the case of Cu-Al, the estimated mass gained
from cathodic flux equalled the erosion for a
peak current of 1250 A. At a peak current of
2050 A, the erosion (15 mg) was 8 times larger
than the gain from the cathodic flux.

BA-2 Arc Current and Electric Field Measurements in a
Transverse Magnetic Field Metal Plasma Arc Switch - C.
Scheffler, D. Dettman and R. Dollinger, St. U. of NY at
Buffalo.* -- Measurements of the arc currents to each
anode quarter of a Westinghouse type [1] of Metal Plasma
Arc Switch (MPAS) shows non-uniform current distribution.
Single electric probe measurements show the existence of
a thin anode sheath and a Hall electric field. These
new measurements and high speed photographs for the case
of ringing circuit current will be compared to previous
data [2] for nonringing circuit current. The implica-
tions associated with thin anode sheath in connection
with the fluctuating current density will be discussed.

[1] C. W. Kimblin, et.al., EPRI Final Reports of Phase 1,
EL-393, 1977; Phase 2, EL-1221, 1979 and of Phase 3
(Research Project RP-564 to be available in 1982.)
[2] R. Dollinger, et.al., 3rd IEEE International Pulsed
Power Conference, p. 428, June 1-3, 1981 and Final
Report of EPRI Research Project RP-993-3 (1983).

BA-3 Characteristics of Metal Plasma Arc Switches -
J. Sullivan, C. Scheffler, C. King, D. Dettman and R.
Dollinger, St. U. of NY at Buffalo.* -- Four different
Metal Plasma Arc Switches (MPAS) which are characterized
by a high burning arc voltage (100 V - 10 kV) and con-
trollability have been developed recently. (These oper-
ating characteristics are quite different from those of
standard vacuum arcs.) Measurements have been done
[1,2,3,4] to determine the cause of the high voltage and
the results show that all MPAS devices rely on the de-
velopment of an anode sheath for proper operation. The
device physics and the external circuitry were found to
be interdependent primarily because the plasma density
at the plasma sheath boundary is related to current and
the sheath thickness is related to voltage.

*Supported by Electric Power Research Institute (EPRI)
and in part by Sandia Laboratories

[1]Dollinger, , EPRI Final Report EL-1947, 1981 and Final
Report of Research Project RP-993-3 (1983).
[2]Kimblin, , Phase 1: EPRI EL-393, 1977; Phase 2: EL-1221,
1979 and Phase 3: Final Report of RP-564 (1982).
[3]Dethlefsen, , Gould-Brown Boveri, ERPI EL-1187, 1979.
[4]Burrage, , McGraw Edison Co., EPRI EL-2266, 1982.

BA-4   Bouncing Expansion of the Cathodic Plasma in
Vacuum along the Transverse Applied B. Field. M.G.DROUET
and J.L. MEUNIER, IREQ, Varennes, JOL 2PO, Canada.
As predicted, the cathodic plasma is found not only to
expand in the cathode plane, along the magnetic field
lines[1], but also to bounce against the field.[2] For an
arc of 100 A burning in vacuum between tungsten elec-
trodes and with an applied magnetic field of 8.5×10^{-2} T,
the bouncing period is approximately 12 μs.

[1]M.G. Drouet, "The Physics of the Retrograde Motion of
the Electric Arc," Jap. J. Appl. Phys. 20, 1027-36
(1981).

[2]D.K. Bhadra, "Expansion of a Resistive Plasmoid in a
Magnetic Field," Phys. Fluids 234-39 (1968).

BA-5 Experimental Study of Arc Spot Motion on a Conical Cathode -- H.P. MERCURE, R. RAJOTTE and M.G. DROUET IREQ, Varennes, Canada.-- This paper describes an experimental study of the motion of low-pressure-arc spots on a coninal cathode in a strong axial magnetic field. The varying parameters include arc current, magnetic field intensity, background pressure and cone tip angle. The main experiment is conducted in a cylindrical glass vessel with a coaxially symmetric magnetic field (up to 1 T) using a pulsed arc current (up to 10 kA) in 3 Torr of helium.

Uniform, quite reproducible, spiral patterns are generated at the surface of the conical cathode, and the geometrical elements of these arc spot patterns are collerelated with the varying physical parameters.

A companion experiment will also be described in order to illustrate our interpretation of this peculiar arc spot behavior in which the resultant motion of the spots occurs in neither the I x B nor the -I x B direction.

BA-6 Anode Fall Measurements in High Intensity Arcs - N. SANDERS and E. PFENDER, U. of Minnesota*--Potential probes passing through the surface of a water cooled flat anode have been used for measuring anode falls in high intensity, atmospheric pressure, argon arcs with different arc configurations. For arc currents from 100 to 250 A, the anode falls are negative ranging from -2.08 V to -1.36 V. These results are contrary to previous findings, but they are in agreement with recent analytical predictions [1]. Electron temperatures in front of the anode, derived from probe characteristics, range from 8,800 to 9,800 K. These electron temperatures are used in conjunction with measured floating potentials to determine local values of the space potential. Spectrometric measurements of LTE temperatures close to the anode (1 mm distance) compare favorably with the probe measurements. All the results are consistent with calorimetric energy balances based on a revised anode heat transfer model which takes negative anode falls into account [1].

[1] H.A. Dinulescu and E. Pfender, J. Appl. Phys. 51 (6), 3149 (1980).

BA-7 Study of a Free-Burning High Intensity Argon Arc-
K. ETEMADI, K.C. HSU and E. PFENDER, U. of Minnesota*--
Although the high intensity, free-burning argon arc has
been the object of many studies, modeling of the entire
arc has been precluded because of the lack of realistic
boundary conditions, in particular, close to the cathode.
For establishing the most crucial boundary condition
which is the current density close to the cathode, the
maximum current density has been determined experimental-
ly by measuring the size of the molten cathode tip (thor-
iated tungsten) for a given arc current. Calculated tem-
perature profiles for a 200 A atmospheric pressure argon
arc (electrode gap of 1 cm) are in good agreement with
spectrometric measurements based on absolute line and
continuum intensities. The arc current and arc current
distribution are not only responsible for the temperature
distribution in the arc, but also for the MHD pumping ac-
tion in the cathode region, i.e. the arc behavior is main-
ly controlled by the current. In contrast to the sensi-
tivity of the current density boundary condition on the
results, the calculations show that variations of the
boundary condition for the flow field are insignificant.

BA-8 Comments on Applications of One-Dimensional Mod-
els to Steady-State and Dynamic Arc Plasmas – S.S. AHMED
and D.M. BENENSON, State U. of New York at Buffalo and
D.T. TUMA, Carnegie-Mellon U.* -- The formulation of the
one-dimensional model, e.g., that of Tuma[1], includes, as
inputs, the net radiation emission coefficient and the
pressure distribution, as well as parameters relating to
the temperature and flow fields. The effects of various
representations of these inputs and parameters upon tem-
perature, arc size, arc resistance, electric field, and
flow field are discussed. Both steady-state and dynamic
operation are considered for the dual flow configuration.
In the steady-state: upstream of the nozzle throat, the
results were strongly dependent upon the representation
of the inputs (e.g., at the stagnation point, the temper-
ature could take on values in the range from 17,500K to
27,000K). Downstream of the throat, the solutions were
relatively independent of the particular representations.
In the transient [with $dI/dt = -24A/\mu s$ prior to current
zero and dV/dt prescribed after current zero]: results
(e.g., at current zero, recovery performance) were also
nearly independent of the choice of representation.

[1]D.T. Tuma, IEEE PAS, 99, 2129 (1980).

BA-9 Physical Mechanisms of Sliding Discharges at the
Surface of Moist Polluted Insulating and/or Semiconduct-
ive Surfaces -- H.P. MERCURE, IREQ, Varennes, Canada.
The sudden disruptive event characterized by the steady
elongation of a weak sliding discharge at the surface of
moist polluted insulating materials or semiconductive
layers subjected to high voltages is usually referred
to as contamination-induced flashover.

The physical mechanisms responsible for the elongation
of such low-current discharges at the surface of an
electrolyte, for instance, are explained in terms of a
simple model based on experimental observations. These
results were obtained using a novel probe technique
allowing dynamic monitoring of the current distribu-
tion in the root of the discharge as it progresses along
the surface.

A look at the so-called stabilizing nature of semicon-
ductive glazes proposed for high-voltage insulators is
of particular interest to power utilities concerned
with the reduction of contamination-induced flashovers.
Cases involving clean semiconductive layers will also
be presented. The various results will be discussed and
compared with other experimental and theoretical studies
published recently.

SESSION BB
10:30 A.M., TUESDAY, OCTOBER 19, 1982

LASERS

CHAIRPERSON: J. G. EDEN
UNIVERSITY OF ILLINOIS

BB-1   Efficient Discharge Excitation of an X-Ray
Preionized XeCl Laser - D.E. ROTHE, J.I. LEVATTER,
T. PETACH, C. WALLACE & R. SANDSTROM, Helionetics, Inc.* -
The transfer of electric energy from the pulse-forming
network (PFN) to the laser medium is complicated by the
dynamic nature of the electric discharge in the high-
pressure gas mixture. Primary considerations are: the
finite avalanche formation rate as a function of over-
voltage, impedance and voltage matching considerations,
discharge instabilities and the stabilizing effects of
the PFN. The problems and physical principles which
prevent complete energy transfer have been identified.
By properly shaping the excitation pulse, it should be
possible to reach energy efficiencies close to the
measured power efficiencies of 5%. Other effects which
limit laser efficiency are also discussed (e.g. build-
up of absorbing species which reduce the optical
extraction efficiency).

BB-2   Measurement of the Threshold X-Ray Flux for
Preionizing an XeCl Laser - C.R. TALLMAN, and IRVING J.
BIGIO, Los Alamos National Laboratory*--Using a hot
cathode x-ray source we have determined that the
discharge of a large volume (250 cm^3) XeCl laser can be
effectively stabilized with as little as 0.1 mRad of
x-rays in the energy range 20-40 kV. The laser operated
at 4 atmospheres total gas pressure, with an electrode
gap of 4 cm and a discharge voltage of ~60 kV. The
delay between the 50 ns x-ray pulse and the onset of the
voltage rise at the discharge electrodes could be varied
from 0-200 ns with little effect on the laser output.
The laser's volumetric efficiency was 5 J/ℓ. The same
laser produced 35% less energy when operated with uv
preionization. The measured threshold indicates that
excimer lasers can be operated with an energy for the
preionizer only 0.2% that of the stored energy for the
main discharge.

BB-3   STIMULATED EMISSION FROM RADIATIVE COLLISIONS IN HE-N$_2$. * L.W. Downes, S.D. Marcum and W.E. Wells, Miami University, Oxford OH and K.Y. Tang and R.A. Tilton, Western Research Corporation, San Diego CA.

A high pressure He-N$_2$ plasma has been studied during the interaction of a ~100 kW/cm^2 pulsed dye LASER at 3538 Å. Stimulated emission from the radiative collision[1,2],

$$\text{He}(2^3S) + N_2 \rightarrow [N_2^R(B,v=4,5) \rightarrow N_2^R(X,v=3,4)+ h\omega] + \text{He}(1^1S),$$
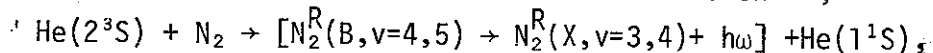
where R refers to a highly excited Rydberg state, has modulated the metastable density, [He(2^3S)]. The [He(2^3S)] has been depressed by approximately 30%. This result is in agreement with previous work.[2,3]

1. L.Gudzenko and L.I.Yakovlenko, Sov. Phys. JETP 35, 877 (1972).
2. L.W.Downes, S.D.Marcum, R.A.Tilton and W.E.Wells, Phys. Rev. A 25, 1798(1982).
3. L.W.Downes, S.D.Marcum, R.A.Tilton and W.E.Wells, Optics Letters 7,22(1982).

BB-4   Enhanced HgBr (B$^2\Sigma^+ \rightarrow$ X$^2\Sigma^+$) Emission – W. P. LAPATOVICH, G. R. GIBBS, and J. M. PROUD, GTE Laboratories, Inc.--We have examined the spectral output of microwave driven (915 MHz), low pressure (2 to 4 torr), diffuse discharges containing HgBr$_2$ and various buffer vapors. The integrated power emitted in the spectral range between 374 and 543 nm due to B$^2\Sigma^+\rightarrow$X$^2\Sigma^+$ transitions in Hg Br was recorded by means of an optical multichannel analyzer system. When mixtures of N$_2$ and I$_2$ vapor are added to the HgBr$_2$ discharges, an increase in B→X radiated power is observed. The excess population of neutral HgBr$_2$ interacts with N$_2$(A) and atomic iodine photons at 206.2 nm. Nearly resonant electronic energy transfer collisions and photodissociative excitation of the dihalide occur to produce additional B state population. The enhanced emission is two orders of magnitude more intense than that observed with pure neon as a buffer at 145°C (~1.6 torr HgBr$_2$).

BB-5   Kinetic Studies of the Triatomic Excimer Xe_2Br^* --
R.A. Williams, W. L. Wilson, R. Sauerbrey, and F.K.
Tittel, Rice U.*--Formation and quenching processes, as
well as the optical emission characteristics of Xe_2Br^*,
centered at 440 - 30 nm were investigated for electron
beam pumped mixtures of argon, xenon and several dif-
ferent bromine donors. Three-body collisional quenching
of XeBr was identified as the primary formation
mechanism for the triatomic species. Quenching rates
for Xe_2Br^* and $XeBr^*$ were measured and the Xe_2Br^*
radiative lifetime was determined to be 245 $\pm$ 30 ns.

BB-6   Flashlamp-Pumped Iodine Monobromide Lasing Char-
acteristics -. L. E. ZAPATA*, Miami U., and R. J.
DEYOUNG, NASA Langley Res. Center -- Xenon flashlamp
energies of 100-1500 J were used to photodissociate IBr
resulting in lasing of Br at 2.7 μm.   Quenching of
$Br(P_{1/2})$ by I_2 and Br_2 is severe and thus IBr must be
highly purified before use.   Peak lasing output of
350 W/cm^2 was achieved at 12 Torr IBr with 750 J flash-
lamp energy.   Neon was found to be the most effective
buffer, producing long pulse (50 μsec) lasing by enhanc-
ing the recombination of the photodissociation products
determined by transient absorption spectroscopy.   With
static-fill IBr, lasing is limited to 50 μsec by buildup
of atomic I and Br_2 quenchers; thus for continuous
operation, gas flow is mandatory.   A gain under optimum
conditions of 0.17% cm^{-1} was measured.   Gas heating
decreased lasing output.   At 300°C, output dropped to
one-third the room temperature value.   Time-dependent
absorption measurements with an Ar^+ laser have correla-
ted the rise of I_2 density with the decrease in IBr las-
ing.   The technique also yields recombination coeffici-
ents for the products of photodissociation.   The recom-
bination rate for pure IBr takes place in 20 msec.   When
Ne buffer is added, this time is reduced to 20 μsec.

BB-7 **Electron Superelastic Efficiency Loss in TE Lasers** - J. MELLIS and A.L.S. SMITH, Strathclyde U., Scotland* - Boltzmann models of the CO_2-N_2-He electrical discharge system[1] usually predict that, with optimum E/N, 50 to 80% of the input energy is used usefully in N_2 and CO_2 (ν_3) vibrational excitation. Thus, allowing for the quantum efficiency, 20 to 33% of the discharge energy should be available as radiation output. We have adapted our vibrational kinetics model[2] to study vibrational temperatures and stored energy in TE laser pulsed discharges and find a serious deterioration in laser efficiency with increasing input energy, caused by electron superelastic losses during the excitation pulse: an effect which should also be important in many other pulsed gas laser systems. Experimental observations support the calculated vibrational temperatures and likewise our predicted 8-12% radiation yield efficiency at optimum excitation is in good agreement with the values realised in working lasers.

[1] J.J. Lowke, A.V. Phelps and B.W. Irwin, J. Appl. Phys. 44, 4664 (1973).

[2] J. Mellis and A.L.S. Smith, Opt. Commun. 41, 121 (1982).

BB-8 **Effects of Diffusion on Characteristics of CW CO_2 Laser Discharges.** GERALD L. ROGOFF, Westinghouse R&D Center—In order to clarify when electron loss by diffusion is important in steady-state CO_2 laser discharges, we have calculated V-I characteristics of positive columns in 1:7:20 CO_2:N_2:He mixtures at pressures ≥ 10 Torr. The calculations are based on an approximate electron continuity equation that includes effects of ambipolar diffusion, one-step electron-impact ionization, attachment, detachment, and recombination. E/N vs I relationships are obtained from a generalized discharge analysis[1] which also gives a measure of the shape of the electron density profile. Results for a 6 cm diameter tube and a current density range given by $10^{-22} \leq j/N \leq 10^{-19}$ A cm indicate that with little detachment, E/N values with and without diffusion differ by less than a few percent if the pressure is ≥ 50 Torr. With strong detachment the same difference requires about 300 Torr. The density profile, which depends on the relative strengths of recombination and diffusion, remains relatively nonuniform for I less than about 400 mA for the 50 Torr case and for I less than about 30 mA for the 300 Torr case.

[1] G. L. Rogoff, J. Appl. Phys. 50, 6806 (1979); 51, 3144 (1980).

SESSION CA
1:30 P.M., TUESDAY, OCTOBER 19, 1982

ARCS II

CHAIRPERSON: W. M. KEEFFE
GTE SYLVANIA

CA-1 Spectroscopic Determination of Operating Pressure in Metal Halide Arcs – W.M. KEEFFE and H.L. ROTHWELL, GTE LIGHTING PRODUCTS, Sylvania Lighting Center -- We have studied the use of van der Waals and resonance interactions on the resonance lines of Na and Hg to determine the operating pressure of wall stabilized 60 Hz LTE arcs containing mercury and metal halide additives such as NaI and ScI$_3$.[1,2] Using a well defined cylindrical arc vessel and a known mercury dosage the spectroscopically determined pressures were within 20% of equation of state calculations. Accurate radial arc temperature profiles out to a reduced radius of .75 and thermo-chemical calculations to determine the depletion of atomic neutrals by molecular formation were found necessary in order to establish a self-consistent method. Application to vertical arcs with axial core temperature gradients (4300 to 5900°K) demonstrates axial pressure commutation to within 10%.

[1] H.L. Rothwell and W. M. Keeffe, 34th GEC (Boston, 1981)

[2] D. Karabourniotis and J.J. Damelincourt, J. Appl. Phys. 53, 2965 (1982).

CA-2 Geometry-Dependent Net Emission Coefficients For Modeling High Pressure Radiative Arcs – R.J. ZOLLWEG, Westinghouse R&D Center--Temperature profiles and the radiative, conductive and convective properties of high pressure arcs can be reliably described in the LTE approximation when the material transport properties and boundary conditions are known. The net radiation emission coefficient is a particularly difficult property since it depends upon the radiance of the whole arc. "Exact" net emission coefficients have usually been calculated with a complex five-fold integral formulation appropriate for the center of an infinite cylinder of specific radius and power. Such results are not appropriate for arcs of different power, wall radius, with spacial composition variations or for the electrode termination region. By taking advantage of unique properties of collision-broadened spectra and imprisonment theory[1], the local volume properties can be separated from the integrated column radiation and good approximate net emission coefficients obtained, even for arcs with numerous optically thick spectral lines. Applications to modeling the electrode termination of the high pressure mercury arc will be presented.

[1] F.E. Irons, J.Quant.Spect.Radiat.Transfer 22,1,(1979).

CA-3 Time Dependent Behaviour of the Contraction
Region of High Pressure Mercury Lamps -
R. SCHÄFER and H.P. STORMBERG, Philips GmbH Forschungsla-
bor Aachen/Germany.--High pressure mercury lamps were.
operated on a periodically pulsed supply voltage. From
optically thin mercury line emission the variation of the
axial arc temperature profile during an a.c. cycle has
been determined. It is found that the time dependence of
the arc temperature changes strongly along the discharge
axis. The temporal variation of the temperature of the
hot spots in the contraction region[1] in front of cathode
and anode is appreciably higher than the column tempera-
ture fluctuation. From the measured radial arc tempera-
ture profiles the time dependent arc conductance per unit
length has been calculated. The results show that a sig-
nificant part of the integral arc conductance decay dur-
ing the current off periods is caused by the contraction
regions, whereas in the current on periods the arc con-
ductance is mainly determined by the arc column.

[1]G. Ecker, Z. Physik 132, 248 (1952)

CA-4
The Effect of Wall Temperature on Sodium
D-Line Radiation in the High Pressure Sodium Arc -
RICHARD P. GILLIARD and JOHN H. INGOLD, General
Electric Co., Cleveland, OH -- The resonance radiation
output of the high pressure sodium arc is strongly
affected by the number density of unexcited sodium
atoms near the wall of the arc chamber. This quantity
in turn is affected by the arc temperature profile
which is dependent upon wall temperature. The
significance of wall temperature change as reported in
the literature, varies widely. A new experimental
determination of the relationship between wall
temperature and sodium D-line radiation efficiency of
the high pressure sodium arc at constant power and
sodium pressure was made. Wall temperature changes
were brought about, independent of sodium pressure and
arc power, by varying heat loss from the wall. Arc
spectral power distributions were measured for varying
wall temperatures which were determined by infrared
pyrometry. The experimental results, which show an
increase in sodium resonance radiation of 4%±1% per
100°K increase in wall temperature, were compared to
results predicted by a theoretical model of the high
pressure sodium arc.

CA-5   Radiant Efficiency of Large Bore Flashlamps -
L. P. BRADLEY, A. E. OREL, and H. T. POWELL, Lawrence
Livermore National Laboratory*--We have measured the
overall radiant efficiency of flashlamps with arc
diameters from 1.0 to 2.7 cm, with pulselengths from
0.2 to 1.4 ms, and with input energies up to 60% of the
explosion limit. Diagnostics include wall temperature
rise, "black box" calorimetry, and pyroelectric
detector measurements of radiated power. Modeling has
determined the role of collisional energy loss to the
wall and optical absorption by the envelope material.

CA-6   Neodymium Pumping Efficiency of Large Bore
Flashlamps - L. P. BRADLEY, A. E. OREL, and H. T.
POWELL, Lawrence Livermore National Laboratory* --We
have measured the Nd:glass pumping efficiencies of
flashlamps with arc diameters ranging from 1.0 to 2.7
cm, with pulselengths from 0.2 to 1.4 ms, and with
input energies up to 60% of the explosion limit. The
difference in pumping efficiency versus input energy
for open lamps and for lamps in a reflective cavity has
been addressed. The measurements have been compared to
simple models.

CA-7 Laser Induced Fluorescence Imaging of Electrode Vapor in a Spark Gap Switch-R.A. DOUGAL, P.F. WILLIAMS, D.C. PEASE, Texas Tech*--Time-resolved two-dimensional pictures of the migration of metal vapor eroded from aluminum electrodes in a laser triggered spark gap switch have been obtained using a new technique based on laser-induced fluorescence. A 1 μs, unipolar, square-wave discharge was produced in a 5 mm gap filled with 700 torr N_2 triggered by a 1.06μ Nd:YAG laser. Electrode material vaporized during the discharge was excited from ground state ($3P^2P_{1_2}^o$) to an upper state ($4S^2S_{1_2}$) with a 394.4 nm dye laser probe, resulting in fluorescence at 394.4 and 396.1 nm. The fluorescence was imaged through a 400 ± 5 nm bandpass filter onto a gated SIT vidicon detector. The aluminum vapor is shown to jet from the electrodes, and then dissipate after about 300 μs.

CA-8 Plasma Processes in Hydrogen Thyratrons J.A. KUNC, S. GUHA, H. COLE, and M.A. GUNDERSEN Univ. of Southern California*--An analysis of the plasma occurring in hydrogen thyratrons, where neutral densities are of the order $1-2\times10^{16}$ cm^{-3} and electron densities are of the order 10^{14} cm^{-3}, during the conductive phase, is presented. Plasma parameters were obtained from spectral emission data and a theoretical analysis of kinetic processes. The electron energy distribution function, the degree of hydrogen dissociation, and other processes are considered.

SESSION CB
1:30 P.M., TUESDAY, OCTOBER 19, 1982

HEAVY PARTICLE COLLISIONS

CHAIRPERSON: M. R. FLANNERY
GEORGIA INSTITUTE OF TECHNOLOGY

CB-1 Enhancement of Charge-Transfer Reaction Rate Constants by Ion Vibrational Excitation. M. DURUP-FERGUSON, H. BÖHRINGER, D. W. FAHEY, and E. E. FERGUSON, Aeronomy Laboratory, NOAA, Boulder, CO 80303. A number of molecular ion charge-transfer reactions with neutral molecules have been studied in a flow-drift system as a function of average kinetic energy from thermal to $\sim$1eV. Varying the buffer gas gives an independent control of the vibrational temperature of the ions. No vibrational excitation has been found for any of the ions in helium buffer gas while extensive vibrational excitation has been found for Ne and Ar buffer gases at kinetic energies above the vibrational excitation threshhold.

The reactions measured include charge-transfer of CO_2^+ ions with O_2 and NO and N_2O^+, SO_2^+, H_2O^+ and NO_2^+ ions with NO. In every case the reaction rate constant is greatly enhanced by vibrational excitation of the ion. The vibrational enhancement has an onset near the lowest frequency bending mode vibrational energy. The reactions proceed via long-lived complexes at low energy and via a direct process at higher energies. A detailed analysis of the dependence of rate constant separately on translational and vibrational energy indicates that the vibrational enhancement occurs in an energy regime in which a long-lived complex reaction mechanism is operative.

CB-2 Vibrational Relaxation of Molecular Ions by Low Energy ($<$1eV) Collisions. E.E. FERGUSON, M. DURUP-FERGUSON, H. BÖHRINGER, and D.W. FAHEY, Aeronomy Laboratory, NOAA, Boulder, CO.--The enhancement of ion-neutral reaction rate constants by vibrational excitation of ions using a flow-drift tube apparatus with various buffer gases has been used as a probe to study ion vibrational excitation and relaxation. It is found that the ions O_2^+, CO_2^+, and N_2O^+ are not vibrationally excited in $\sim$10^3 collisions with He at energies several times greater than vibrational energies of the ions. These ions are fully vibrationally excited in $\sim$10^3 collisions with Ne or Ar at energies only slightly above threshhold. The ions are relaxed very efficiently by charge-transfer with their parent neutral in every case, at near the collision rate. The $O_2^+(v = 1)$ ion is collisionally deexcited with a rate constant near 10^{-11} cm^3 s^{-1} by Ar at near thermal energies. The O_2^+ ions are less efficiently vibrationally excited by N_2 than by Ar and more efficiently deexcited as a consequence of vibrational excitation of neutral N_2 as a competitive process in $O_2^+ - N_2$ collisions. The potential range of applicability of this new technique for the study of vibrational excitation and deexcitation appears to be large.

CB-3   Electron and Ion Collisions with CH_4, C_2H_6, SiH_4, and Si_2H_6 - H. CHATHAM, D. HILS, R. ROBERTSON and A. GALLAGHER,* JILA, Univ. of Colo. & NBS.--Electron collisional ionization cross sections of CH_4, C_2H_6, SiH_4, and Si_2H_6 have been measured. The total ionization cross sections as well as the product-ion distributions will be reported. Rate coefficients for charge-exchange reactions of He^+, Ne^+, and Ar^+ with these four gases have also been measured in a drift tube as a function of E/P, for mean ion energies typically of 0.03-1 eV. Product ion distributions have also been measured for these reactions, although with considerable uncertainty in some cases as the diffusion corrections for the product-ions are calculated using assumed mobilities. The total charge-exchange rate coefficients are within a factor of 2 of Langevin values, with the exception of Ar^+ + SiH_4 and Si_2H_6 for which they are ~30 times smaller in spite of >3 eV exothermicity. These cross sections and rate coefficients are important for modeling of discharges and ion-chemistry in these gases.

*Staff Member, Quantum Physics Division, NBS.

CB-4   Charge Transfer from H_2 to Near-Thermal O^{2+} and O^{3+} Ions, D. A. CHURCH AND H. M. HOLZSCHEITER, Texas A&M U. -- Using an ion storage technique, the rate constants for charge transfer from H_2 to ion gases composed of O^{2+} and O^{3+} were measured. The ions were at a temperature of $1.45(0.6) \times 10^4$ K and $2.5(0.6) \times 10^4$ K respectively. Studies of relaxation of the motional degrees of freedom by pulsed cyclotron resonance followed by axial energy transfer aided in establishing the thermal properties of the gas. The measured rate of constants are $k(O^{2+},H_2) = 1.7(0.4) \times 10^{-9}$ cm^3/sec and $k(O^{3+},H_2) = 1.2(0.3) \times 10^{-8}$ cm^3/sec. Evidence for metastable level effects in the O^{2+},H_2 interaction will be discussed.

CB-5　Charge Transfer in Ne^{8+}-Ne Collisions between 1 and 100 eV Impact Energy. S. HAGMANN, C. L. COCKE, P. RICHARD, A. SKUTLARTZ, Kansas State University and H. SCHMIDT-BÖCKING, Universität Frankfurt, R. SCHUCH, Universität Heidelberg.--We have used the 0.5 MeV/u F^{9+} beam of the KSU FN tandem accelerator to produce highly charged low velocity Ne recoil ions. It has been shown through spectroscopic identification[1] that these ions with energies of a few eV and charge states up to the one electron ion may in a secondary collision capture an electron into an excited state and decay subsequently to the ground state. We have now investigated the velocity dependence of this secondary collision process for extremely low collision velocities, equivalent to 1 to 100 eV impact energy: through a coincidence between the primary projectile scattered under a certain angle and the delayed electron from the excited state of the Ne ion we determine kinematically its velocity. We will discuss the oscillations appearing in the transfer cross sections.

1) R. Mann, F. Folkmann, H. F. Beyer, J. Phys. B 14, 1161 (1981).

CB-6　Chemistry of Some Negative Cluster Ions of Atmospheric Interest - H. BÖHRINGER, D.W. FAHEY, AND F.C. FEHSENFELD, NOAA, Aeronomy Laboratory -- Thermodynamical data for some negative cluster ions have been determined from equilibrium constant measurements in a flowing afterglow. Specifically, it was found that a ligand of H_2O_2 bonds significantly stronger to negative ions than a ligand of H_2O (for example D (Cl$^-$-H_2O_2) is about 6.5 kcal/mol larger than D (Cl$^-$-H_2O) and also about 0.5 kcal/mol larger than D (Cl$^-$-SO_2)). This may imply that H_2O_2 cluster ions exist in small concentrations in the lower atmosphere. Chemical reactions other than simple ligand switching reactions have been observed for negative H_2O_2 cluster ions, like the reaction $NO_2^- \cdot H_2O_2 + SO_2 \rightarrow HSO_4^- + HNO_2$. These measurements will be reported and their implication for the chemistry of the lower atmosphere will be discussed.

CB-7 Collision Studies of O⁻ Ions With H₂ and D₂ -
R.L.C. WU, Y. ICHIKAWA, AND T.O. TIERNAN, Wright
State Univ., Dayton, Ohio 45435*--Excitation functions
for the reactions, $O^- + H_2(D_2) \rightarrow$ products have been inves-
tigated extensively utilizing a tandem mass spectrometer
and a crossed ion-molecular beam apparatus. Reaction
cross sections and energy thresholds have been measured
for the following reaction channels:

$$O^- + H_2(D_2) \quad \rightarrow \quad \begin{cases} H_2O\ (D_2O) + e & (1) & \quad -3.63 \\ OH^-\ (OD^-) + H\ (D) & (2) & \quad -0.32 \\ H^-(D^-) + OH\ (OD) & (3) & \quad +0.73 \end{cases}$$

with $\Delta E(eV)$ values shown at right.
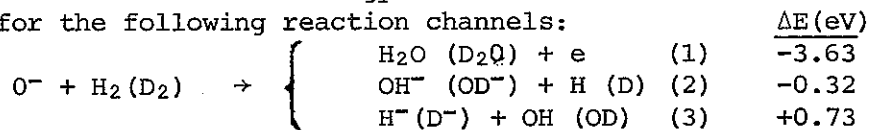
The results demonstrated that, in the near-thermal energy
region, reaction (1) is the dominant reaction channel,
but as the energy of the system increases, reaction (2)
becomes dominant, and reaction (3) also becomes signifi-
cant. The cross sections for both processes (2) and (3)
attain a maximum at about 0.8 eV. The angular and ener-
gy distributions of the products from reaction (2) have
also been measured in the relative energy range 0.6 -
5 eV. The data obtained in this study will be presented
and discussed in terms of understanding the microscopic
mechanism and the energy surface on which these pro-
cesses occur.

CB-8   Drift Tube Energy Transfer Processes of N_2^+
Studied with Laser-Induced Fluorescence - M.A. DUNCAN
and S. R. LEONE, JILA, NBS & Univ. Colo., and Dept. of
Chem., Univ. of Colo.--Internal excitation of ions in
a drift field has previously been suggested as a pos-
sible explanation for the unusual energy dependence of
certain ion-molecule reaction rates measured in this
environment. This question has subsequently been the
topic of a detailed theoretical study. In the current
work the translational to rotational energy transfer
processes of drifted N_2^+ in collisions with a helium
buffer gas are observed directly using laser-induced
fluorescence. The final rotational state distribution
is measured as a function of E/N using the $X^2\Sigma_g^+ \rightarrow B^2\Sigma_u^+$,
(0-0) transitions (~3900 Å). Over the E/N range of
the experiment (0-30 Td), the rotational state distri-
bution is well characterized by a single Boltzmann
temperature corresponding to the mean center of mass
collision energy. Over the same E/N range, vibration-
al excitation is predicted to be small and indeed is
not observed. Additional experiments are now under
way to test the possibility of vibrational excitation
under different drift tube conditions with the goal of
measuring vibrational deactivation rates.

SESSION D
3:15 P.M., TUESDAY, OCTOBER 19, 1982

WORKSHOP ON CHEMICAL PROCESSES IN PLANETARY ATMOSPHERES

This workshop convenes in the honor and presence of Professor Sir David Bates, F.R.S. His imaginative foresight and pioneering studies laid the foundation of our current understanding of the basic atomic and molecular processes controlling the collisional and radiative economy of the atmospheres of the earth and neighboring planets. The session will provide an overview of the increased understanding of such fundamental atomic processes as a result of the flights of the Voyager, Mariner and Pioneer spacecrafts and the Atmospheric Explorer Mission.

CHAIRPERSON: A. DALGARNO
HARVARD UNIVERSITY

PROCESSES OBSERVED AND PROBLEMS ENCOUNTERED IN ATMOSPHERES
OF VENUS AND MARS

A. I. STEWART

UPPER ATMOSPHERE PHYSICS AND CHEMISTRY OF THE OUTER PLANETS

J. C. McCONNELL

ESCAPE OF GASES FROM PLANETARY ATMOSPHERES

M. B. McELROY

PROGRESS IN ATMOSPHERIC CHEMISTRY SINCE THE LAUNCH OF THE
ATMOSPHERE EXPLORER SATELLITES

W. B. HANSON AND E. L. BREIG

GENERAL DISCUSSION

SESSION EA
9:00 A.M., WEDNESDAY, OCTOBER 20, 1982

PHOTON INTERACTIONS

CHAIRPERSON: P. VICHARELLI
JILA/N.B.S. & UNIV. COLORADO

EA-1 Optogalvanic Spectroscopy of a Hollow Cathode Discharge R. SHUKER, A. BEN-AMAR and G. EREZ Ben-Gurion University Beer-Sheva, Israel.

Several spectroscopic applications of the optogalvanic effect in plasma discharges are discussed. This effect is utilized by us in investigating population inversion detection, two photon and optical double resonance and Penning ionization spectroscopy. We use neon to demonstrate the spectroscopic uses of the optogalvanic effect. A phenonenological model of the resulting optogalvanic signal is described which deals, in details, with the time development of the signal. The model deals with the various cases encountered in the optogalvanic effect due to transitions in neon. We have particularly investigated single step laser excitation of the 3s→sp and from the 3p manifold to higher levels in neon.

We will demonstrate experimental results of measurement of inverted population on the 3p→3s transitions.

The signal relevant to uninverted pupulation will also be shown. The results of the model are in good agreement with the experiments.

EA-2 Experimental and Theoretical Investigation of Optogalvanic Effects in the Neon Positive Column – D. Doughty and J. E. Lawler, U. of Wisconsin[*]--An experimental and theoretical investigation of the 594.5 nm optogalvanic effect in the Ne positive column is described. The effect is a decrease in discharge current (or increase in discharge voltage) due to laser induced depletion of metastable atoms. Absolute measurements of the effect per unit of absorbed laser power are reported for radius-pressure products of 0.1 cm-Torr to 1.0 cm Torr and for sustaining direct currents of 1 to 16 mA. The effect is modeled in this regime by applying perturbation theory to key rate equations.[1] The model predictions are in agreement with the experimental measurements. Associated measurements of absolute metastable densities indicate that the studied regime covers the transition from a discharge sustained primarily by single step electron impact ionization to a discharge sustained primarily by two step ionization via the $2p^53s$ metastable levels.

[1]J. E. Lawler, Phys. Rev. A 22, 1025 (1980).

EA-3 <u>Optogalvanic Effects in the Obstructed Glow Discharge</u> - J. E. Lawler and D. Doughty, <u>U. of Wisconsin</u>* --The obstructed glow discharge occurs between plane parallel electrodes at low pressure. It corresponds to operation on the "left side" of the Paschen curve where the breakdown voltage increases with decreasing pressure. We observe a 594.5 nm optogalvanic effect in a Ne discharge at 1.0 Torr with a 1.0 cm electrode spacing which is 75 times larger than the 594.5 nm effect in the Ne positive column. The effect is a laser induced depletion of metastable atoms which play an important role in electron emission from a cold cathode. Most of the discharge current at the cathode surface is carried by returning ions rather than emitted electrons, hence the cathode fall region provides a natural gain mechanism. Low electron concentrations in the cathode fall region also minimize competition between inelastic electron collisions and laser photons. The absolute size of a steady state optogalvanic effect is characterized by a dimensionless ratio of the change in power delivered to the load resistor over the absorbed laser power. Ratios of -400 are observed in obstructed glow discharges. Application of the effects in opening switch technology are discussed.

EA-4 <u>Multiphoton Ionization in Xenon and Xenon-Nitrogen Mixtures</u>-S.K. DHALI and P.F. WILLIAMS, <u>Texas Tech</u>*-- We studied the multiphoton ionization (MPI) process in xenon and xenon-nitrogen mixtures in order to use it as a controlled source of charge in other experiments on fast breakdown of under-volted spark gaps. We investigated extensively the MPI process in xenon involving a three-photon transition from the ground state to a 5d level followed by a saturated, one-photon, ionizing transition. In all regions we find MPI to be a clean and relatively convenient source of free charge for studies of charge motion in electric fields. In studies of ionization strength as a function of laser power, we find three distinct regions. At the lowest powers, ionization varies as the cube of the laser power. Starting at a power of ~3Kw corresponding to a total charge production of ~10^8 electrons, the dependence becomes approximately quadratic, due to the onset of space-charge effects. Finally, at higher powers (~30Kw) corresponding to a total charge production of ~10^{10} electrons the dependence becomes roughly linear. We believe this final saturation effect to be due to the complete ionization of the xenon atoms in the focal volume of the laser.

EA-5 <u>Photodetachment as a Control Mechanism for Dif-</u>
<u>fuse Discharge Switches</u>-G. SCHAEFER, P.F. WILLIAMS, and
K.H. SCHOENBACH, <u>Texas Tech</u>* and J. MOSELEY, <u>Univ. of</u>
<u>Oregon</u>--We report the results of experiments designed to
test the suitability of photodetachment of negative ions
as an optical control of diffuse discharges, with appli-
cations to optically-controlled switches. We observed
significant effects on $He-O_2$ and $Ar-O_2$ glow discharges
and flowing afterglows caused by photodetachment of 0^-
with a moderate power, pulsed dye laser. The dependence
of the photodetachment signal on laser wavelength and
laser fluence are consistent with the known photodetach-
ment cross section of 0^-. We found that the voltage
across the discharge (excluding cathode and anode falls)
could be substantially decreased (50%) with laser fluence
above a moderate threshold. The results support the
optical control concept for diffuse discharge switches.

EA-6 <u>Laser Irradiation of Sodium Vapor: Comparison</u>
<u>of Pulsed and cw Experiments.</u> V.S. KUSHAWAHA, W.P.
GARVER, C.E. BURKHARDT, and J.J. LEVENTHAL, <u>U. of MO-</u>
<u>St. Louis</u>--Effects produced by cw and pulsed dye laser
irradiation of Sodium vapor have been investigated at
low density ($\sim 10^{13}$ atom cm^{-3} and 10^{11} dimer/cm^{-3}).
Strikingly different results were obtained. For
example, pulsed laser light at 6000Å produces Na_2^+ ions
and D-line radiation, however, neither are detected with
6000Å cw laser light. The ions probably result from
resonance enhanced 3-photon ionization of Na_2, while the
D-line is indicative of $Na_2(A)/Na(3s)$ excitation
transfer. These observations illustrate the difficulty
in comparing results of experiments using cw and pulsed
lasers.

EA-7 Branching Ratio Measurements Relevant to the Interpretation of Voyager Euv Spectra - M. D. MORRISON and A. J. CUNNINGHAM, Univ. of Texas at Dallas.--The results of a new application of the branching ratio method[3] in the determination of transition probabilities of ionized sulfur and oxygen emissions are presented. The relevant emissions were excited in a hollow cathode discharge lamp containing SO_2, H_2S or O_2. Singly and doubly ionized sulfur emissions and singly ionized atomic oxygen emissions were dispersed using a vacuum ultraviolet spectrometer capable of $0.5A°$ resolution throughout the interval $500-1800A°$. Branching ratios were obtained through measurements of the photon intensities of transitions orginating from common upper levels. The present measurements for SII and SIII suggest the need for a reevaluation of models of the radiative economy of the Io torus.

SESSION EB
9:00 A.M., WEDNESDAY, OCTOBER 20, 1982

BASIC PROCESSES IN HgBr LASERS

CHAIRPERSON: J. J. EWING
               MATH SCIENCES NORTHWEST

EB-1 Dissociative Excitation of $HgBr_2$ by Low Energy Electron Impact. *J.R. TWIST, M.L. LAKE, Universal Energy Systems, Inc., Dayton, Ohio, D.C. Vansickle--The optical excitation function for dissociative excitation of $HgBr_2$ to the $B^2\Sigma^+$ state of HgBr by electron impact has been measured by observing the fluorescence produced by the transition $HgBr(B^2\Sigma^+) \rightarrow HgBr(X^2\Sigma)$ at 502 nm. The pressure of the $HgBr_2$ sample was 0.5 millitorr and the temperature was $350^\circ K$. Radiation near 502 nm ($\Delta\lambda = 0.8$ nm) from the decay of the $HgBr(B^2\Sigma^+)$ state is recorded over the range of electron energies from near zero to 50eV. The excitation function exhibits a steep slope above threshold. The peak above the 6.4eV threshold is located at 8.5eV. The optical excitation function exhibits several oscillations from electron energies of 8.5 to 50eV. These oscillations may be caused by cascades from states having thresholds above the $B^2\Sigma^+$ state of HgBr.

EB-2 HgBr*(B) Production by Electron Impact on $HgBr_2$ †
C. L. CHEN and P. J. CHANTRY, Westinghouse R&D Center.--
A magnetically collimated electron beam (1-200eV) crossed by a molecular beam of $HgBr_2$ has been used to measure the cross section for HgBr*(B) production from $HgBr_2$. The apparatus permits simultaneous measurements of negative ion, positive ion, and wavelength resolved photon production from $HgBr_2$, and from permanent bottled gases. The relative wavelength dependence of the photon counting system has been determined from 280 to 640 nm using standard lamps. By comparison with known ionization and total emission cross sections in He it is possible to measure total emission cross sections for other molecules whose ionization cross sections are known. The HgBr*(B) emission extends from 510 nm to beyond 350 nm, and appropriate integration over wavelength is necessary. The resulting cross section has a sharp onset at 6.0 eV and rises rapidly to a plateau with a mean value of 3.2 (-16) cm^2. In the region (3-5 eV) of dissociative attachment HgBr*(B) production is undetectable, corresponding to $\sigma < 1$ (-18) cm^2.

EB-3 Pseudo-Optical Absorption Spectra in $H_gC\ell_2$ and H_gBr_2 from 4 to 14 eV. — DAVID SPENCE, R.-G. WANG, and M.A. DILLON, Argonne Natl. Lab.[*]—Using a high-resolution electron-impact spectrometer we have obtained electron energy loss spectra of electrons scattered in the forward direction from $H_gC\ell_2$ and H_gBr_2, for incident electron energies of 200 eV. Under these experimental conditions, the energy-loss spectra correspond closely to optical absorption spectra. In addition to the well known $^1\Pi_u$ and $^1\Sigma_u$ absorption bands we observe many new energy loss processes beginning at 7.9 eV in H_gBr_2 and 8.60 eV in $H_gC\ell_2$. The relative cross sections and energies of these energy loss processes are in excellent agreement with those predicted by Nighan and Brown[1] as being necessary to account for discharge and flourescence measurements in e-beam sustained mercuric bromide lasers. On heating $H_gC\ell_2$ to about 200°C, we observe many additional strong lines, which we attribute to the presence of $H_gC\ell$ in our target beam.

EB-4 Total Quenching Cross Sections of Metastable Atoms and Molecules by HgBr2[*]--J. L. DANIELS and L. D. SCHEARER, University of Missouri-Rolla--The total quenching cross sections of thermal beams of Ar, He, and N_2 metastables by HgBr2 have been measured. The metastable beam is passed through a stainless steel cell containing a saturated vapor of HgBr2. The attenuation of the metastable beam intensity as a function of the HgBr2 number density provides the total quenching cross section. The beam energies range between 45 and 66 meV. Cross sections on the order of 10^{-15} to 10^{-16} cm^2 are obtained.

EB-5 Relative Fluorescence Efficiencies for Mercury-Halide Vapors Excited by Collisions with $N_2(A^3\Sigma)$.*-
L. D. Schearer-University of Missouri-Rolla.--Using a fast flowing afterglow in nitrogen we have determined the relative fluorescence efficiencies of $HgX(B^2\Sigma)$ produced in energy transfer collisions with nitrogen metastable $(A^3\Sigma)$ molecules where X is Cl, Br, or I. Nitrogen gas from an expanding nozzle is excited by a weak (<5 watts) microwave discharge at the entrance to the reaction region. A heated pyrex chamber is the source of the HgX vapor. We observe the emission spectra of the three species under identical conditions. Assuming that there is no significant collisional quenching of the emitting states we obtain:

Species	Peak	Integrated Flux
HgCl	558 nm	1.0
HgBr	503 nm	8.3
HgI	443 nm	10.3

EB-6 Reanalysis of the B →X Transitions in the Mercury Halides - J. TELLINGHUISEN, P. C. TELLINGHUISEN, J. GAIL ASHMORE, and K.S. VISWANATHAN, Vanderbilt*-- The $B(^2\Sigma^+) \rightarrow X(^2\Sigma^+)$ transitions of HgI, HgBr, and HgCl are reanalyzed from spectra obtained using Tesla discharge sources containing the single isotopic species, $^{200}Hg^{127}I$, $^{200}Hg^{129}I$, $^{200}Hg^{79}Br$, $^{200}Hg^{81}Br$, $^{200}Hg^{35}Cl$, and $^{200}Hg^{37}Cl$. The results corroborate the earlier work of Wieland qualitatively but not quantitatively, in that the assignments deviate from his for high v'' levels, leading to significantly lower estimates of the X state dissociation energies in all three molecules. For HgI the isotope effect indicates that the v'' numbering should be decreased by one unit. Franck-Condon calculations yield ΔR_e values which are larger than reported previously; correspondingly the Franck-Condon distributions are altered significantly. Preliminary rotational analyses for HgCl and HgBr indicate R_e' values of ~3.00 and 3.056 Å, respectively, both close to recent theoretical estimates.

SESSION FA
10:45 A.M., WEDNESDAY, OCTOBER 20, 1982

ELECTRON COLLISIONS

CHAIRPERSON: J. N. BARDSLEY
UNIVERSITY OF PITTSBURGH

FA-1 CALCULATION OF ELECTRON EXCITATION CROSS-SECTION OF 3P STATE OF SODIUM. Z. Azar and R. Shuker, <u>Physics Department, Ben-Gurion University of the Negev Beer-Sheva, ISRAEL</u>.

The electron-excitation cross-section of the 3P state of sodium has been calculated at several incident electron energies between 2.5 and 250 eV by two state 3S-3P close coupling method without core and exchange. We use approximate atomic wave functions that enable us to extend the range of calculation to the high energy range.

The calculated theoretical cross section is in good agreement with recent experimental results.

It converges to the Born cross section in the high energy range, and it is in very good agreement with detailed four states close coupling calculation including core and exchange by Moores and Norcross in the low energy range that they calculated. In the intermediate energy range our results are close to those obtained by Korff et. al. using two and seven state close coupling calculation.

FA-2 Electron-Impact Excitation of the Xenon Atom.* – J. E. GASTINEAU, F. A. SHARPTON, L. W. ANDERSON, and CHUN C. LIN, <u>Univ. of Wisconsin-Madison</u>.--Absolute optical cross sections for some 100 emission lines of the xenon atom produced by electron-impact excitation have been measured from threshold to 100 eV. From these optical data, direct excitation cross sections have been determined for all ten 2p levels (of the $5p^56p$ configuration). The peak direct excitation cross sections of the ten 2p levels, in the order of $2p_1$ to $2p_{10}$, are 5.7, 2.1, 6.0, 2.8, 23, 13, 13, 57, 43, 50, in units of 10^{-18} cm^2. Using the technique of laser-induced fluorescence,[1] we have measured the electron-impact excitation cross sections of the metastable $1s_3$ level ($5p^56s$, J=0). The excitation function of the $1s_3$ level shows a sharp maximum and the peak direct excitation cross section is 7.5 x 10^{-18} cm^2.

1. M. H. Phillips, L. W. Anderson, and C. C. Lin, Phys. Rev. A <u>23</u>, 2751 (1981).

FA-3 Rotational Transitions in the Ionization-Excitation of Cold N_2 Beams by Electron Impact - J.P. DOERING, S. HERNANDEZ, and P.J. DAGDIGIAN, Johns Hopkins U.*--N_2^+ first negative system emissions excited by 60-1500 eV electron impact on cold (<10K), supersonic N_2 beams have been measured with high spectral resolution. Excited N_2^+ B state rotational populations have been calculated from the spectra and used to derive the original N_2 ground state populations. The N_2 rotational state population in the beam is found to be non-Boltzmann with a large population in the first few rotational states and a long tail to high J. Changes in the excited state rotational populations as the electron energy is lowered show that the electric dipole rotational selection rule ($|\Delta J| = 1$) which is valid for 1500 eV electrons breaks down at electron energies below 800 eV.

FA-4 Electron-Impact Excitation of the $D^3\Sigma_u^+$ State of the Nitrogen Molecule.* - A. R. FILIPPELLI, S. CHUNG, CHUN C. LIN, Univ. of Wisconsin-Madison, and EDWARD T. P. LEE, Air Force Geophysics Laboratory--Absolute optical emission cross sections have been measured for the $D^3\Sigma_u^+ \to B^3\Pi_g$ Fourth Positive band system of the nitrogen molecule excited by controlled electron impact on ground-state N_2 molecules. Polarization of the optical emission was found to be less than 3%. The branching ratios determined for the seven bands studied [$D^3\Sigma_u^+$(v'=0) $\to$ $B^3\Pi_g$(v"=0,1,2,3,4,5,6)] were 0.19, 0.27, 0.29, 0.13, 0.08, 0.03, and 0.01 respectively. The sum of the measured optical emission cross sections gives an apparent cross section for electron-impact excitation of the v'=0 level of the $D^3\Sigma_u^+$ state of 1.4 x 10^{-19} cm^2 at maximum. The excitation functions of all seven bands studied show a principal maximum at 15.7 eV and a secondary maximum at 25 eV. The shape of the optical emission excitation functions will be discussed.

FA-5 Production of Atomic Oxygen Emission by Electron-Impact Dissociation of O_2.[*] – F. A. SHARPTON[†], M. R. PEDERSON, A. R. FILIPPELLI, L. W. ANDERSON, CHUN C. LIN, U. of Wisconsin-Madison, and R. E. MURPHY, Air Force Geophysics Laboratory.--Production of excited oxygen atoms in the $2p^33p$, $2p^35s$, and $2p^3nd$ configurations has been observed in an experiment with an electron beam passing through oxygen molecules. Optical cross sections for the emission lines of the excited oxygen atoms (e.g., $3p\ ^3P \rightarrow 3s\ ^3S$, $4d\ ^5D \rightarrow 3p\ ^5P$, etc.) have been measured for incident electron energies from threshold to 500 eV. The excitation functions exhibit a broad maximum at about 90 eV with a slight shoulder near 35 eV. This shoulder structure is similar to but less prominent than the corresponding case of electron-impact dissociation of N_2. The peak optical cross section for the $3p\ ^5P \rightarrow 3s\ ^5S$ emission is $3.6 \times 10^{-18} cm^2$.

SESSION FB
10:45 A.M., WEDNESDAY, OCTOBER 20, 1982

MODELING OF HgBr LASERS

CHAIRPERSON: W. H. LONG
NORTHROP RESEARCH

FB-1 Mercury Bromide Kinetic Model,* L.J. PALUMBO, R.L. TAYLOR and H.L. CHEN, Research & Laser Technology, Inc.--The kinetics of the HgBr laser have been analyzed with a detailed computer model which considers all relevant electron and heavy particle reactions. Comparisons with experimental data provided model verification and indicated the principal mechanisms affecting laser performance and long duration, unattended operation. Agreement between calculations and experiments supports the hypothesis that the only significant upper laser level formation channel is direct electron-impact dissociation of $HgBr_2$. Laser energy extraction is limited by bottlenecking of $HgBr(X, v \approx 22)$ and by absorption by $HgBr(X)$; both effects increase with pulse duration and volumetric laser power. The discharge modeling points out the need for further studies of electron production and loss mechanisms and of other processes affecting the electron energy distribution function. Several potential issues relevant to long-term operation have been identified. These analyses generally support the belief that an efficient HgBr laser can be developed for application to blue-green optical communications.

FB-2 HgBr(B→X)/$HgBr_2$ Laser Kinetics* - W.L. NIGHAN, R.T. BROWN, J.J. HINCHEN, and W.J. WIEGAND - United Technologies Research Center, East Hartford, CT - An investigation of fundamental kinetic processes influencing discharge and laser properties of the 502 nm HgBr(B→X)/$HgBr_2$ dissociation laser has been carried out. Experimental results obtained using both an electron swarm apparatus[1] and an e-beam controlled discharge[2] will be presented for several gas mixtures. A set of electron-$HgBr_2$ cross sections for vibrational and electronic excitation has been inferred on the basis of interpretation and analysis of the experimental data. These cross sections will be discussed along with the effect of electron-electron collisions on laser medium properties.

1. W.L. Nighan, J.J. Hinchen and W.J. Wiegand, J. Chem. Phys. (Oct. 1982, in press).
2. W.L. Nighan and R.T. Brown, J. Appl. Phys. (Nov. 1982 in press).

FB-3 Electron Kinetics Analysis for HgBr Lasers Using a Measured B State Excitation Cross Section, L. E. KLINE, C. L. CHEN, P. J. CHANTRY and L. J. DENES, Westinghouse R&D -- Electron kinetics analysis of the HgBr laser has been hindered by a lack of cross section data. We have used our recent measurements of the cross section for electron impact excitation of the HgBr blue-green fluorescence to make a new analysis of the electron kinetics of the HgBr laser. The measured cross section has a threshold at 6 eV and rises to a plateau value of 3.2 $\mathring{A}^2$ above 9 eV. We have assumed two additional electronic processes with thresholds at 5 eV and 7.9 eV as in previous analyses. When previous cross section estimates for these processes are used in the analysis the predicted peak HgBr B state formation efficiency in an Ar-0.8%HgBr$_2$ mixture is 26% which is much higher than the measured formation efficiency of 5%. Predicted values of formation efficiency in approximate agreement with experiment can be obtained by using step function 5 eV cross section with a value of 3 $\mathring{A}^2$. Predicted values of the sum of the ionization and attachment coefficients which agree with experiment can be obtained by using a step function 7.9 eV cross section with a value of 10 $\mathring{A}^2$.

FB-4 Electron Cross Sections for Neon in the Range 7 to 100 eV., L. E. KLINE, Westinghouse R&D -- Neon is widely used as a buffer gas in discharge-pumped rare gas-halide and metal-halide lasers. A consistent set of collision cross sections has been determined for neon in the electron energy range 7 to 100 eV by analyzing available electron collision cross section and transport data. When these cross sections are used to predict values of the drift velocity, longitudinal diffusion coefficient, and ionization coefficient for electrons in neon the predicted values agree well with available experimental data in the E/N range 10 to 300 Td. The momentum transfer cross section reported here is about twice as large, for energies above 20 eV, as a neon momentum transfer cross section which has been used in several analyses of XeCl and HgBr lasers. This smaller momentum transfer cross section results in 30-50% overestimates of the electron drift velocity and 20-30% overestimates of the ionization coefficient in the E/N range studied here. However, the predicted electron transport and laser pumping behavior for HgBr laser mixtures containing 0.1 to 0.8% HgBr$_2$ in neon are the same to within a few percent for both neon momentum transfer cross sections.

SESSION G
1:30 P.M., WEDNESDAY, OCTOBER 20, 1982

DISTRIBUTION FUNCTIONS AND ELECTRON TRANSPORT

CHAIRPERSON: W. F. BAILEY
AIR FORCE INSTITUTE OF TECHNOLOGY

G-1 Electron Multiplication in Gases: The Stochastic Ionization Coefficient and the E/N Limit of the Townsend Ionization Coefficient*-E.E. KUNHARDT, Y. TZENG, and J. P. BOEUF, Texas Tech U.--Using Monte Carlo methods, we have done an extensive investigation of avalanche development in helium and nitrogen over a wide range of E/N. We have obtained avalanche size distribution, $P(n,x)$, and the energy distribution of electrons $f(v,x,n)$. From this we have determined a limit of validity for the Townsend ionization coefficient, α_T, and obtained the stochastic ionization coefficient, $\alpha(n,x)$ (i.e. the ionization probability per unit distance for an electron in an avalanche of size n). At high E/N, $\alpha(n,x)$ is found to have a maximum as a function of n. This occurs when some electrons can acquire energy above that corresponding to the maximum in the ionization crossection. The probability for small size avalanches increases and the non-equilibrium region of an avalanche is no longer finite. The value of E/N is 300 Td for helium and 1750 Td for nitrogen. We will discuss the behavior of $P(n,x)$ and $\alpha(n,x)$, with E/N as a parameter, with reference to the collisional processes in the gas. In light of this study, the range of usefulness of the Townsend ionization coefficient α_T, will be discussed.
*Work supported by ONR under contract #N00014-81-0655.

G-2 Non-equilibrium Development of an Electron Swarm in Nitrogen: A Monte Carlo Study with Statistical Enhancement for High Energy Electrons*-Y. TZENG and E.E. KUNHARDT, Texas Tech U.--The temporal and spatial evolution of electron swarms between two infinite parallel plates have been studied for E/N values ranging from 300 Td to 3000 Td using Monte Carlo simulations. A renormalization and weighting technique has been developed to enhance the resolution in the high energy tail where the visitation frequency is low. With this method we have investigated the response of the electron velocity distribution, ionization rate and drift velocity, to temporal variations of the applied uniform electric field. We have also studied the effect on the above swarm properties and their spatial characteristics of four different ways of partitioning the energy among the two electrons after an ionization event. Significant differences have been observed in the velocity distribution and the spatial characteristics of the swarm, especially at the high E/N. From these temporal and spatial characteristics of swarms run-away electrons have been observed at E/N values higher than 1500.

*Work Supported by ONR under Contract #N00014-81-K-0655.

G-3   The Effects of Space Charge on Avalanche Development: A Self-consistent Microscopic Study Using Monte Carlo Technique*–Y. TZENG and E.E. KUNHARDT, Texas Tech U.--We present the simulation results of the evolution of avalanches initiated by an electron pulse on the cathode under the action of both space charge induced and externally applied electric field. A self-consistent treatment of the evolution has been achieved using Monte Carlo methods to simulate the electron kinetics and a two dimensional (cylindrical symmetry) Poisson solver to compute the space charge field. With this method, we have investigated the temporal and spatial characteristics of electron energy distribution in the avalanche and the transport coefficients. All avalanche characteristics, i.e. average energy, diffusion coefficients, drift velocity and ionization rate, have been observed to change significantly with increasing space charge. The electron energy distribution is highly space dependent. There is no equilibrium under this condition.

G-4   Nonlocal Boltzmann Code for Electron-Beam-Generated Plasma Channels,* S. S. YU and R. E. MELENDEZ, Lawrence Livermore Nat'l. Lab. —— A time-dependent nonlocal Boltzmann code (NUTS) has been constructed to study the evolution of plasma channels created by an intense electron beam passing through a gaseous medium. The code is based on a two-term expansion of the Boltzmann Equation. Two independent vector components are retained to allow for current flow in both the axial and the radial directions. All inertial, spatial, electric and magnetic terms as well as effects of atomic collisions are included. Time-dependent electromagnetic fields are calculated self-consistently from the evolving plasma currents. Code results and comparisons with experimental data from the LLNL Experimental Test Accelerator (ETA) will be presented.

G-5 Electron Conductivity in a Rapidly Increasing Electric Field - J. N. BARDSLEY and B. M. PENETRANTE, U. of Pittsburgh* -- During the opening stage of a diffuse discharge switch the electric field is expected to grow rapidly, with E/N increasing from below 10 Td to over 100 Td. To prevent breakdown, the gas must contain molecules which absorb momentum, thereby reducing the transfer of power from the field to the electrons, absorb energy and attach electrons. Monte Carlo simulations are performed for gas mixtures of N_2 and N_2O with time scales between 10^{-9}s and 10^{-7}s. The calculated attachment probabilities are compared with the results of adiabatic calculations in which rates appropriate to the instantaneous value of E/N are integrated over time.

G-6 Electron Energy Distributions in Microwave Discharges - J. N. BARDSLEY and R. CHAKRABARTI, U. of Pittsburgh* -- The behavior of electrons under the influence of high-frequency AC fields is studied, using the theory of Margenau[1], for gas mixtures containing small fractions of molecular gases such as H_2, NO, O_2, CO, CO_2, H_2O and NH_3 in rare gas buffers. The energy distribution and effective temperature are calculated as a function of the strength of the microwave field. With argon as a buffer, the presence of the Ramsauer-Townsend minimum in the momentum transfer cross section leads to a bottleneck in the electron energy distribution. The presence of only a few parts per million of these molecular gases can have a significant effect on the average energy of electrons in Ar.

1. H. Margenau, Phys. Rev. 69, 508 (1946); 73, 297 (1948).

G-7 Effects of Various Secondary Electron Energy Distributions on Electron Transport in N_2 - S. YOSHIDA and A.V. PHELPS,[*]--JILA, U. of Colorado and NBS, and L.C. PITCHFORD,[+] Sandia Nat'l. Labs.--The Boltzmann equation solution of Brunet and Vincent[1] is extended and used to investigate the effects of changes in the distribution in energy of the electrons produced by ionization at high E/n in N_2. For example, at $E/n = 1500 \times 10^{-21}$ Vm^2 the rate coefficient for ionization, the electron drift velocity and the ratio of the diffusion coefficient to the mobility D/μ decrease and the mean electron energy increases as the mean energy of the secondary electrons is increased. The electron energy distributions $f(\varepsilon)$ decrease slowly with energy ε above 200 eV and the effective electron temperature at these energies decreases as the mean energy of the scattered electrons decreases.

[1]H. Brunet and P. Vincent, J. Appl. Phys. 5-, 4700 and 4708 (1979).

G-8 Cross-Section Data for High Mobility Gases - A. GARSCADDEN and G. L. DUKE, AFWAL/POOC, Wright-Patterson AFB, Ohio, 45433 -- A number of gases or gas mixtures display high electron conductivity when a large inelastic cross-section exists near the onset of a rapidly increasing momentum transfer cross-section. The usual two-term Legendre expansion for calculation of the electron energy distribution function that has been applied to derive, these cross-sections iteratively, does not include the influence of inelastic collisions on f_1. This has led to sets of cross-sections and transport properties that are self-consistent but incorrect. Thus they cannot be used to derive collisional data for significantly different gas mixtures or different excitation conditions. The high conductivity gases are especially subject to this effect. New calculations, allowing for inelastic collisions on f_1, are compared with the previous works. Methane, which is a candidate switching gas, is taken as an example. It is demonstrated that the momentum transfer cross-section must be adjusted down by a factor of approximately two near the Ramsauer minimum. An ~8% increase in the vibrational cross-section is also required to predict measured transport properties.

G-9   Transport Coefficients and Collisional Cross Sections of SF_6 - J.P. NOVAK and M. FRECHETTE, IREQ, Varennes, Québec, Canada -- The Boltzmann equation method has been used to reevaluate the transport coefficients of SF_6 on the basis of revised collisional cross sections, in particular: the plateau value of the momentum transfer cross section, 2×10^{-15} cm^2, and the pronounced minimum at about 1eV; SF_6^- attachment cross s. according to Chutjian;[1] and the excitation cross s. based on data of Trajmar and Chutjian.[2] The calculated diffusion coefficient agreed well with experimental values but the calculated drift velocity proved to be about 20% lower. Fitting of the ionisation coefficient was used to determine the profiles of the excitation cross sections. The largest difference (about 30% for the reduced fields between 30 and 170 Vcm^{-1} torr^{-1}) was observed for the attachment coefficient. Good agreement has been achieved by reducing the width of the SF_6^- cross section to about 30% and by increasing the higher energy attachment cross sections (except SF_5^-) to about 130%.

[1] A. Chutjian, Phys. Rev. Lett. 46, 1511 (1981).

[2] S. Trajmar and A. Chutjian, J. Phys. B 10, 2943 (1977).

SESSION H
3:15 P.M., WEDNESDAY, OCTOBER 20, 1982

WORKSHOP ON ATOMIC AND MOLECULAR COLLISION PROCESSES
IN DENSE PLASMAS

This workshop will focus on fundamental atomic and molecular processes, such as ion-ion recombination, electron-ion recombination, ion-molecule reactions, bimolecular and termolecular charge transfer and Penning ionization, occurring in plasmas formed in high pressure gases. Theory, experiment and computer simulation of such processes will be discussed. Ample time has been provided for general discussion of these topics.

CHAIRPERSON: M. R. FLANNERY
GEORGIA INSTITUTE OF TECHNOLOGY

ION-ION RECOMBINATION AND RELATED PROCESSES
                    D. R. Bates

MEASUREMENT AND MODELLING OF ION-MOLECULE REACTIONS
AT ATMOSPHERIC PRESSURE
                    C. B. Collins and F. W. Lee

KINETIC PROCESSES IN DENSE HELIUM-NITROGEN AND HELIUM-
HYDROGEN PLASMAS
                    J. Stevefelt

COMPUTER EXPERIMENTS AND RECOMBINATION THEORY
                    W. L. Morgan

GENERAL DISCUSSION

SESSION IA
7:15 P.M., WEDNESDAY, OCTOBER 20, 1982

POSTER SESSION

IA-1 Negative Ion Concentrations, Electron Energy Distributions, and Vibrational Population Distributions in Hydrogen Discharges*. J.R. HISKES and A.M. KARO, Lawrence Livermore National Laboratory--The formation and destruction processes leading to the equilibrium negative ion concentrations in hydrogen discharges are discussed for discharge densities in the range 10^8 to 10^{13} electrons cm^{-3}. Analytic expressions are developed for the high energy portion of the electron energy distribution. Three electronic excitation processes predominate: excitation through the H_2^- resonances, singlet excitations, and triplet excitations through the $c^3\pi_u$ state. At low densities, the vibrational distribution arises from these electronic excitations in equilibrium with wall de-excitation processes. Vibrational relaxation via wall collisions are discussed in the context of molecular dynamics methods. At high densities singlet excitations predominate in equilibrium with atom-molecule exchange de-excitation processes. Negative ion generation is discussed for a two-chamber tandem system in which vibrational excitation occurs in a high power, high temperature discharge chamber, $kT_e = 5$ eV, and dissociative attachment occurs in a low temperature, 1 eV, plasma chamber.

IA-2 Electron Temperature Dependence of the Recombination of Electrons with H_3^+ and H_5^+ Ions - J. A. MACDONALD, M. A. BIONDI and R. JOHNSEN, U. of Pittsburgh* -- Dissociative recombination involving the trimer ion H_3^+ is a very efficient electron removal process which affects the ionization level in the upper atmospheres of the outer planets. Also, the thermalization of the neutral products of this reaction may play a role in determining the temperature of dense interstellar clouds. We have studied the dissociative recombination of H_3^+ and H_5^+ ions with electrons in an admixture of H_2 and neon using a low-temperature, microwave afterglow-mass spectrometer apparatus employing microwave heating. In 20 Torr of neon with $\sim$ 1 mTorr of H_2, the measured recombination coefficient $\alpha(H_3^+)$ does not show a simple power-law dependence on electron temperature. At T = 265K, $\alpha(H_3^+) = (2.0 \pm 0.3) \times 10^{-7}(T_e/300)^{-0.88}$ cm^3/sec for 400 K $\leq T_e \leq$ 4000 K. However, over the range 265 K $\leq T_e \leq$ 400 K, $\alpha(H_3^+) \sim 1.5 \times 10^{-6}$ cm^3/sec, independent of T_e. In similar admixtures of H_2 and neon at 128 K, H_5^+ ions dominate the afterglow ion mass spectrum. We find $\alpha(H_5^+) = (1.8 \pm 0.2) \times 10^{-6} (T_e/300)^{-0.69}$ cm^3/sec, valid over the range 128 K $\leq T_e \leq$ 4000 K.

IA-3 <u>Basic Microscopic Theory of Ion-Ion Recombination</u> - M. R. FLANNERY and E. J. MANSKY, <u>Georgia Institute of Technology</u>*--The basic coupled integro-differential equations[1] for the distribution $\rho(E,R)$ of ion pairs in both internal energy E and internal separation R are solved as a function of gas density N. At low N, energy transfers, via collision with the gas, are very slow in comparison to orbital motion so that equilibrium in R is established. As N is increased energy transfer and orbital motion are coupled. For all N, changes of internal angular momentum L of the ion pair occur very rapidly in comparison to E and R changes such that equilibrium in L is instantaneously established. The recombination rate α versus N is determined from $\rho(E,R)$ for the cases of symmetrical resonance charge transfer and hard-sphere ion-neutral gas collisions.

[1]M. R. Flannery, Phil. Trans. Roy. Soc. A <u>304</u>, 447 (1982).

IA-4 <u>Ultraviolet Photodissociation of Rare Gas Dimer</u> Ions (Xe_2^+, Kr_2^+)*- A.W. McCOWN, M.N. EDIGER, S.M. STAZAK, and J.G. EDEN, <u>U of IL</u>--An optical method for detecting rare gas dimer ions (Xe_2^+, Kr_2^+) in real time has been demonstrated by photodissociating the ion with a UV laser and by observing recombination-fed, excited state fluorescence. Initially, atomic ions are produced by multiphoton ionization using an ArF laser (193 nm : 2γ for Xe, 3γ for Kr) and for pressures greater than 100 Torr, dimerization rapidly occurs (< 1 μs). A second excimer laser is sequentially fired and photodissociation takes place, involving the $1(1/2)_u \rightarrow 2(1/2)_g$ molecular transition. This results in a suppression of the fluorescence since the species feeding the excited states is depleted, and quenching by ground state atoms is very fast (e^{-1} decay time < 1ns). The amount of fluorescence suppression depends upon the intensity of the dissociating laser. A computer model has been developed which accurately predicts the dimerization and recombination coefficients from fluorescence waveforms, and this is being used to calculate the spectral variation of the dissociation cross section. These results will be presented.

IA-5   Improved Absolute Free-Free Emission Coefficients for Electrons in Argon*-S. J. BUCKMAN and A. V. PHELPS, JILA, U. of Colorado and NBS-Through the use of improved data handling, more accurate calibrations, and measurements at wavelengths where the background is minimized we have reduced scatter and statistical uncertainties in derived excitation coefficients from $\pm15\%$ in previous measurements[1] to less than $\pm5\%$ for electric field to gas density rations E/n above 7×10^{-22} Vm^2. The estimated uncertainty in the absolute excitation coefficients is $\pm20\%$. Our free-free excitation coefficients agree to within $\pm10\%$ with values calculated using the theory of Kas'yanov and Starostin[2] and momentum transfer cross sections for electrons in argon derived from transport data. Similar agreement is obtained with Geltman's theoretical value.[3] Comparisons will be made with other theory and experiments.

1. C. Yamabe and A. V. Phelps, Bull, Am. Phys. Soc. 27, 100 (1982).
2. V. Kas'yanov and A. Starostin, Zh. Eksp. Teor. Fiz. 48, 295 (1965).
3. S. Geltman, J. Quant. Spectros. Radiat. Transfer, 13, 601 (1973).

IA-6   Transition Probability Measurements for Some Ar I 4s-4p Transitions - D.W. JONES, W.L. WIESE, and K. MUSIOL*, National Bureau of Standards.--Absolute transition probabilities for 13 lines of the Ar I 4s-4p (1s-2p in Paschen notation) transition were measured by analyzing high resolution spectra from a wall-stabilized arc. The arc source was 10 cm long and 3 mm in diameter and operated at atmospheric pressure with axial temperatures of about 13 000° K and electron densities of about 10^{17} cm^{-3}. An on-line microcomputer was used to acquire and analyze high resolution line profiles; the analysis included corrections for dark current, spectral sensitivity, self-absorption, continuum radiation, blended lines and line-wing truncations. In order to minimize the contribution of uncertainties in the temperature determination to the overall uncertainty of the transition probabilities, the relative transition probabilities measured in this experiment were normalized to an absolute scale with the aid of the precise laser-fluorescence lifetime measurements of Chang and Setser.[1]

*Present address: Jagellonian U., Krakow, Poland

[1]R.S.F. Chang and D.W. Setser, J. Chem. Phys. 69, 3885 (1978).

IA-7 <u>Kinetic Processes in Dense Helium-Hydrogen</u>
<u>Plasmas</u> - J. STEVEFELT, O. MOTRET, and A. BOUCHOULE, U.
<u>of Orléans, France.</u>-- A fast pulsed discharge (4 kA, 7
nsec, 10 Hz) was used to create an afterglow plasma with
initial electron density over 10^{15} cm^{-3} in a mixture of
hydrogen (0 - 400 mtorr) and helium (310 - 760 torr).
The afterglow radiation was emitted in He_2 transitions as
well as in atomic hydrogen spectral lines, with Lα being
particularly intense. The H(n = 1) concentration was
estimated from the profile of the self-absorbed Lα line,
indicating a significant dissociation of the hydrogen by
the discharge pulse. Destruction frequencies for
metastable 2^3S helium atoms have been determined and
analyzed in terms of rate coefficients for quenching
processes.

IA-8 <u>Reaction Rate Coefficients for C^+, CO^+, and CO_2^+</u>
<u>+ O_2.</u> -THOMAS M. MILLER,[*] RODNEY E. WETTERSKOG,[*] and JOHN
F. PAULSON, <u>Air Force Geophysics Laboratory</u>--Rate coef-
ficients have been measured for C^+, CO^+, and CO_2^+ ions
reacting with O_2 over the temperature range 90-300 K.
Charge transfer is the only reaction channel observed
except for $C^+ + O_2$ which yields O^+ and CO^+ products. The
reaction rate coefficients agree with the measurements
of others at 300 K. The $C^+ + O_2$ rate coefficient is rela-
tively independent of temperature for 90-300 K. The
rate coefficients for $CO^+ + O_2$ and $CO_2^+ + O_2$ decrease with
increasing temperature, by factors of 0.6 and 0.3, re-
spectively, between 90-300 K. A variable-temperature
selected-ion flow-tube (SIFT) apparatus was used in this
work. We will discuss evidence for a shock effect as-
sociated with the SIFT helium injector, which fits the
description given by Dupeyrat et al.[1]

[*]Permanent address: Dept. of Physics and Astronomy,
Univ. of Oklahoma, Norman, OK 73019.
[1]G. Dupeyrat, B. R. Rowe, D. W. Fahey, and D. L.
Albritton, Int. J. Mass Spectrom. Ion Phys. (in press).

**IA-9   Temperature Dependence of 3-Body Association
Reactions of Ions in Nitrogen** – S. DHEANDHANOO,
R. JOHNSEN, and M. A. BIONDI, U. of Pittsburgh[*] — Rate
coefficients for the association of N^+, N_2^+, O_2^+, and NO^+
ions in nitrogen have been measured as a function of gas
temperature in a drift tube–mass spectrometer apparatus.
The following results were obtained:

reaction	rate coeff. (cm^6/sec)
$N^+ + 2N_2 \rightarrow N_3^+ + N_2$	$2.0 \times 10^{-29}(T/300)^{-2.0}$
$N_2^+ + 2N_2 \rightarrow N_4^+ + N_2$	$5.0 \times 10^{-29}(T/300)^{-2.2}$
$O_2^+ + 2N_2 \rightarrow O_2^+ \cdot N_2 + N_2$	$1.0 \times 10^{-30}(T/300)^{-3.2}$
$NO^+ + 2N_2 \rightarrow NO^+ \cdot N_2 + N_2$	$3.0 \times 10^{-31}(T/300)^{-4.4}$

The range of temperatures covered by the experiments was
110 to 420 K for the first reaction, 120 to 480 K for
the second and 110 to 180 K for the third and fourth
reactions.

**IA-10   Kinetic Order of the He^+ to He_2^+ Conversion in
Helium** – R. JOHNSEN and M. A. BIONDI, U. of Pittsburgh[*]
— We have tried to find experimental evidence for a
4–body contribution in the conversion of He^+ to He_2^+ ions
in helium. This reaction mechanism has recently been
invoked by deVries and Oskam[1] in order to explain their
afterglow data. Our experiments, carried out in a drift
tube–mass spectrometer apparatus at pressures between
0.25 and 4.5 Torr, gave results compatible with the
3–body mechanism usually assumed for this type of
reaction. It will be shown that the 4–body effects
reported by deVries and Oskam are considerably larger
than expected on the basis of simple theoretical
considerations.

[1]C. P. deVries and H. J. Oskam, Phys. Rev. A 22, 1429
(1980).

IA-11 Prompt and Delayed Photolysis of Cs_2 and Cs_2Kr[*].
F. DAVANLOO, F. W. LEE and C. B. COLLINS, Univ. of Texas
at Dallas; A. S. NAQVI, King Saud Univ. of Riyadh.--In
this work a time-delayed, double resonance technique
was used for the study of the state selective photolysis
Cs_2 and Cs_2Kr with particular attention being placed
on the production of the fine structure components of
the 5^2D state of Cs. Not only were the prompt sources
from dissociation and predissociation of excited states
of CsKr and Cs_2Kr confirmed, but new kinetic channels
for delayed photolysis were found. Over the visible
wavelength range two delayed processes for the produc-
tion of $Cs(5^2D)$ atoms were characterized. One appeared
to involve the intermediate production of CsKr $(7p\Pi)$
and the other was tentatively identified as proceeding
through the precursor, Cs_2 $(^1\Delta u)$.

IA-12 Solar Photodetachment Rate of Atomic Anions - E.M.
Helmy, Delaware State College and S.B. Woo, Univ. of
Delaware[*] -- The solar detachment rates of all stable
atomic anions belonging to elements in the main body of
the periodic table have been calculated. Multi-channel
photodetachment effects owing to fine structure levels[1]
and temperature effects are included in the treatment.
All-told the solar detachment rates of thirty-one
anions at 300°K and 10,000°K are made available. The
rates show strong correlation to the column position in
the periodic table. The higher the column-number of the
element is the lower will be its detachment rate. Cesium
has the highest detachment rate of 82 sec^{-1}. Fluorine
has the lowest rate of 0.069 sec^{-1}. This implies that
the life time, if controlled by photodetachment, of Cs$^-$
in the ionsphere is only about 1/1,000 that of F$^-$.
Implications of this drastic difference in life time
will be discussed.

[1]W.B. Clodius, R.M. Stehman and S.B. Woo, "Extended zero
core- contribution model applied to multichannel photo-
detachment", to be published in the Jan. issue of Phys.
Rev. A, 1983.

SESSION IB
7:15 P.M., WEDNESDAY, OCTOBER 20, 1982

POSTER SESSION

IB-1 Near-Threshold Vibrational Excitation in Electron-CO_2 Collisions--A Simple Model - B. L. WHITTEN, Lawrence Livermore Natl. Lab., and N. F. LANE, Rice U.*--A simple two-state numerical model is used to illustrate the influence of strong low-energy σ_g scattering on near-threshold excitation of the different vibrational modes of CO_2. In the case of 000→100 symmetric-stretch excitation, the model provides an extrapolation of a previously-determined adiabatic-nuclei result down to threshold. For all modes, the "virtual-state" feature of the σ_g scattering gives rise to strong enhancement of the excitation cross sections just above threshold. The calculated cross sections for all modes are reasonably consistent with low energy beam and swarm measurements.

IB-2 Non-Maxwellian Electrons in a Laser Produced Sodium Plasma-W.L. MORGAN, Lawrence Livermore Nat. Lab*.-- Time dependent Boltzmann calculations of the electron energy distribution function in a laser excited Na plasma will be presented. Such non-LTE plasmas are produced in alkali metal vapor, such as in the Lucatorto and McIlrath[1] experiment, by laser irradiation of the ns-np resonance line. The electrons in such plasmas are heated by super-elastic collisions with atoms in the np state. The distribution of electrons in energy is characterized by a series of spikes at energies separated by $\Delta\epsilon=\epsilon(np)-\epsilon(ns)$. This feature had been suggested by Morgan, et al.[2] and has recently been observed in the laboratory by Le Gouët, et al.[3]

[1]T.B. Lucatorto and T.J. McIlrath, Phys. Rev. Letts. 37, 428 (1976).
[2]W.L. Morgan, R.D. Franklin, and R.A. Haas, Appl. Phys. Letts. 38, 1 (1981).
[3]J.L. Le Gouët, J.L. Picqué, et. al., Phys. Rev. Letts. 48, 600 (1982).

IB-3 Electron Impact Collision Strengths for Excitation from the 2p Levels to All Levels with n = 3, 4 and 5 in He-like Ions – D. H. SAMPSON and S. J. GOETT, Penn State Univ*., R. E. H. CLARK, Los Alamos Nat. Lab. – A Coulomb-Born-Exchange Method that is well suited for treating many members of an isoelectronic sequence simultaneously has been used to calculate electron impact collision strengths for all transitions of the kind $1s2p\,^{2S+1}P_J$ – $1sn'\ell'\,^{2S+1}L'_J$, with n' = 3,4 and 5 in 20 different He-like ions with nuclear charge number Z $\geq$ 4. For each transition the calculations have been made for the 9 impact electron energies in threshold units ε = 1.0, 1.2, 1.5, 1.9, 2.5, 4.0, 6.0, 10.0 and 15.0. The results have been fitted to simple functions of the impact electron energy that are readily integrated over a Maxwellian to obtain collision rates. The parameters for obtaining collision strengths and rates for excitation from the $1s^2\,^1S_0$ and $1s2s\,^{2S+1}S_J$ levels to all levels with higher n values $\leq$ 5 are also given. The calculated collision strengths include the effects of intermediate coupling, but do not include the effects of resonances.

IB-4 Electron Collisional Excitation of Na 3P Atoms to the 3D State – B. STUMPF and A. GALLAGHER,* JILA, Univ. of Colo. & NBS--The cross section Q for electron collisional excitation of Na(3P) J=3/2, M_J=3/2 atoms to the 3D state has been measured for electron energies from threshold (1.5 eV) to 1500 eV. The expected high-energy behavior QE $\cong$ A+B log E is observed above ~50 eV and is used to normalize the data to the Born cross section at high energies. Polarization measurements are under way to correct these Q_{90} to total cross sections and to obtain additional details regarding M_L dependences of the cross section. The cross section is observed to rise very abruptly at threshold, essentially within our electron energy resolution of 0.3 eV, to an approximately constant value, then decrease gradually above ~20 eV. The 3S→3D excitation, on the other hand, is observed to rise much more gradually above threshold. This abrupt onset for 3P-3D is reminiscent of H Lyman α threshold excitation, which is finite at threshold due to negative ion resonances, but the Na level structure is quite different.

IB-5   Plasma Electron Heating in a DC Multidipole Plasma.

M.D. HAWORTH and R.E. KRIBEL, Auburn U.-- Experimental results are given for plasma electron heating by isotropically injected test electrons in a DC multidipole plasma. This device is characterized by a large volume of plasma with essentially zero magnetic field, along with uniform electron temperature and density profiles. Plasma densities range from 10^9 cm^{-3} to 10^{11} cm^{-3} with corresponding electron temperatures of 10 eV to 2 eV. The injection energy of the test electrons is kept below 16 eV to prevent further ionization of the argon plasma. The plasma electron heating rate at $t = 0$ is compared with theory via the Fokker-Planck equation.

IB-6 Effects of Electron Loss Due to Attachment on Swarm Parameters in SF_6-N_2 Mixtures - L.C. PITCHFORD*, Sandia National Laboratories, and A.V. PHELPS†, JILA, U. of Colorado and NBS--We have shown that the effect of electrons lost to the electron energy distribution due to attachment, analogous to the problem of the inclusion of electrons born in ionization events, is important for an accurate calculation of electron swarm parameters in SF_6-N_2 mixtures. At 1×10^{-21} Vm^2 and 100 ppm SF_6, the drift velocity and attachment rate coefficient are reduced by 11% and 23%, respectively, when attachment is properly included in the calculation. Over the range of SF_6 concentrations (1-100 ppm) and E/N values (1-20 $\times 10^{-21}$ Vm^2) investigated thus far, these effects scale with the ratio of the attachment to the energy exchange frequency.

IB-7 Ion Runaway Induced by Model Ion-Atom Potentials
- I. R. GATLAND, Georgia Institute of Technology--The runaway of protons and deutrons in helium gas, predicted by ion mobility calculations[1] and later observed in flow-drift experiments[2], appears to be associated with "soft" short range potentials. To obtain more information about the onset of runaway the phenomenon is being simulated by a Monte-Carlo calculation based on a truncated Coulombic potential. Such macroscopic effects as the rate of runaway vs. E/N (ratio of applied electric field to neutral gas number density) may be studied. Also microscopic features, including the roles of small angle scattering, long inter-collision times, and the neutral gas velocity distribution, may be observed. Results so far indicate that the rate of runaway is an exponentially increasing function of E/N, in the region of interest, and that the initial runaway is related to a combination of microscopic features.

[1]S. L. Lin, I. R. Gatland, and E. A. Mason, J. Phys. B. 12, 4179 (1979).

[2]F. Howorka, F. C. Fehsenfeld, and D. L. Albritton, J. Phys. B. 12, 4189 (1979).

IB-8 Characteristics of a microwave generated surface wave plasma in a standing waves structure.- J.MAREC,E.BLOYET,E.DERVISEVIC,P.LEPRINCE, M.POUEY,S.SAADA,Paris-Sud U.- A microwave discharge is generated by standing surface waves at 2.45 GHz(discharge tube diameter 2-mm,argon gas pressure 2 torr).Radial electric field E_r outside the plasma and intensities of ArI(430.0 nm) and ArII(434.8 nm) are measured along the discharge.A standing wave pattern is observed for E_r^2 and the both lines intensities.Intensity maxima and E_r^2 minima have same location.Inside the plasma,E_z is the main component and is 90° out of phase with respect to E_r.Thus,the maxima of intensity and E_z have the same location.Assuming that ArI and ArII lines intensities are proportional to E_z^2 and to n and n^3 respectively (n is the electron density)like in microwave capillary discharges,n can be deduced from the intensities ratio and the wavelength of surface wave.E_z^2 and n exhibit similar variations pattern.

IB-9 Wave Propagation During Ignition of Low Pressure Hg-Rare Gas Discharges - J. F. LOWRY and M. D. NAHEMOW, Westinghouse R&D Center -- We have investigated the ignition process in low pressure mercury - rare gas mixtures (1 mTorr Hg, 2.5 Torr rare gas) contained in 3.8 cm diameter cylindrical glass tubes having a thin internal conductive layer with a thin dielectric overlay. Using a scanning photodiode and synchronous detector, we observed that the ignition mechanism involves the propagation of subacoustic luminous waves from the electrode regions -- a relatively intense wave from the anode end and a weaker wave from the cathode. If the applied voltage is sufficiently high the waves meet to form a continuous ionized channel, whereupon ignition occurs. Changes in the resistivity of the conductive coating and the properties (e.g., thickness, dielectric constant) of the dielectric coating affect both the amplitudes and velocities of the luminous plasma waves. We propose a dielectric wave model in which the velocity of the luminous front in the plasma is controlled by the dielectric properties of the wall. Wave velocities predicted by the model are in close agreement with measured values.

IB-10 The Helical Magnetic Instability of Arcs - Theoretical and Experimental Determination of the Growth Rate - H. G. HÜLSMANN, J. MENTEL, Ruhr-Universität Bochum FRG[+]-- We have developed a time dependent linear perturbation theory of the helical magnetic instability of electric arcs including an external axial magnetic field B_e. The main differential equations are the mass-, momentum- and energy balance, its solution is simplified by introducing a channel model for the current distribution and by omitting the mass inertia. We have calculated the growth rate Ω of the helix amplitude for a hydrogen arc burning in a water-cooled tube of 20 mm diam. at a pressure of 1040 mbar in dependence on the current ($\Omega \gtrless 0$ for $I \lessgtr 9.3$ A, $B_e = 0$) and in dependence on B_e. The growth rates are a function of the pitch with a maximum for a certain value. The growing of an arc helix of this critical pitch with the corresponding Ω is observed when the arc is switched suddenly from a stable to an unstable state by applying rectangular pulses of a supercritical B_e. Ω measured in this way agree very well with theory. To determine Ω experimentally also for $B_e = 0$ we have developed an automatic control loop stabilization of the unstable arc by a time varying axial magnetic field. Ω is measured by turning off the stabilization for a short time.- Sponsored by DFG, FRG.

IB-11 Probing a XeCl* gain module with a 0.0004Å bandwidth ($\Delta\nu \sim 100$ MHz) probe pulse by O.L. Bourne and A.J. Alcock, NRC, Ottawa, Ont. A 0.0004Å bandwidth probe pulse was used to study the gain profile of a XeCl* gain module. No rotational structure was resolved but four vibrational bands were observed. By monitoring the gain on the $B_{v=0} \to X_{v=1}$ and $B_{v=1} \to X_{v=1}$ under lasing conditions a quenching rate of 2×10^{-11} cm^3 sec^{-1} was derived as the Ne two body quenching rate for the two upper state vibrational levels. Evidence for strong coupling of the ground vibrational states was also observed. Under injection locking conditions the line width of either of the two main transition ($B_{v=0} \to X_{v=1}$ or $B_{v=0} \to X_{v=2}$) could be reduced from 0.5Å to 0.0004Å without sacrificing the net output energy. However, the performance could not be maintained over the entire gain profile. Evidence obtained from the temporal evolution at the output spectrum under injection locked conditions suggest that this may be due to hole burning in the gain profile.

IB-12 Temperature-Dependent Kinetics of XeF Using SSRL – D.C. LORENTS, K.Y. TANG, and D.L. HUESTIS, SRI International, M. DURRETT, L. HOUSTON, and G.K. WALTERS, Rice U.†--The synchrotron radiation source at SSRL has been used to study various kinetic processes in the formation and decay of XeF at temperatures ranging from −65°C to 200°C. Photoexcitation of Xe in Ar/Xe and Ne/Xe mixtures containing the halogen donors NF_3, N_2F_4, or XeF_2 and photodissociation of XeF_2 was used to produce XeF*, whose intensities and time decays were measured using the fluorescence at 350 and 470 nm. The yields of XeF* were measured as a function of Xe* level in the $^3P_1$, $^1P_1$, and higher states for each of the donors as well as for NF_2 obtained from dissociation of N_2F_4 at 200°C. Formation rates from Xe($^3P_1$) and ($^1P_1$) were obtained from the time-dependent fluorescence by modeling studies and data fitting. Radiative and quenching rate data were also obtained. The temperature dependence of the ratio of intensities of the B and C states of XeF were used to determine the B-C energy separation.

IB-13 Calculation of the Charge and Radius of Break-
down Channels in Gases at Atmospheric Pressure,
B.Eliasson and S.Strässler, Brown Boveri Research Center,
CH-5405 Baden, Switzerland. - By using a very simple
stationary model we have calculated the characteristic
parameters of streamer breakdown in an arbitrary gas at
around atmospheric pressure. Our approach has been
based on the concepts of runaway electrons as presented
recently in the literature. By postulating a runaway
condition we are able to present a one-dimensional model
of charge propagation as a function of overvoltage and
gas density times gap distance. The calculated values
for O_2, N_2, and air are compared to measured values
which have been published in the literature.

SESSION J
9:00 A.M., THURSDAY, OCTOBER 21, 1982

BREAKDOWN I

CHAIRPERSON: E. E. KUNHARDT
TEXAS TECH. UNIVERSITY

J-1   Runaway Electrons in Fast Gas Discharges -
W.W. BYSZEWSKI and G. REINHOLD*, GTE Labs, Inc.--
Passive x-ray diagnostic techniques were used to verify
the presence of runaway electrons in transient gas dis-
charges. Impact ionization by these electrons at the
front of the avalanche plays a major role in breakdown
development. Runaway electrons stopped by the anode
produce bremsstrahlung and characteristic x-ray radia-
tion. Radiation in the keV range was observed and
detected in a transmission line pulse system used to
generate highly overvolted conditions in a test gap.
The effect of the type of gas, its pressure and the
applied voltage will be presented. The results will be
analyzed with respect to breakdown development described
by a model based on two groups of electrons present in
the discharge.[1]

*On leave from University of Dusseldorf, W.G.

[1]E.E. Kunhardt, W.W. Byszewski, Phys. Rev. A $\underline{21}$, 2069
   (1980).

J-2   Electron Shock Structure in the Electrical
Breakdown of N_2 - H. JURENKA and E. BARRETO, Atm. Sci.
Res. Center, State U. of N.Y. at Albany* - - A low
energy spark in nitrogen at atmospheric pressure in a
uniform field and between metal electrodes (2 mm apart)
shows a characteristic 25° cone of luminosity[1]. When the
energy available for the discharge increases from $\sim 2 \times 10^{-4}$
Joule, a considerably brighter core, extending from the
cathode surface into the gap, appears in the discharge
channel during the final stage of the breakdown. The
regularly repeating variation of luminosity in this
filamentary core is interpreted as evidence of supersonic
flow of electrons, provided by a cathode spot, into the
previously ionized media in the gap. The results support
the concept of wave propagation through the collision
dominated electrons in the fluid dynamical description
of the electrical breakdown of gases[2,3].

*Supported by the Office of Naval Research.
[1]E. Barreto, Electrostatics 1979 (Institute of Physics,
Bristol and London, 1979) p. 135.
[2]E. Barreto, S.I. Reynolds, and H. Jurenka, J. Appl.Phys.
$\underline{45}$, 3317 (1974).
[3]H. Jurenka and E. Barreto, J. Appl. Phys. $\underline{53}$, 3581 (1982).

J-3 Dielectric Collapse in Small High Pressure Discharges - E. Barreto and H. Jurenka, _Atm. Sci. Res. Ctr., SUNY at Albany, NY 12222._* In a 2 mm spark in air at atmospheric pressure it is known that rapid electron thermalization and subsequent gas heating occur when the ion density reaches $10^{17} cm^{-3}$. Time resolved photography confirms that a rapid deposition of most of the energy in the capacitance is preceded by a comparatively very long time of the order of 10^{-6} sec in which electrons are maintained through Coulomb interactions as a hot isotropic gas. The rapid energy deposition is associated with the formation of a single cathode cell produced by the accumulation of ions on the oxide covered cathode. Increase of the available energy produces enhanced emission which is associated with the onset of interaction between the plasma in the gap and field emission from the metal. It starts only a few nanoseconds after the plasma becomes strongly ionized and leads to a more "stable" cathode spot. Thus it is postulated that in gases, liquids, solids and even vacuum sparks the final collapse is associated with strong gradients at an interface and with a collision dominated isotropic plasma in which electron pressure forces dominate.

J-4 Statistical Delay Times and Breakdown Probability in N_2, Ar, H_2, and SF_6 - R.V. HODGES, R.N. VARNEY, and J.F. RILEY, _Lockheed Palo Alto Research Laboratory_ -- An expression for the probability that a free electron in a spark gap will initiate breakdown was derived by Wijsman in 1949.[1] We have obtained breakdown probabilities as a function of overvoltage for N_2, Ar, H_2, and SF_6 from measurements of the spark delay time in a uniform field gap provided with a small current ($\sim 10^{-15}$ A) of free electrons by UV illumination of the cathode. Laue plots of the delay times yielded straight lines with slope $i_0 P$, where i_0 is the free electron current and P is the breakdown probability. The breakdown probabilities were in excellent agreement with theory for N_2, Ar, and H_2, but not for SF_6. The deviation in SF_6 was greater at lower E/N where electron attachment is stronger.

[1] R. A. Wijsman, Phys. Rev. 75, 833 (1949).

J-5   <u>Initiation of Electron Avalanches by Photo-detachment in Irradiated Gaps Containing O_2 or SF_6</u> - R. J. VAN BRUNT and M. MISAKIAN, <u>National Bureau of Standards</u>* -The role of photodetachment in the initiation of electron avalanches near a positive point electrode was investigated using radiation between 254 and 630 nm from a chopped, tunable cw laser or filtered Hg-discharge lamp. The negative ion flux was controlled by uv-irradiation of the cathode. Consistent with estimates based on known cross sections, photodetachment for light beams with intensities up to 450 mW was found to make a negligible contribution to avalanche initiation in SF_6 or O_2 at pressures from 100 to 400 kPa. The dominant electron release mechanism appears to be collisional detachment. Previously reported[1] enhancements in avalanche rates during irradiation of a positive point can be explained by increases in negative ion densities arising from attachment of photoelectrons ejected by scattered radiation.

[1]R. J. Van Brunt and D. Leep, J. Appl. Phys. <u>52</u>, 6588 (1981).

SESSION K
10:30 A.M., THURSDAY, OCTOBER 21, 1982

LARGE APERTURE DISCHARGE LASERS

CHAIRPERSON: L. F. CHAMPAGNE
NAVAL RESEARCH LABORATORY

K-1 Performance Measurements of an 8 Liter Self Sustained Discharge TEA Laser - M.J. PECHERSKY and R.J. SPREADBURY, Westinghouse R&D Center* -- A series of measurements including small signal gain, near field energy extraction, discharge current and voltage waveforms and intra-pulse density variations were made on an 8x10x100 cm^3 UV preionized discharge. The main gas mixtures studied were: 1:14:0.5 - CO_2:N_2:H_2 and 1:7:8 - CO_2:N_2:He. Both mixtures operated at 800 torr and room temperature and contained 30 ppm of Tripropylamine. The parameters varied were: pulse width (8, 12 & 16 µsec), energy loading (200-375 J/liter), preionization density, and the output coupling of the stable resonator (R = 25, 45 and 65%). The extraction measurements yielded outputs in excess of 500 Joule for both mixtures with efficiencies of about 20%. The effect of hydrogen on the gain was also measured, where the addition of H_2 greatly improved small signal gain in mixtures containing no helium. The effect of reducing the rate rise of current and voltage was also investigated. A strong correlation between rate of rise and energy loading was observed.

K-2 Hook Measurements in Large Copper Lasers, B E WARNER AND G V SEELY, LLNL* -- The modern hook method[1] was used to measure excited state populations of copper and neon in a large bore copper vapor laser. Use of a pulsed dye laser light source permitted nanosecond time resolution during the excitation pulse of the copper laser. Spatially resolved information was obtained by scanning the probe leg of the interferometer over the 8 cm aperture. Measurements of the Cu ^{2}P copper laser levels indicate a spacially dependent sequential excitation due to plasma skin effects. Relaxation of the CVL plasma to its prepulse state was monitored through measurement of various copper and neon excited states.

[1] I. Smilanski, L. A. Levin, & G. Erez, Optics Ltrs. 5, 92 (1980).

K-3   Large Bore Copper Vapor Laser Discharge Kinetics
M.J. KUSHNER and B.E. WARNER, LLNL*--A temporally and
spatially dependent discharge and kinetics code is used
to characterize laser performance for various
geometries. In high repetition rate CVL's electron
densities in excess of 10^{13}/cm^3 can be sustained.
The resulting skin depth associated with the penetration
of the applied electric field into the plasma can be
comparable to or less than the diameter of the discharge
tube for lasers greater then 6 cm in diameter. This
results in a time and spatially dependent excitation of
the laser, and a lengthening of the laser pulse as the
diameter of the discharge tube increases. The thermal
stability of CVL discharges is found to be due in part
to a more uniform heating of the gas, a consequence of
skin depth effects.

K-4

Aperture Scaling of Discharge-Pumped XeCl Lasers,
B. L. Wexler and R. Burnham, Naval Research Laboratory.

In order to study the scalability of discharge-
pumped rare-gas halide lasers, we have operated an x-ray
preionized XeCl laser with 10 x 7.5 x 40 cm discharge
dimensions. The laser has been pumped by an 0.67 ohm,
200 nsec water line charged to 80 kV. Output pulses of
3.6 and 6.0 Joules with durations of 100 and 150 nsec
have been obtained at laser pressures of 2 and 3 atmo-
spheres respectively. Discharge widths of 6-7 cm are
indicated by laser burn patterns. The overall efficiency
of the laser with respect to the primary energy-storage-
capacitor is 1.3%. We have also studied the effects
of varying the current and voltage risetimes of the
discharge on laser output. Results of these studies
indicate that scaling to discharge volumes consistent
with 100 J of laser output should be possible with little
sacrifice in efficiency.

SESSION LA
1:30 P.M., THURSDAY, OCTOBER 21, 1982

NEGATIVE IONS AND ATTACHMENT

CHAIRPERSON: H. BÖHRINGER
                NOAA AERONOMY LAB

LA-1   Volume Production of Hydrogen Negative Ions in Plasmas.- M. Bacal*, A.M. Bruneteau, M. Nachman, Ecole Polytechnique, Palaiseau, France, M. Péalat, J.P.E. Taran and J. Taillet, O.N.E.R.A., Châtillon, France.- Volume production of H^- and D^- ions in plasma has been recently found to be a useful element of possible high-power negative-ion based neutral beam systems. Experimental evidence for volume production will be presented, based on measurements of high density (5×10^{10} cm^{-3}) and high fractions (10-35 %) of H^- and D^- ions in plasmas, using the photodetachment method, and on measurements of ro-vibrational populations using coherent anti-Stokes Raman scattering (CARS). These measurements are discussed in terms of a theoretical model relying on the assumption that the dominant negative ion production process is dissociative electron attachment to highly vibrationally excited molecules[1,2].

[1.] J.N. Bardsley and J.M. Wadehra, Phys. Rev. A20, 1398 (1979).
[2.] M. Allan and S.F. Wong, Phys. Rev. Lett. 41, 1791(1978)

LA-2   Effect of Rot-Vibrational Excitation on Dissociative Attachment of H_2 - J.M. WADEHRA, Wayne State University*--Resonant scattering model is used to calculate the cross sections for dissociative attachment of electrons to H_2 when the molecule is both rotationally and vibrationally excited. The cross sections are obtained for attachment to all possible (v,J) levels of H_2. It is found that the vibrational excitation is more important in enhancing the cross section than the rotational excitation. For example, for the initial states (0,15), (2,8) and (3,0), all of which have the same internal energy, the threshold attachment cross sections are 3.1(-19), 3.7(-18) and 6.0(-18) cm^2, respectively.

LA-3 Measurement of Attachment Coefficients at High Pressures--P. BLETZINGER, Air Force Wright Aeronautical Laboratories, WPAFB, OHIO--Attachment coefficients can be determined from the decay characteristics of discharges ionized by a pulsed electron beam. As little as 0.015% of an attaching gas was added to a non-attaching carrier gas (CH_4 at atmospheric pressure). Using a nonlinear least square fit, both attachment and recombination coefficients were determined as a function of the reduced electric field. Since in an E-beam ionized discharge the cathode fall voltage depends on many parameters, it was measured for each discharge condition using a movable electrode. To improve the switch-off characteristics of E-beam controlled switches, gases with an attachment coefficient sharply increasing with the applied electric field are desired. Recently proposed[1] as well as other gases with such attachment characteristics have been measured. Some of the halocarbon gases such as C_2F_6 show the increasing attachment rate as well as good stability under E-beam discharge conditions, however not at the desired reduced electric field. Measurements for C_3F_8, NF_3, HCl and other attachers will be reported.

[1] L.G. Christophorou et.al.,Appl.Phys.Lett.41,147,JUL82.

LA-4 Measurements of Attachment and Ionization Coefficients in CCl_4* - D. K. DAVIES, Westinghouse R&D Center -- Measurements of attachment (η/N) and ionization (α/N) coefficients together with negative- and positive-ion mobilities have been made in pure CCl_4 over the range $300 \leq E/N \leq 950 \times 10^{-17}$ Vcm^2 using a pulsed drift tube. Measurements of electron drift velocity have been restricted to the range $850 \leq E/N \leq 950 \times 10^{-17}$ Vcm^2 due to the large attachment coefficient which increases with decreasing E/N. The limiting value of E/N, (E/N)*, at which $\alpha = \eta$, is determined to be $(880 \pm 2) \times 10^{-17}$ Vcm^2. In the vicinity of (E/N)*, the net ionization coefficient, $(\alpha - \eta)/N$, increases linearly with increasing E/N, characteristic of strongly-attaching gases. Over the respective ranges $650 < E/N < 950 \times 10^{-17}$ Vcm^2 and $750 \leq E/N \leq 950 \times 10^{-17}$ Vcm^2 the coefficients $(\alpha - \eta)/N$ and α/N (in cm^2) are described to within $\pm 3\%$ by $(\alpha - \eta)/N = 3.81 \times 10^{-19}$ $[(E/N) - (E/N)*]$ and $\alpha/N = 2.73 \times 10^{-14}$ $\exp [-6000/(E/N)]$, where E/N is in units of 10^{-17} Vcm^2. The arrival spectra of both negative and positive ions are dominated by a single species. In the ionization region, the negative-ion mobility is approximately twice the positive-ion mobility.

LA-5 **A Swarm Study of Electron Attachment to the Perfluoroalkanes** - S. R. HUNTER and L. G. CHRISTOPHOROU, ORNL*--Total electron attachment rate constants, k_a, for the perfluoroalkane series, $C_N F_{2N+2}$, where $N = 1$ to 6, have been measured in high pressure (0.133 MPa $\leqslant P_T \leqslant$ 1.6 MPa) buffer gases of N_2 and Ar over the mean electron energy, $\langle \epsilon \rangle$, range of 0.04 to 4.8 eV. The $k_a(\langle \epsilon \rangle)$ for CF_4 and $C_2 F_6$ are independent of P_T since these molecules capture electrons dissociatively. The $k_a(\langle \epsilon \rangle)$ for the larger perfluoroalkanes are very dependent on P_T since for these molecules moderately short-lived parent negative ions are formed. As the size of the molecule increases, however, the parent negative ion lifetime increases, and $k_a(\langle \epsilon \rangle)$ again becomes pressure independent over the pressure range of our experiments. From the measured $k_a(\langle \epsilon \rangle)$, we have obtained electron attachment cross sections using a swarm unfolding technique. These measurements are compared with the relative cross sections obtained in a beam experiment.[1]

*Operated for USDOE by Union Carbide Corporation under contract W-7405-eng-26.

[1] S. M. Spyrou, I. Sauers, and L. G. Christophorou, submitted to *Journal of Chemical Physics*.

LA-6 **Fragmentation of Fluoroethers and Fluorosulphides Under Low-Energy ($\leqslant$10 eV) Electron Impact** - S. M. SPYROU and L. G. CHRISTOPHOROU, ORNL*--Fragment negative ions from four fluoroethers (CF_3OCF_3, CF_3OCF_2H, CF_2HOCF_2H, and CF_3OCH_3) and two fluorosulphides (CF_3SCF_3 and CF_3SCH_3) formed by low-energy (0-10 eV) electron impact have been studied using a time-of-flight mass spectrometer. The types and relative intensities of these fragment anions depend strongly on the number and relative position of the fluorine atoms in the molecule and on the O to S substitution. The observed negative ions (in decreasing order of intensity) are: F^- and CF_3O^- from CF_3OCF_3; CF_3O^-, HF_2^-, F^-, CFO^-, and CF_3^- from CF_3OCF_2H; CF_3O^-, HF_2^-, F^-, and CFO^- from CF_2HOCF_2H; F^- from CF_3OCH_3; CF_3S^- and F^- from CF_3SCF_3; CF_3S^- from CF_3SCH_3. The fluorosulphides attach electrons of lower energy than the fluoroethers. The magnitude of the total cross section for negative ion formation increases[1] with increasing F substitution.

*Operated for USDOE by Union Carbide Corporation under contract W-7405-eng-26.

[1] S. R. Hunter and L. G. Christophorou, *Journal of Chemical Physics* (to be published).

SESSION LB
1:30 P.M., THURSDAY, OCTOBER 21, 1982

CORONA AND BREAKDOWN II

CHAIRPERSON: H. JURENKA
STATE UNIV. OF NEW YORK

LB-1 <u>Theory of Trichel Pulses in Oxygen</u> - R. Morrow and J.J. Lowke, <u>CSIRO</u>, Division of Applied Physics, Sydney, Australia 2070.--Theoretical predictions have been made which describe 'Trichel Pulse' corona in oxygen between a negative sphere and a positive plane. The continuity equations for electrons, positive ions and negative ions are solved numerically, together with Poisson's equation. The effects of ionization, attachment, drift, recombination, electron diffusion and photo emission from electrodes are included. The distortion of the electric field due to space-charge is calculated using the 'cylinder method', modified to include images of space-charges in the sphere and the plane. Results have been calculated for the experimental results of Bugge[1] for oxygen at 50 torr for an applied voltage of 2160 V. We obtain fair agreement with the experimental pulse rise times of 20 ns, pulse widths of 50 ns, pulse currents of 1 mA, and pulse repetition frequencies of 100 kHz. Effects of variations of pressure and zero attachment are also calculated.

[1]C. Bugge, Technical Report EIP 68-1, Norwegian Institute of Technology (1968).

LB-2 <u>Toward a Fundamental Model for Steady Point-Plane Coronas</u>--B. L. Henson, <u>University of Missouri-St. Louis</u>--Poisson's equation, expressed in prolate spheroidal coordinates, is used as a basis for the development of a mathematical model for the space charge region of point to plane coronas in the steady regime. Arbitrary geometries are initially assumed for both the surface of the point electrode and the corresponding corona glow discharge boundary. Also in the initial equations an arbitrary field dependent mobility model for charge transport is used. In the model's more general form the analysis culminates in an integral-differential equation whose solution yields the potential distribution. Cylindrically symmetrical solutions of this equation for constant charge carrier mobilities are discussed with respect to their correlation with known laws and other empirical relations for coronas.

LB-3 A Simple Model of Laser-Triggered Breakdown-P.F. WILLIAMS and R.A. DOUGAL, Texas Tech*--We present a simple model of the closing phase of gas-filled, laser-triggered, spark gap switches. The model is based on a process, which has been applied to conventional over-volted breakdown by several researchers,[1,2] in which the gas conductivity is continuously enhanced due to ohmic heating. Results of preliminary numerical calculations based on this model which describe well the qualitative features of laser-triggered electrical breakdown will be presented. Properly implemented, the model should serve as a suitable basis for a reliable numerical algorithm for the engineering design of laser-triggered spark gap switches.

[1]E. Marode, F. Bastien, and M. Bakker, J. Appl. Phys. 50, 140 (1979).

[2]M. Kekez, M. R. Barrault, and J. D. Craggs, J. Phys. D: Appl. Phys. 3, 1886 (1970); and references therein.

LB-4 Spectral and Temporal Evolution of Laser Break-down in SF_6 - P. J. HARGIS, JR., Sandia National Labora-tories*--Experiments were carried out on the initiation of gas breakdown in SF_6 by a Q-switched Nd:YAG laser operated at wavelengths of 266-nm and 1064-nm. Light emitted by the breakdown spark was recorded with a spec-tral resolution of 0.1 nm over the pressure range from 10-Torr to 1000-Torr SF_6. Strong molecular emission from the multiphoton photodissociation of SF_6 was observed from the 266-nm laser spark for gas pressures below 100 Torr; whereas, molecular emission was completely absent from the 1064-nm laser spark. Above 100 Torr, both the 266-nm and 1064-nm spark spectra were dominated by atomic fluorine emission and a blackbody continuum. A fast photodiode was used to record the temporal evolution of the breakdown spark with a resolution of 0.5 nsec. Time scales for the formation of the breakdown spark are much slower at 1064-nm than at 266-nm. The data presented in this paper demonstrate the importance of multiphoton photodissociation in the threshold region of gas break-down at 266-nm. The data also demonstrate that the threshold for gas breakdown in SF_6 is determined by laser fluence rather than intensity at both 266-nm and 1064-nm.

LB-5 Multifrequency Laser Breakdown in SF_6 -
P. J. HARGIS, JR., L. C. PITCHFORD, T. A. GREEN,
J. R. WOODWORTH, and R. A. HAMIL, Sandia National Labora-
tories*--A Q-switched Nd:YAG laser was used to study the
effect of the simultaneous presence of 266-nm and 1064-nm
laser pulses on optical breakdown in SF_6. When both
pulses were spatially and temporally overlapped in the
center of a gas cell containing 1000-Torr SF_6, the
intensity of the breakdown spark was enhanced by factors
of 3 to 10 over that produced by either laser pulse alone.
The spectrum of the enhanced laser spark showed an
increase in the atomic fluorine emission and blackbody
continuum with no increase in the molecular emission asso-
ciated with the 266-nm multiphoton photodissociation of
SF_6. In addition, the enhanced spark preserved the fast
risetime characteristic of 266-nm laser breakdown in SF_6.
These results are consistent with the concept that the
266-nm laser pulse produces a source of seed electrons by
the rapid multiphoton ionization of SF_6 followed by
heating and enhancement of the seed electrons by the
1064-nm laser pulse. Results on the multifrequency laser
triggering of a 500-kV SF_6-insulated switch will also be
presented in this paper.

LB-6 A Parametric Study of Laser Triggering of a
500-kV Gas-Filled Switch - J.R. WOODWORTH and P.J.
HARGIS, JR. Sandia National Labs* - We have per-
formed a parametric study of laser triggering of a
500-kV, SF_6-insulated electric switch. Laser wave-
lengths of 248 nm, 266 nm, and 1064 nm and laser
pulselengths of 2 nsec, 4 nsec and 20 nsec were used
to trigger the switch. Triggering was accomplished by
focusing the laser output to form a breakdown arc in
the SF_6 between the switch electrodes. We find that
triggering in the UV (248, 266 nm) gives results which
are a dramatic improvement over triggering in the IR
(1064 nm). Switch breakdown jitter of less than 0.2
nsec was obtained with UV laser triggering. Our
results also indicate that the optimum laser pulse-
length is equal to the turn-on time of the switch,
i.e., the time between the arrival of the laser pulse
in the switch and the rise of the switch current
pulse. Implications for large multi-switch systems
will be discussed.

LB-7 Theory of R.F. Breakdown in Nitrogen – R. Morrow, CSIRO, Division of Applied Physics, Sydney, Australia 2070.--Theoretical predictions are presented of the development of R.F. breakdown in nitrogen in a parallel plate electrode system with a 10 MHz radio frequency voltage applied. The continuity equations for electrons and positive ions, including ionization and photo-emission from the electrodes, are solved numerically, together with Poisson's equation. The effect of space-charge on the electric field is calculated using the cylinder method, with multiple images in the electrodes. Results for nitrogen at 90 torr show that with an electrode separation of 3 cm and a 10 MHz voltage of 16.7 kv peak, most of the ionization occurs near the centre of the gap, with only a small contribution from the electrodes due to photo-emission. Preliminary results give comparable times to breakdown to those measured in air by Haydon et al[1].

[1] S.C. Haydon, I.C. Plumb and G.A. Woolsey "Studies of Electrical Charges and Plumes on High Power H.F. Aerials" III, Dept of Phy, UNE. Australia.

LB-8 Breakdown of Rod-Plane Gaps under High Frequency Voltages – M. S. ABOU-SEADA, H. ANIS and S. M. SALEM, Cairo U. Egypt--
A theoretical study of breakdown in air-gaps under simulated oscillatory surges is conducted. The surges are made up of high frequency voltages superimposed upon a dc bias. This combination serves to simulate switching surges in power systems when a power line is energized. Breakdown is said to occur when the travel distance of the positive space charge lies within the physically determined boundaries of the ionization zone. The model is applied to rod-plane gaps of various dimensions and under frequencies of oscillation up to 1 MHz. It is found that the breakdown field decays with increasing product of the frequency and the rod's radius of curva-ture, but at a slower rate as the dc bias is increased. The calculated breakdown voltages are compared to published experimental results of breakdown in air gaps subjected to high frequency voltages. A reasonable agreement is reported.

LB-9 Two Dimensional Description of the Development of Transient Gas Discharges - W.W. BYSZEWSKI, K.C. CHUNG and J.M. PROUD, GTE Labs, Inc.--Development of fast gas discharges between plane-parallel electrodes was theoretically modeled in axial symmetry. Continuity equations for electrons and for positive and negative ions together with Poisson's equation formed a hyperbolic system of partial differential equations. This system was solved numerically with boundary conditions governed by circuit impedance and secondary processes on electrodes. A finite difference method with fourth order Runge-Kutta techniques and Fast Fourier Transformation was applied. The effect of initial ionization and the sensitivity of the solution to the accuracy of the data for material properties have been analyzed. Some results for N_2 and SF_6 will be shown. The current waveform and the formative lag time will be compared with experimental data obtained in a transmission line pulse system. The space dependence of the particle density and electric field will be presented and discussed.

LB-10 Simulation of Probability Distributions for the Breakdown Voltage of Surface Discharges M. J. KUSHNER, LLNL*--Probability distributions for the breakdown voltage between closely spaced electrodes ($\approx$10 mils) on insulated surfaces are studied with results from a Monte Carlo simulation. The probability distributions, experimentally measured to be bimodal under certain conditions,[1] are found to be characterized by the number of ionizations per primary electron emitted at the triple junction that is required to initiate the electron avalanche. Bimodal distributions represent a transition region between low variance and high variance normal distributions, requiring low and high multiplication coefficients, respectively, for the avalanche to occur. Preionization and low electron loss rates to the surface not only lower the breakdown voltage but also reduce bimodal distributions to single distributions.

[1]E. W. Gray, D. J. Harrington, J. Appl. Phys. 53, 237 (1982)

LB-11 Analysis of Discharge Damage and Breakdown in Gaseous Cavities in Insulating Materials -- A.A. HOSSAM-ELDIN, U. of Alexandria, Egypt --

Insulating systems invariably contain some micro-cavities within the insulation or on boundaries between the insulation and the electrodes. These cavities are filled with a gas or liquid having a lower electric strength than the main dielectric. Partial discharges in cavities lead to the deterioration and complete break-down of insulating media.

Ion and electron bombardment have been considered as independently accountable for the failure of dielect-rics by sustained partial discharges. However, experi-mental results indicate that electron bombardment is primarily dominant and that the rate of degradation is accelerated linearly by increasing the frequency, magni-tude and time of applied voltage. Furthermore filling the cavities with hydrogen or helium gases, at slightly higher pressures than atmospheric, or even by insulating liquids decreases the rate of deterioration and increases the life time.

SESSION MA
9:00 A.M., FRIDAY, OCTOBER 22, 1982

METASTABLE COLLISIONS

CHAIRPERSON: R. BIENIEK
UNIVERSITY OF MISSOURI-ROLLA

MA-1 <u>Velocity Dependent Total Scattering</u>
<u>Cross Sections for Metastable Helium on He, Ne,</u>
<u>Ar, Kr and Xe</u>[†], J.W. SHELDON and K.A. HARDY,
<u>Florida International Univ.</u> - The title data are
obtained by measuring the attenuation of a time-
of flight analyzed metastable helium beam on
passing through a collision cell. The computer
interactive experiment allows extended data ac-
quisition times and thereby provides precise da-
ta over a wider relative velocity range than was
previously accessible.[1] The velocity dependence
of the He* + He cross section is relatively flat
and monotonic over the observed 1600 m/s to 5000
m/s velocity range. As heavier rare gas targets
are used the long range van der Waal forces are
stronger and the available minimum relative ve-
locity is lower so that with argon one glory un-
dulation in the cross section is observed and
with xenon two undulations are resolved.

[1]E.W. Rothe, R.H. Neynaber and S.M. Trujillo, J.
Chem, Phys. 42, 3310 (1966).

MA-2

<u>Temperature Dependence of De-excitation Rate</u>
<u>Constants for Neon Excited Atoms</u> - C. AKOSHILE*, JERRY
CLARK* and A. J. CUNNINGHAM, <u>Univ. of Texas at Dallas.</u>-
Investigations of de-excitation processes for neon
excited atoms in their parent gas and in helium neon
mixtures are reported. The studies were conducted at
temperatures of 150, 300 and 400°K and de-excitation
rate constants of Ne ($^3P_2$, $^3P_1$ and $^3P_0$) by Ne and He
were determined using time resolved absorption spec-
troscopy. The measured temperature dependence of both
the two- and three-body rate coefficients indicate the
need for refinements of available potential curves.

MA-3 The Ionization Coefficient in Ar-Hg Mixtures - A.L.J. BURGMANS, and A.H.M. SMEETS, Philips Research Labs., Eindhoven, The Netherlands. -- The first Townsend ionization coefficient[1] is measured in Ar-Hg mixtures for E/n values between 6×10^{-21} Vm^2 and 2×10^{-18} Vm^2 and for a mercury atom fraction varying from 2×10^{-4} to 2×10^{-2}. The experiments are performed with a parallel-plate apparatus in which the current is measured as a function of the plate separation at constant electric field. The ionization coefficient is determined by ionization processes in argon and by ionization of mercury via excited argon states through Penning ionization and associative ionization. Experimentally the ionization coefficient is found to be a function of E/n and the mercury atom fraction only. Small admixtures of mercury lead to a large increase in the ionization coefficient. From the experimental results the effective rate coefficient for excitation to the appropriate argon states is obtained as a function of E/n, as well as the ratio of the rate coefficients for destruction of these excited argon states by collisions with argon and mercury atoms respectively.

[1] J.M. Meek and J.D. Craggs, Electrical Breakdown of Gases (John Wiley & Sons, 1978).

MA-4 Observation of ^{5}S Nitrogen Metastable State in Charge Exchange Collisions - K. B. McAfee, Jr., C. R. Szmanda, and R. S. Hozack, Bell Laboratories -- The charge-transfer reactions of excited metastable nitrogen atomic ions with argon are reported. The principal contributor to the reaction cross section is N$^+$ (^{5}S; $1S^2 2S2P^3$) while small contributions are made by the ^{1}S ^{3}P states of N$^+$. The experiment quite uniquely allows a clear identification of the specific electronic state which undergoes a charge transfer reaction. Excited atomic nitrogen ions are important in interstellar and synthetic plasmas.

MA-5 Metastable Ions and the F-Region Photochemistry of N_2^+.* - E. L. BREIG, W. B. HANSON, J. H. HOFFMAN, Univ. Texas at Dallas and D. G. TORR, Utah State Univ.-- Comprehensive in situ measurements with the Atmosphere Explorer aeronomy satellites have permitted study, direct in the atmospheric environment, of the uncertain roles of metastable $O^+(^2D)$ and vibrational excitation in the photochemistry of N_2^+. Results are described for a unique subset of data that spans distinct regions near the daytime F-peak wherein either chemical reactions or electron processes alternatively control the N_2^+ abundances. Concentrations for N_2^+ calculated with recent laboratory data for $O^+(^2D)$ losses via N_2 exceed these measurements by a consistent factor of ~2, despite good agreement for the companion NO^+ ion. The nature of the data imposes severe constraints on any simple modification of current theory. Improved agreement, however, is achieved with a more complex model involving losses of vibrationally-excited N_2^+ through resonant-type reactions with O, thus reducing its net production from $O^+(^2D)$.

MA-6 Time Resolved Observations of $O(^1D)$ Energy Transfer - G. A. Germany, G. J. Salamo, and R. J. Anderson, University of Arkansas*--A pulsed fluorine excimer laser operating at $\lambda1570$ A wavelength, 10 ns pulse width, 10 Hz repetition rate and $\sim.7$ MW output power is used to photodissociate ground state molecular oxygen, $O_2(X^3\Sigma_g^-)$. The dissociation products, $O(^1D)$ and $O(^3P)$, are produced with unit quantum efficiency, ~0.4 eV translational energy, and $\sim2\%$ total O_2 dissociation. The energy transfer process $O(^1D) + O_2(X^3\Sigma_g) \rightarrow O_2 (b^1\Sigma_g^+) + O(^3P)$ is monitored by observation of the $O(^1D) \rightarrow O(^3P)$ radiative transition, ($\lambda6300$ A), as a function of O_2 gas pressure over the region 10 to 400 mtorr. The $O(^1D)$ quenching rate constant is determined as 3.5×10^{-11} cm^3/s in agreement with previous observations. All observations are carried out without the aid of a high pressure buffer gas to limit diffusive losses. The data demonstrate the feasibility of using pulsed laser dissociation to produce high densities of $O(^1D)$ and $O(^3P)$ as target atoms for subsequent collision experiments.

MA-7 Measurement of Bimolecular and Termolecular Charge Exchange and Penning Ionization Rate Constants. L.W. Downes, S.D. Marcum and W.E. Wells, Physics Dept., Miami University, Oxford, Ohio 45056.

A long pulse electron beam (10 A/cm^2, 1 μsec) was used to create a helium-nitrogen afterglow plasma over 100 T to 1000 T helium pressures and .05 T, .1 T, .2 T and .5 T partial pressures of nitrogen. The lifetimes of the 3914 Å transition ($N_2^+(B,v=0) \rightarrow N_2^+(X,v=0)$) was observed to determine charge exchange lifetimes (early afterglow) and Penning ionization lifetimes (late afterglow). Using the methods of Lee et al.[1,2], the rate constants obtained were within experimental error (< 40% lower than Lee et al.[1]) for charge exchange rates. For Penning ionization rates the constants were greater than Lee et al.[2] and less than Myers et al.[3]

1. F.W. Lee, C.B. Collins and R.A. Waller, J. Chem. Phys 65, 1605 (1976).

2. F.W. Lee and C.B. Collins, J. Chem. Phys. 65, 5189 (1976).

3. G. Myers and A.J. Cunningham, J. Chem. Phys. 67, 3352 (1977).

MA-8 Rotational Spectra of Nitrogen Ion Transitions Produced by Penning Ionization at High Pressures. L.W. Downes, S.D. Marcum and W.E. Wells, Physics Dept., Miami University, Oxford, Ohio 45056.

A long pulsed electron beam machine with variable repetition rate (10 A/cm^2, 1 μs, up to 2 pps) was used to create helium-nitrogen plasmas with various partial pressures of nitrogen at total pressures ranging from 100 - 2300 Torr. The rotational structure of the $N_2^+(B,v'=0) \rightarrow N_2^+(X,v''=0)$ band at 3914 Å was observed by coupling a scanning spectrometer to the repetitively pulsed e-beam initiated plasma. Fast digitization of light signals emitted during each pulse allowed separation of discharge and early (charge exchange dominated) and late (Penning ionization dominated) afterglow portions of the plasma. No observable differences in the rotational spectra were found for those time domains and in all cases the rotational temperature was close to 300 K. These data and the effects of pressure broadening at elevated pressures will be presented and discussed.

SESSION MB
9:00 A.M., FRIDAY, OCTOBER 22, 1982

GLOW DISCHARGES I

CHAIRPERSON: L. E. KLINE
               WESTINGHOUSE R&D

MB-1 Electron Density Measurements in a Low Pressure Na-Ne Discharge using Doppler-Free Two-Photon Spectroscopy - H.J. CORNELISSEN, and A.L.J. BURGMANS, Philips Research Labs., Eindhoven, The Netherlands. -- In a low pressure Na-Ne discharge the Stark broadening and shift of the Na-4D level due to the presence of the electrons are both of the order of 100 MHz. To measure these quantities the Doppler width which amounts to a few GHz has to be eliminated. This is accomplished by inducing the 3S-4D two-photon transition in sodium using two counter-propagating laser beams of the same frequency. The laser induced 4P-3S fluorescence is detected together with the simultaneously obtained Doppler-free signal from a sodium reference cell. In this way the Stark broadening and shift is measured as a function of the discharge current (0-1 Amp). Using the calculations of Griem[1] values for the electron density are obtained ranging from 10^{18} to 10^{19} m^{-3}. With the present technique the electron density is obtained without disturbance of the discharge and also a good spatial resolution, better than 0.5 mm, is realized.

[1] H.R. Griem, Spectral Line Broadening by Plasmas (Academic Press, 1974).

MB-2 Heating in a Pulsed Nitrogen Discharge*-J.P. BOEUF and E.E. KUNHARDT, Texas Tech U.--The mechanisms for gas heating in pulsed discharges in nitrogen have been invesitgated using a self consistent calculation of the time evolution of the electron distribution function, the vibrational population, and the density of electronically excited states. Results show that two processes are mainly responsible for the short time heating of the gas, the importance of each depending on the value of E/N and the electron number density during the pulse (20<E/N<80 Td)
    - heating by V-V collisions due to the anharmonicity of the nitrogen molecule ("anharmonic heat-up"),
    - heating due to self-quenching of the $N_2(A^3\Sigma u^+)$ molecules.
Energy transfer to the translational degree of freedom of N_2 by V-T collisions (mainly N_2-N), or by deactivation of $N_2(A^3\Sigma u^+)$ by N became significant after a much larger time. The time evolution of the energy balance will be discussed.

MB-3 Monte Carlo Simulation of Electron Properties in Parallel Plate Capacitively Coupled RF Discharges M. J. KUSHNER, LLNL*--Electron properties in parallel plate RF discharges are studied with results from a Monte-Carlo computer simulation. The model calculates the time dependent electron density and sheath potential and thickness by oscillating the applied electric field. Time averaged values for the spatial distribution of electron energy and density are obtained by calculating many RF cycles, periodically undating boundary conditions for a self-consistent solution. The computed electron properties are in systematic agreement with probe measurements made in a plasma etching reactor when a large secondary emission coefficient for electrons by ions is used. The electron distribution function is composed of a large thermal group and an e-beam component resulting from high energy secondary electrons.

MB-4 Microwave capillary discharges- J.MAREC, E.BLOYET,E.DERVISEVIC,P.LEPRINCE,M.POUEY,S.SAA-DA,Paris-Sud U. - A discharge is produced at 2.45 GHz by a surface wave structure[1] in capillary quartz tubes(diameters 2-mm to 5-mm,argon gas pressure 0.1 to 10 torr).In these discharges,the electric field E and the electron density n are together known.Thus,a model[2] based on wave properties and a proportionality assumption between the absorbed power and the total electron number gives the electron density profile along the discharge depending on the pressure and the wave damping.Experimental profiles are in good agreement with theoretical relation. Spectroscopic measurements of ArI and ArII line are also reported.As expected,intensities of ArI lines are proportional to n and E^2(excitation frequencies vary like E^2).As in capillary positive columns,intensities of ArII lines are found to be proportional to n^3 and E^2.

1 M.Chaker et al.,J.Phys.Lett.,43,L71 (1982).
2 V.M.Glaude et al.,J.Appl.Phys.,51,5693 (1980).

MB-5 <u>Radiation Efficiency of the Argon-Mercury</u>
<u>Discharge at High E/N</u>. CHARLES N. STEWART and
J.H. INGOLD, <u>General Electric</u>, Nela Park, Cleveland,
OH.-- The relative radiation efficiency of mercury-
argon mixtures in 11 mm diameter tubes has been
measured as a function of argon pressure. The 254 nm
mercury resonance radiation shows an unexpected maximum
near an argon pressure of two torr. In an attempt to
explain this result, the Boltzman equation for the
electron energy distribution has been solved for the
appropriate argon-mercury mixture. The drop off at
higher argon pressures is caused by increased elastic
losses, as expected. The drop off at lower argon
pressures is caused by excitation of the excited states
of argon. The measurements and the model calculation
for 11 mm diameter will be presented and compared with
results for discharges in 36 mm diameter tubes.

MB-6 <u>Axial Particle Density Gradient in</u>
<u>Direct-Current Discharges</u>* - J. H. INGOLD, <u>General</u>
<u>Electric Company, Cleveland</u>, OH and H. J. OSKAM,
<u>University of Minnesota, Minneapolis, MN</u>. --Particle
density gradients in the positive column of a dc
discharge have been reported previously. An increase
of the density at the cathode end of the discharge tube
is due to the neutralization of ions at the cathode
(cataphoresis), while a density increase at the anode
end is caused by an imbalance of the momenta
transferred by the electrons and ions to the neutral
particles (electrophoresis). A general transport
theory will be presented which incorporates both
effects. An approximate analytic solution shows that
cataphoresis dominates electrophoresis at low gas
pressures in a monatomic gas, while the reverse holds
at high gas pressures. Numerical results will be given
for the complete pressure range.

MB-7 Modelling of He-SiH$_4$-PH$_3$ Gas mixture Glow Discharge Positive Column Plasmas - Jen-Shih Chang, McMaster University, Canada, R.M. Hobson and Y* Ichikawa, York University, Canada -- A numerical model of the positive column in plasmas produced in the gas mixture of He-SiH$_4$-PH$_3$ is developed. The plasma parameters which are important to those conditions applied to the PCVD technique for a-Si solar cell production are emphasized. The range of numerical parameters cover the total gas pressure P from 10^{-1} to 10 torr, the partial silane pressure from 0 to 5×10^{-1} torr, the partial PH$_3$ pressure from 0 to 5×10^{-3} torr, the discharge tube radius from 1 to 3 cm, and the electron density from 10^8 to 10^{12} cm^{-3}. The transport equation of He$^+$, He$_2^+$, He*, SiH$_{\alpha-1}$, PH$_\beta^+$, PH$_{\beta-1}$ and (H+H$_2$) has been numerically solved together with electron temperatures. Numerical results show that: (1) electron temperature decreases with increasing SiH$_4$ and PH$_3$ partial pressure; (2) for lower gas pressure, dominant ion species is SiH$_\alpha^+$, ($\alpha \leq 3$), except He$^+$ at smaller discharge tube radius; (3) for higher gas pressure, silane free radical density is much larger than that of the silane ions; (4) significant amount of hydrogen was observed only at the lower pressure; (5) the role of Helium metastable particles observed to be important in the plasma parameters in the positive columns for this combination of gas mixtures (* presently in Wright State Univ.)

MB-8 Particle Balance and Plasma Parameters in Oxygen Glow Discharge Positive Column - Y. ICHIKAWA, R. L.C. WU, T.O. TIERNAN, Wright State Univ.*, and T. Kaneda, Tokyo Denki U., Japan.--A numerical analysis of a pure oxygen positive column plasma has been made in order to predict the composition of neutral and charged particles and their plasma parameters. In the modeling of the discharge plasma, a total of thirteen species, including electrons, O_n (n=1∿3), O_m^+,O_m^- (m=1∿4), and metastable O_2(a'∆g), have been taken into consideration. More than thirty reactions involving these thirteen species have been included in the model. Under typical glow discharge conditions (electron density $\cong 10^{11}$ cm^{-3}, tube radius ∿1cm and total pressure = 1∿10 torr), the calculations yield the following conclusions: (1) the major neutral species are O_2 and O_2(a'∆g), and O_3 is usually less than 1% of the total neutral species; (2) the major positive and negative ions are O_2^+ and O^- respectively; (3) the electron temperature increases slightly as the plasma density increases. The calculated results will be compared with experimental data also determined in the present study.

MB-9 <u>Studies of a Glow Discharge Electron Beam</u>* – Z. YU, J. MEYER, J. ROCCA, and G. COLLINS, <u>Colorado St. U.</u>—Glow discharge electron beams have been <u>recently used</u> to excite cw ion lasers[1,2]. We have measured the energy spectrum of a kilovolt electron beam produced by a glow discharge operating in helium at pressures between .15 and .8 Torr. The electron beam energy spectrum measured at 17 cm from the electron gun presents an energy width at half-maximum of 100 eV to 300 eV. The electron beam energy spectrum gets narrower as the discharge current is incremented up to a critical current value, at which it abruptly degrades into a broad energy profile. This change in the electron beam energy spectrum is coincident with the sudden appearance of a plasma region with a very intense luminosity and with the emission of intense microwave radiation. This phenomena is attributed to the generation of plasma oscillations driven by the electron beam. We suggest the use of the beam-plasma interaction as a method to efficiently deposit the electron beam energy into the plasma for the excitation of ion lasers.

[1] J. Rocca, J. Meyer and G. Collins, APL, 301, <u>40</u>, 1982 and
[2] JQE, 326, <u>18</u>, 1982.

SESSION N
10:45 A.M., FRIDAY, OCTOBER 22, 1982

GLOW DISCHARGES II AND BOUNDARY PHENOMENA

CHAIRPERSON: A. GARSCADDEN
               AIR FORCE WRIGHT AERONAUTICAL LABS

N-1 Theory of the Boundary Layer in a
Partially Ionized Plasma* – K.-U. RIEMANN,
Ruhr-Universität Bochum,FRG. The build-up of
a collision free space charge layer in front
of a negative wall is possible only if the
ions are accelerated within the plasma (in
the "presheath") to a sufficiently high velo-
city (Bohm criterion). The theoretical ana-
lysis of the presheath region requires the
selfconsistent determination of the potential
and ion distribution. This analysis is com-
plicated by the strong inhomogeneity of the
boundary layer. For representative models of
the collision free and collision dominated
plasma the solution can be given analytically.
Generally, the formulation of the ion kinetics
yields fundamental conclusions concerning the
nature of the Bohm criterion and the structure
of the plasma-sheath transition. These results
are of practical importance for the self-
consistent description of the core and
sheath of a plasma column.

N-2 Theory of the Electron Distribution
Function in Strong Inhomogeneities* – A.
SCHUMACHER, Ruhr-Universität Bochum,FRG. The
angular relaxation of the distribution func-
tion in the strongly inhomogeneous boundary
layer of a Lorentz gas can be treated by the
rather involved Case-Zweifel-formalism of
singular integral equations. This formalism,
however, cannot be generalized to include the
strong and inhomogeneous electric fields
which are essential for the electron kinetics
in the boundary layer. Therefore we start
from a parametrization of the angular depen-
dency of the electron distribution function,
which is based on physical arguments and
accounts for the special conditions of the
plasma-wall transition region. An estimate of
the error shows the validity of this pro-
cedure. For the field-free case the results
can be compared with analytical and numerical
solutions in the literature, which yields
excellent agreement.

N-3 Electron Wall Current and Floating Potential in a Weakly Ionized Plasma* - A. SCHUMACHER, Ruhr-Universität Bochum FRG. The calculation of the electron wall currents in a weakly ionized plasma requires a kinetic treatment of the electrons in the plasma-wall transition sheath. Using the method of matched asymptotic expansions we solve the kinetic equation on two different scales corresponding to the characteristic lengths of momentum and energy exchange, respectively. The consistent matching yields the angular and energy dependency of the electron distribution function in the whole boundary layer. We calculate the electron wall current to a planar negative wall and find order of magnitude deviations from the Hertz-Knudsen-formula and a correspondingly large shift in the floating potential. As an example we discuss the application of our results to the theory of electrostatic Langmuir probes.

N-4 Body Fitted Non-Linear Electric Field in Glow Discharges* - W.M. MOENY, H.J. HAPP, Tetra Corp.-- P.J. ROACHE, Ecodynamics Res. Assoc. --A new approach to analyzing 2-D, steady state electric fields in self-sustained and e-beam controlled glow discharges has been developed. Our approach uses a body-fitted coordinate system to calculate the electric fields on physical boundaries, such as electrode surfaces, so that the effects of subtle changes in electrode shape are properly modeled. We use a numerical coordinate transformation to solve the non-linear Poisson Equation, which describes the electric field including non-uniform plasma distribution effects. We then do the reverse transformation to obtain the electric fields in physical space. This approach enables design of self-sustained and e-beam glow discharge electrodes with a precision not previously possible. It also enables detailed analysis of the interaction between non-uniform plasma and the electric field distribution. A time-dependent version of the code is under development, along with a 3-D steady-state version. Comparisons with known solutions will be presented, along with examples of electrode design and analysis.

N-5 Cathode Sheath Formation in a Pulsed, High-Pressure Discharge -
W. H. LONG, JR., Northrop Research and Technology Center
The formation of a sheath at the cathode of a high pressure discharge is analyzed in a two-component plasma by solving the continuity equations for ion species and the gas dynamic equations for neutrals. The electron energy distribution is assumed to be in equilibrium with the local electric field. A uniform field gap is coupled to an external circuit and then preionized to initiate breakdown. The electrons are swept away from the cathode until the space charge field generated by the sheath is strong enough to drive an ionization wave back against the drift. The cathode fall potential increases at first to over 1000 V before relaxing back to its steady value of about 100 V. Sheath development is essentially complete before gas heating has significantly altered the neutral density. At later times the sheath expands, driving a shock wave out from the cathode surface. The dependence of sheath formation on external circuit parameters and preionization uniformity is examined with regard to discharge stability.

N-6 Analysis of Positive Ion Mass Spectra at the Cathode of a Glow Discharge - M.C. SIDDAGANGAPPA, and M.S. NAIDU, I.I.Sc., Bangalore, India. --
The data of mass analysis of the positive ions in the cathode region of a glow discharge will be of considerable help for an understanding of the basic physical processes occurring in a glow discharge. Mass spectra of the positive ion species in the cathode region of a glow discharge in air, N_2, O_2 and CO_2 was obtained using a quadrupole mass spectrometer built in our laboratory. The discharge source consists of two plane electrodes separated by a distance of 6 mm and operates over the pressure range of 0.1 to 1 torr. Stabilised power source was used to supply the discharge current upto 30 mA. An aperture of 0.5 mm dia in the cathode facilitates the flow of ions into the mass analyzer region. Analysis of the mass spectras obtained shows that with N_2, only N^+ ions were recorded and presumably these are formed due to electron bombardment of N_2 according to reaction: $N_2 + e \longrightarrow N^+ + N + 2e$. Similar reactions were found to be predominant when only C^+, O^+ and CO^+ were observed in CO_2 and O^+ was abundant in O_2. O^+/O_2^+ ratio over the discharge current range of 5 to 20 mA was observed to increase from 10 to 90. In air N^+ and O^+ were dominant with N_2^+ and O_2^+ forming only 5% of the total ion current.

INDEX OF ABSTRACTS

Collins C. B. IA-11

Collins, G. MB-9

Cornelissen, H. J. MB-1

Cunningham, A. J. EA-7, MA-2

Dagdigian, P. J. FA-3

Daniels, J. L. EB-4

Davanloo, F. IA-11

Davies, D. K. LA-4

Denes, L. J. FB-3

Dervisevic, E. IB-8, MB-4

Dettman, D. BA-2, BA-3

DeYoung, R. J. BB-6

Dhali, S. K. EA-4

Dheandhanoo, S. IA-9

Dillon, M. A. EB-3

Doering, J. P. FA-3

Dollinger, R. BA-2, BA-3

Dougal, R. A. CA-7, LB-3

Doughty, D. EA-2, EA-3

Downes, L. W. BB-3, MA-7, MA-8

Drouet, M. G. BA-5

Duke, G. L. G-8

Duncan, M. A. CB-8

Durrett, M. IB-12

Durup-Ferguson, M. CB-1, CB-2

Eden, J. G. IA-4

Ediger, M. N. IA-4

Eliasson, B. IB-13

Erez, G. EA-1

Etemadi, K. BA-7

Fahey, D. W. CB-1, CB-2, CB-6

Fehsenfeld, F. C. CB-6

Ferguson, E. E. CB-1, CB-2

Filippelli, A. R. FA-4, FA-5

Flannery, M. R. A-4, IA-3

Frechette, M. G-9

Gallagher, A. CB-3, IB-4

Garscadden, A. G-8

Garver, W. P. EA-6

Gastineau, J. E. FA-2

Gatland, I. R. IB-7

Germany, G. A. MA-6

Gibbs, G. R. BB-4

Gilliard, R. P. CA-4

Goett, S. J. IB-3

Goldsmith, S. BA-1

Green, T. A. LB-5

Guha, S. CA-8

Gundersen, M. A. CA-8

Hagmann, S. CB-5

Hamil, R. A. LB-5

Hanson, W. B. MA-5

Happ, H. J. N-4

Hardy, K. A. MA-1

Hargis, P. J., Jr. LB-4, LB-5, LB-6

Haworth, M. D. IB-5

Helmy, E. M. IA-12

Henson, B. L. LB-2

Hernandez, S. FA-3

Hils, D. CB-3

Hinchen, J. J. FB-2

Hiskes, J. R. IA-1

Hobbs, R. H. A-2

Hobson, R. M. MB-7

Hodges, R. V. J-4

Hoffman, J. H. MA-5

Holzscheiter, H. M. CB-4

Hossam-Eldin A. A. LB-11

Houston, L. IB-12

Hozack, R. S. MA-4

Hsu, K. C. BA-7

Huestis, D. L. IB-12

Hülsmann, H. G. IB-10

Hunter, S. R. LA-5

Ichikawa, Y. CB-7, MB-7, MB-8

Ingold, J. H. CA-4, MB-5, MB-6

Johnsen, R. IA-2, IA-9, IA-10

Jones, D. W. IA-6

Jurenka, H. J-2, J-3

Kaneda, T. MB-8

Karo, A. M. IA-1

Keeffe, W. M. CA-1

King, C. BA-3

Kline, L. E. FB-3, FB-4

Kribel, R. E. IB-5

Kunc, J. A. CA-8

Kunhardt, E. E. G-1, G-2, G-3, MB-2

Kushawaha, V. S. EA-6

Kushner, M. J. K-3, LB-10, MB-3

Lake, M. L. EB-1

Lane, N. F. IB-1

Lapatovich, W. P. BB-4

Lawler, J. E. EA-2, EA-3

Lee, E. T. P. FA-4

Lee, F. W. IA-11

Leone, S. R. CB-8

Leprince, P. IB-8, MB-4

Levatter, J. I. BB-1

Leventhal, J. J. EA-6

Lin, C. C. FA-2, FA-4, FA-5

Long, W. H., Jr. N-5

Lorents, D. C. IB-12

Lowke, J. J. LB-1

Lowry, J. F. IB-9

MacDonald, J. A. IA-2

Mansky, E. J. IA-3

Marec, J. IB-8, MB-4

Marcum, S. D. BB-3, MA-7, MA-8

McCown, A. W.   IA-4

McAfee, K. B., Jr.   MA-4

Melendez, R. E.   G-4

Mellis, J.   BB-7

Mentel, J.   IB-10

Mercure, H. P.   BA-5, BA-9

Meunier, J. L.   BA-4

Meyer, J.   MB-9

Michels, H. H.   A-2

Miller, T. M.   IA-8

Misakian, M.   J-5

Moeny, W. M.   N-4

Morgan, W. L.   A-5, A-6, IB-2

Morrison, M. D.   EA-7

Morrow, R.   LB-1, LB-7

Moseley, J.   EA-5

Motret, O.   IA-7

Murphy, R. E.   FA-5

Musiol, K.   IA-6

Nachman, M.   LA-1

Nahemow, M. D.   IB-9

Naidu, M. S.   N-6

Naqvi, A. S.   IA-11

Nighan, W. L.   FB-2

Novak, J. P.   G-9

Orel, A. E.   CA-5, CA-6

Oskam, H. J.   MB-6

Palumbo, L. J.   FB-1

Paulson, J. F.   IA-8

Péalat, M.   LA-1

Pease, D. C.   CA-7

Pechersky, M. J.   K-1

Pederson, M. R.   FA-5

Penetrante, B. M.   G-5

Petach, T.   BB-1

Pfender, E.   BA-6, BA-7

Phelps, A. V.   A-1, G-7, IA-5, IB-6

Pitchford, L. C.   G-7, IB-6, LB-5

Pouey, M.   IB-8, MB-4

Powell, H. T.   CA-5, CA-6

Proud, J. M.   BB-4, LB-9

Rajotte, R.   BA-5

Reinhold, G.   J-1

Richard, P.   CB-5

Riemann, K. -U.   N-1

Riley, J. F.   J-4

Roache, P. J.   N-4

Robertson, R.   CB-3

Rocca, J.   MB-9

Rogoff, G. L.   BB-8

Rothe, D. E.   BB-1

Rothwell, H. L.   CA-1

Saada, S.   IB-8, MB-4

Salamo, G. J.   MA-6

Wang, R. -G. EB-3

Warner, B. E. K-2, K-3

Wells, W. E. BB-3, MA-7, MA-8

Wetterskog, R. E. IA-8

Wexler, B. L. K-4

Whitten, B. L. A-6, IB-1

Wiegand, W. J. FB-2

Wiese, W. L. IA-6

Wilson, W. L. BB-5

Williams, P. F. EA-4, EA-5, CA-7, LB-3

Williams, R. A. BB-5

Woo, S. B. IA-12

Woodworth, J. R. LB-5, LB-6

Wu, R. L. C. CB-7, MB-8

Yoshida, S. G-7

Yu, Z. MB-9

Yu, S. S. G-4

Zapata, L. E. BB-6

Zollweg, R. J. CA-2

ADAMS, DAN
UTD BOX 688, PHYSICS DEPT
RICHARDSON, TX 75080

AKOSHILE, CLEM
UTD BOX 688, PHYSICS DEPT
RICHARDSON, TX 75080

ALLIS, WILLIAM P.
RM 36-231, MIT
CAMBRIDGE, MA 02138

ALVAREZ, IGNACIO
INST. DE FISICA, U.A. DE MEX.
MEXICO 01000, D.F.

ANDERSON, RICHARD J.
UNIV. ARKANSAS
FAYETTEVILLE, AR 72201

ASSAL, WILLIAM
BAT. 212 UNIV PARIS-SUD
91405 ORSAY FRA.

BACAL, MARLHE
ECOLE POLYTECHNIQUE
PALAISEAU, FRANCE

BAILEY, WILLIAM F.
A.F. INSTITUTE OF TECHNOLOGY
HUBER HEIGHTS,OH 45424

BARISLEY, J. NORMAN
UNIV OF PITTSBURGH
PITTSBURGH, PA 15260

BATES, DAVID R.
QUEENS UNIV.
BELFAST, N. IRELAND

BEATY, EARL C.
NBS DIV. 524.10
BOULDER, CO 80303

BENDSEN, KAY
UTD BOX 688, NB 11
RICHARDSON, TX 75080

BENENSON, D.M.
ST. UNIV. OF NY AT BUFFALO
AMHERST, NY

BIBLARZ, OSCAR
NAVAL POSTGRADUATE SCHOOL
MONTEREY, CA 93940

BIENIEK, RONALD
UNIV MISSOURI-ROLLA
ROLLA, MO 65401

BLAVER, JAY A.
ROCKETDYNE/ROCKWELL
CANOGA PARK., CA 9130R

BLETZINGER, PETER
AFWAL/WPAFB
DAYTON, OH 45324

BOEUF, JEAN-PIERRE
TEXAS TECH. UNIV.
LUBBOCK, TX 79401

BOHLER, CHRIS
UNIV MO.- ROLLA
ROLLA, MO 65401

BOHRINGER, HANS
NOAA, ERL, AERONOMY LAB.
BOULDER, CO 80303

BOURNE, ORSON L.
NAT'L. RES. COUNCIL OF CANADA
OTTAWA, CANADA

BRADLEY, LAIRD P.
LLL P.O. BOX 5508, L-470
LIVERMORE, CA 94550

BREIG, ED
UTD BOX 688, PHYSICS DEPT
RICHARDSON, TX 75080

BRICKS, B.G.
GE - SSD MI339, BOX 8555
PHILADELPHIA, PA 19101

BROWN, ROBERT T.
MS 85, UNITED TECH. RES. CORPE.
HARTFORD, CT 06108

BUCKMAN, STEPHEN J.
JILA, UNIV OF COLORADO
BOULDER, CO 80309

BURFORD, GLENDA
UTD BOX 688, PHYSICS DEPT
RICHARDSON, TX 75080

BURGMANS, ADRIANUS L.J.
PHILIPS RES LAB. 5600 JA
EINDHAVEN, NETHERLANDS

BURKHARDT, CHARLES
UNIV. OF MISSOURI-ST. LOUIS
ST. LOUIS, MO 63121

BURNHAM, R.
NAVAL RESEARCH LAB.
WASHINGTON, DC 20375

BURROW, PAUL D.
BEHLEN LAB. UNIV. NEBRASKA
LINCOLN, NE 68588

BYRON, STAN
MSNW, 2755 NORTHUP WAY
BELLEVUE, WA 98004

BYSZEWSKI, WAJCIECH
40 SYLVAN RD.
WALTHAM, MA 02254

CANTRELL, CYRUS D.
UNIV TEXAS AT DALLAS, BOX 688
RICHARDSON, TX 75080

CENTER, ROBERT E.
MSNW, 2755 NORTHUP WAY
BELLEVUE WA 98004

CHAMPAGNE, LOUIS F.
NRL, 6306 WILLOWEED LN.
ALEXANDRIA, VA 22310

CHANIN, L.M.
123 CHURCH ST. UNIV. MINN.
MINNEAPOLIS, MN 55455

CHANTRY, P.J.
WESTINGHOUSE R&D CENTER
PITTSBURGH, PA 15235

CHEN, ZONGSHU
UTD BOX 688, PHYSICS DEPT
RICHARDSON, TX 75080

CHEN, C.L.
WESTINGHOUSE R&D CENTER
PITTSBURGH, PA 15235

CHIO, SHIU-SHIN
SES INC, 1 TRALEE IND. PARK
NEWARK, DE 19711

CHURCH, DAVID A.
PHYS. DEPT. TEXAS A&M UNIV.
COL. STATION TX 77843

CLARK, JERRY
UTD BOX 688, PHYSICS DEPT
RICHARDSON, TX 75080

COLEY, ROBIN
UTD BOX 688, PHYSICS DEPT
RICHARDSON, TX 75080

COLLINS, CARL B.
UTD BOX 688, PHYSICS DEPT
RICHARDSON, TX 75080

CRANE, JOHN
LLL PO BOX 5508, L-459
LIVERMORE, CA 94550

CUNNINGHAM, A.J.
UTD BOX 688, PHYSICS DEPT
RICHARDSON, TX 75080

DAKIN, JAMES T.
GENERAL ELECTRIC
SCHENECTANY, NY 12301

DALGARNO, ALEXANDER
CNTR ASTROPHYS.,60 GARDEN ST.
CAMBRIDGE, MA 02138

DAMDMIO, TONY
VOUGHT CORP., RT.1, BOX 231
DESOTO, TX 75115

DANIELS, JOHNNY L.
UNIV. MISSOURI - ROLLA
ROLLA, MO 65401

DAVANLOO, FARZIN
UTD BOX 688, PHYSICS DEPT
RICHARDSON, TX 75080

DAVIES, D.K.
WESTINGHOUSE R&D CENTER
PITTSBURGH, PA 15235

DEMIS, ANDY
UTD BOX 688, PHYSICS DEPT
RICHARDSON, TX 75080

DEPAOLA, BRETT
UTD BOX 688, PHYSICS DEPT
RICHARDSON, TX 75080

DEHOOG, FREDERIK J.
EINDHOVEN UNIV. 5600 MB
EINDHOVEN, NETHERLANDS

DEWITT, R.N.
NAVAL SURFACE WEAPONS CNTR.
DAHLGREN, VA 22448

DEYOUNG, RUSSELL
NASA LANGLEY, 8 LUANITA LANE
NEWPORT NEWS, VA

DHALI, SHIRSHAK
TEXAS TECH UNIV.
LUBBOCK, TX 79401

DOERING, J.P.
JOHNS HOPKINS UNIV.
BALTIMORE, MD 21218

DOLLINGER, RICH
ST. UNIV OF NY AT BUFFALO
AMHERST, NY 14226

DONALDSON, ANTHONY
BOX 4439, TEXAS TECH. UNIV.
LUBBOCK, TX 79409

DOUGAL, OGER
TEXAS TECH. UNIV.
LUBBOCK, TX 79401

DOUGHTY, DOUG
UNIV. WIS. STERLING HALL -8412
MADISON, WI 53705

DOWNES, LAWRENCE W.
MIAMI UNIV.
OXFORD, OH 45056

DUKE, GARY L.
AFWAL/DOOC-3, WRIGHT-PAT. AFB
DAYTON, OH 45433

DUNCAN, MICHAEL A.
JILA, UNIV OF COLORADO
BOULDER, CO. 80309

DURRETT, MIKE
PHYS. DEPT. RICE UNIV.
HOUSTON, TX 77251

DURUP-FERGUSON, MARIE
UNIV. PARIS SUD
ORSAY, FRANCE

EBERHARD, CAROL A.
UTD BOX 688, PHYSICS DEPT
RICHARDSON, TX 75080

EDEN, J.G.
UNIV. ILLINOIS
URBANA, IL 61801

EDIGER, MARWOOD
UNIV. OF ILLINOIS
CHAMPAIGN, IL 61820

ERNIE, DOUGLAS W.
DEPT. E.E. UNIV OF MINN.
MINNEAPOLIS, MN 55455

EWING, J.J.
MSNW, 2755 NORTHUP WAY
BELLEVUE, WA 98004

FARRALL, GEORGE A.
G.E. R&D CENTER, 1 RIVER RD.
SCHENECTADY, NY 12301

FARRELL, MARY
COLORADO ST. UNIV.
FT. COLLINS, CO 80526

FERGUSON, ELDON
AERONOMY LAB. NOAA
BOULDER, CO 80303

FILIPPILI, ALBERT R.
UNIV. OF WISCONSIN
MADISON, WI 53706

FLANNERY, RAYMOND
SCHOOL OF PHYS. GA. TECH.
ATLANTA, GA 30332

FRANZ, FRANK A.
INDIANA UNIV.
BLOOMINGTON, IN

FRASER, MARK
UNIV. MISSOURI - ROLLA
ROLLA, MO 65401

GALLAGHER, ALAN
JILA, UNIV. COLORADO
BOULDER, CO 80309

GARSCADDEN, ALAN
FWAL - POOC-3, WRIGHT-PAT AFB
DAYTON, OH 45433

GARVER, WAYNE
UNIV. OF MISSOURI-ST. LOUIS
ST. LOUIS, MO 63121

GASTINEAU, JOHN
UNIV. WISCONSIN
MADISON, WI 53706

GATLAND, IAN R.
GEORGIA INST. TECH.
ATLANTA, GA. 30332

GERARDO, JAMES B.
SANDIA NAT. LAB., DEPT 1120
ALBUQUERQUE, NM 87185

GERMANY, GLYNN
UNIV. ARKANSAS
FAYETTEVILLE, AR 72201

GILLIARD, RICHARD P.
G.E. LR+TSD, #1310, NELA PARK
CLEVELAND, OH 44112

GORDON, LLOYD B.
LLL PO BOX 5504, L-153
LIVERMORE, CA 94550

GUTHRIE, JOHN
UTD BOX 688, PHYSICS DEPT
RICHARDSON, TX 75080

GYLYS, TOM
UTD BOX 688, PHYSICS DEPT
RICHARDSON, TX 75080

HANSON, W.B.
UNIV. TEXAS AT DALLAS
RICHARDSON, TX 75080

HARGIS, PHILIP J. JR.
SANDIA NAT. LAB., BOX 5800
ALBUQUERQUE, NM 87185

HARRIS, LAWSON F.
G.E. PO BOX 8
SCHENECTADY, NY 12301

HARSHAW, ROBERT C.
UTD BOX 688, PHYSICS DEPT
RICHARDSON, TX 75080

HAUCK, JIM P.
ROCKWELL INTERNAT'L
SANTA ANA, CA 92705

HAWORTH, MIKE
PHYS. DEPT., AUBURN UNIV.
AUBURN, AL 36848

HELMY, E.M.
DELAWARE STATE COLLEGE
DOVER, DE 19901

HENSON, BOB L.
UNIV. OF MISSOURI-ST. LOUIS
ST. LOUIS, MO 63127

HICKMAN, ALBERT P.
SRI, 333 RAVENSWOOD AVE-PS071
MENLO PARK, CA 94025

HILL, ALAN E.
PLASMATRONICS INC. BOX 5444-A
ALBUQUERQUE, NM 87185

HILL, ROBERT M.
SRI, 2950 ALEXIS DR.
PALO ALTO, CA 94304

HISKES, JOHN R.
LLL BOX 55511, L-630
LIVERMORE, CA 94550

HOBBS, ROBERT
UNITED TECH RES. CNTR. MS-72
E.HARTFORD, CT 06108

HODGES, RONALD
PALO ALTO RES LAB 3251 HANOVER
PALO ALTO, CA 94304

HOHLA, KRISTIAN
LAMBDA PHYSIK GMBH
3400 GOTTENGEN, FRG

HOMSEY, ROBERT J.
GE - SSD BOX 8555
PHILA, PA 19101

HORN, LYNDA
UTD BOX 688, NB11
RICHARDSON, TX 75080

HOUSTON, LOUIS
RICE UNIV.
HOUSTON, TX 77054

HUESTIS, DAVID L.
SRI INT. 333 RAVENSWOOD AVE
MENLO PARK, CA 94025

HUNTER, SCOTT R.
OAK RIDGE NAT LAB. BOX 45005
OAK RIDGE, TN 37830

HUTCHISON, SHELDON B.
XMR, INC. 3581 SHAFER RD.
SANTA GARA, CA 95051

ICHIKAWA, YUKIMI
BREHM LAB. WRIGHT STATE UNIV.
DAYTON, OH 45435

INGOLD, JOHN
G.E. LIGHTING BUSINESS GROUP
CLEVELAND, OH 44112

ISLAM, M. AZAD
JILA, CAMPUS BOX-440 U. COL.
BOULDER, CO 80309

JACQUES, JOLLY
UNIV. PARIS-SUD
ORSAY - FRANCE

JOHNSEN, RAINER
UNIV OF PITTSBURGH
PITTSBURGH, PA 15260

JOHNSON, BRIAN
UTD BOX 688, PHYSICS DEPT
RICHARDSON, TX 75080

JOHNSON, PETER D.
G.E. R&D CENTER BOX 8
SCHENECTADY, NY 12301

JONES, DOUGLAS W.
NBS RM. A267 BLDG. 221
WASHINGTON DC 20234

JUNKER, BOB
ONR CODE 412, 800 N. QUINCY
ARLINGTON, VA 22217

JURENKA, HENRY
ASRC SUNY AT ALBANY
GUILDERLAND, NY 12084

KEEFFE, WILLIAM M.
100 ENDICOTT ST.
DANVERS, MA 01923

KLINE, L.E.
WESTINGHOUSE R&D
PITTSBURGH, PA 15235

KRIBEL, ROBERT E.
PHYS. DEPT. AUBURN UNIV.
AUBURN, AL 36849

KROMPHOLZ, HERMANN G.
5702 50TH, #79
LUBBOCK, TX 779414

KUNC, JOSEPH A.
UNIC PARK - MC 1341, USC
LOS ANGELES, CA 90089

KUNHARDT, ERICH E.
TEXAS TECH. UNIV.
LUBBOCK, TX 79413

KUSHAWAHA, V.
UNIV. OF MISSOURI
ST. LOUIS, MO

KUSHNER, MARK J.
LLL BOX 808, L-467
LIVERMORE, CA 94550

LAKE, MAX
UNIVERSAL ENERGY SYSTEMS
DAYTON, OH 45432

LANE, NEAL F.
PHYS.DEPT., RICE UNIV.
HOUSTON, TX 77001

LANGLEY, JOE
2612 HIGHWOOD
DALLAS, TX 75228

LAPATOVICH, WALTER P.
GTE LAB., 40 SYLVAN RD.
WALTHAM, MA 02254

LAWLER, JAMES E.
PHYS. DEPT. UNIV. WIS.
MADISON, WI 53706

LEE, FRANCIS W.
U TEXAS DALLAS, BOX 688, NB11
RICHARDSON, TX 75080

LEVENTHAL, JACOB J.
UNIV. OF MISSOURI - ST.LOUIS
ST. LOUIS, MO 63121

LIN, CHUN C.
UNIV. WISCONSIN
MADISON, WI 53706

LOEB, MRS. LEONARD B.
2615 ETNA ST.
BERKLEY, CA 94704

LONG, WILLIAM H.
NORTHROP RES. & TECH. CENTER
PALOS VERDES, CA 90274

LORANC, MARK
UTD BOX 688, PHYSICS DEPT
RICHARDSON, TX 75080

LORENTS, DONALD C.
SRI INT'L, 333 RAVENSWOOD AVE
MENLO PARK, CA 94025

LOWRY, J.F.
WESTINGHOUSE R&D CENTER
PITTSBURGH, PA 15235

LUO, JHY-MING
UTD BOX 688, PHYSICS DEPT
RICHARDSON, TX 75080

MALINS, ROBERT J.
UTD BOX 688, PHYSICS DEPT
RICHARDSON, TX 75080

MANSKY, ED
SCHOOL OF PHYSICS, GA. TECH.
ATLANTA, GA 30308

MARCUM, S. DOUGLAS
MIAMI UNIV.
OXFORD, OH 45056

MAREC, J.
UNIV. PARIS-SUD
ORSAY 91405 CEDEX FRA.

MCAFEE, KENNETH B.
BELL TELEPHONE LAB.
MURRAY HILL, NJ 07920

MCCONNELL, JOHN C.
YORK UNIV.
ONT., CANADA

MCGEOCH, MALCOLM W.
AVCO EVERETT RES. LAB. INC.
EVERETT, MA 02149

MCKAY, JIM
TEXAS INSTR.
GARLAND, TX 75042

MCKNIGHT, WILLIAM B.
UNIV OF ALABAMA - HUNTSVILLE
HUNTSVILLE, AL 35802

MELLIS, JOHN
UNIV. OF STRATHCLYDE
GLASGOW 940N7 SCOTLAND

MENTEL, JUERGEN
RUHR-UNIV BOCHUM
BOCHUM 1, FRG

MERCURE, HUBERT
IREQ BOX 1000
VARENNES, CANADA

MERTS, A.L.
LOS ALAMOS NAT. LAB
LOS ALAMOS, NM 87545

MEYER, JACK
COLORADO ST. UNIV.
FT. COLLINS, CO 80521

MICHELS, H. HARVEY
UNITED TECH. RES. CENTER
E. HARTFORD, CT 06108

MILLER, THOMAS M.
DEPT. PHYS. UNIV. OKLAHOMA
NORMAN, OK 73019

MILTON, LYNN
UTD BOX 688, PHYSICS DEPT
RICHARDSON, TX 75080

MOENY, WILLIAM M.
71075 SOMERRELL ST. NE
ALBURQUERQUE, NM 87112

MONTGOMERY, JOHN
LUMONICS, 105 SCHNEIDER RD.
KANATA, ONT. CANADA

MORGAN, WILLIAM L.
LLL BOX 808
LIVERMORE, CA 94550

MORRISON, DANNY
UTD BOX 688, PHYSICS DEPT
RICHARDSON, TX 75080

MORROW, RICHARD
CSIRO APPLIED PHYSICS
SYDNEY, NSW, AUSTRALIA

MURRAY, GORDON A.
TACHISTO INC. 13 HIGHLAND CIR
NEEDHAM, MA 02184

MYERS, GARY D.
MS 220-12, VOUGHT CORP.
DALLAS, TX 75265

NAQVI, ATHAR S.
KING SAUD UNIV.
RIYADH, SAUDIA ARABIA

NOVAK, J.P.
IREQ BOX 1000
VARENNES, QUE, CANADA

OREL, ANN E.
LLL P.O. BOX 808, L-472
LIVERMORE, CA 94550

OSKAM, H.J.
DEPT. E.E., UNIV MINN
MINNEAPOLIS, MN 55455

PALUMBO, LOUIS J.
CVI INC. 35 INDUSTRIAL PRKWY
WOBURN, MA 01801

PEASE, DENNIS
BOX 4437, TEXAS TECH. UNIV.
LUBBOCK, TX 79409

PECHERSKY, MARTIN J.
WESTINGHOUSE R&D CENTER
PYH. PA 15253

PETERSON, GARY L.
UTD BOX 688, PHYSICS DEPT
RICHARDSON, TX 75080

PFENDER, EMIL
125 MECH. ENG. BLDG., U MINN.
MINNEAPOLIS, MN 55455

PHELPS, ARTHUR V.
JILA BOX 440, UNIV COLORADO
BOULDER, CO 80309

PITCHFORD, LEANNE
SANDIA NAT LAB. ORG. 1126
ALBUQUERQUE, NM 87185

POWELL, HOWARD T.
LLL P.O. BOX 5508, L-470
LIVERMORE, CA 94550

RASSOUL, HAMID
UTD BOX 688, PHYSICS DEPT
RICHARDSON, TX 75080

RENFROW, MARGIE
UTD BOX 688, PHYSICS DEPT
RICHARDSON, TX 75080

RESCIGNO, TOM
LLL P.O. BOX 5508, L-470
LIVERMORE, CA 94550

RIEMANN, KARL-ULRICH
RUHR-UNIV. BOCHUM
BOCHUM, FRG

RISBERG, L.A.
GTE LABS., 40 SYLVAN RD.
WALTHAM, MA 02254

ROGOFF, G.L.
WESTINGHOUSE R&D 1310 BEULAH
PITTSBURGH, PA 15235

ROHRBAUGH, RON
UTD BOX 688, PHYSICS DEPT
RICHARDSON, TX 75080

ROSOCHA, LOUIS
LOS ALAMOS NAT'L. LAB.
LOS ALAMOS, NM 87545

ROTHE, DIETMAR E.
HELIONETICS
SAN DIEGO, CA 92123

ROTHWELL, HAROLD L.
100 ENDICOTT ST.
DANVERS, MA 01923

RUTFORD, ROBERT
UTD BOX 688
RICHARDSON, TX 75080

RYAN, LARRY
UTD BOX 688, PHYSICS DEPT
RICHARDSON, TX 75080

SADIGHI-BONABI, RASOOL
UTD BOX 688, PHYSICS DEPT
RICHARDSON, TX 75080

SALAMO, GREG
UNIV. ARKANSAS
FAYETTEVILLE, AR 72201

SAMPSON, DOUGLAS H.
PENN. STATE UNIV.
UNIV. PARK, PA 16802

SANDERS, NICHOLAS A.
BELL LABS., 29 KENSINGTON RD.
MADISON, NJ 07940

SCHAEFER, GERHARD
DEPT. E.E. BOX 4439
LUBBOCK, TX 79405

SCHAFER, RALF
PHILIPS RES. LABS
D-51 AACHEN, FRG

SCHEARER, LAIRD D.
UNIV. MISSOURI - ROLLA
ROLLA, MO 65401

SCHMIDT, ERIC
UTD BOX 688, PHYSICS DEPT
RICHARDSON, TX 75080

SCHNIEDER, GREG R.
AFWAL/MOOC-3, WRIGHT-PAT. AFB
DAYTON, OH 45433

SCHOENBACH, KARL H.
TEXAS TECH.
LUBBOCK, TX 79410

SCHRAM, DANIEL C.
UNIV. MONTREAL
MONTREAL, QUE, CANADA

SCHUMACHER, ALEX
RUHR - UNIV.BOCHUM
BOCHUM 1, FRG

SHANKAR, INAMDAR ARVIND
A G COLLEGE, STAFF QUARTERS
PUNA MAHAVASHTI INDIA

SHARPTON, FRANCIS A.
N.W. NAZARENE COLLEGE
NAMPA, ID 83651

SHAVL, SHALEV
49 HAMEYASDIM ST.
RAMAT-HASHARON, ISRAEL

SHELDON, JOHN W.
DEPT PHYS SCI FLORIDA INT'L U.
MIAMI, FL. 33199

SHEMWELL, DAVID M.
UTD BOX 688, PHYSICS DEPT
RICHARDSON, TX 75080

SHEPP, TOM
LLL PO BOX 5508 L-459
LIVERMORE, CA 94550

SHIPSEY, EDWARD J.
UNIV. OF TEXAS AT AUSTIN
AUSTIN, TX 78712

SHUKER, REUBEN
PHYS. DEPT, BEN-GURION UNIV.
BEER-SHEVA, ISRAEL

SIERRA, R.
LOS ALAMOS NAT'L LAB.
LOS ALAMOS, NM 87544

SMITH, ANTHONY L. S.
UNIV. STRATHCLYDE
GLASGOW G40NG SCOTLAND

SPENCE, DAVID
ARGONNE NAT. LAB.
ARGONNE, IL 60434

SPYROU, SPYROS M.
OAK RIDGE NAT LAB.BOX X.45005
OAK RIDGE, TN 37830

ST. JOHN, ROBERT M.
DEPT. PHYS., UNIV. OKLAHOMA
NORMAN, OK 73019

STEVEFELT, J.
GREMI UNIV. ORLEANS
45046 ORLEANS CEDEX.FR

STEWART, A.I.F.
L.A.S.P., UNIV OF COLORADO
BOULDER, CO 80309

STRASSLER, S.
BROWN BOVERI RES. CENTER
SWITZERLAND

STRUENSEE, MICHAEL C.
UNIV TEXAS AT AUSTIN
AUSTIN, TX 78712

STUMPF, BERNHARD
JILA UNIV.COLORADO
BOULDER, CO 80309

TALLMAN, CHARLES R.
165 LA CUEVA
LOS ALAMOS, NM 87544

TANG, KENNETH Y.
WESTERN RESEARCH CORP.
SAN DIEGO, CA 92121

TANNEN, PETER D.
8920 MATTHEW NE
ALBUQUERQUE, NM 87112

TELLINGHUISEN, JOEL
DEPT. CHEM, VANDERBILT UNIV.
NASHVILL, TN 37235

TEFFENHART, BILL
UTD BOX 688, PHYSICS DEPT
RICHARDSON, TX 75080

TRAINOR, DANIEL W.
AVCO-EVERETT RES. LAB. INC.
EVERETT, MA 02149

TURNER, CHARLES E. JR.
ROCKETDYNE/ROCKWELL
CANOGA PARK, CA 9130R

TWIST, BOB
UNIVERSAL ENERGY SYSTEMS
DAYTON, OH 45324

TZENG, YONHUA
TEXAS TECH. UNIV.
LUBBOCK, TX 79401

VALLADARES, CESAR
UTD BOX 688, PHYSICS DEPT
RICHARDSON, TX 75080

VAN BRUNT, RICHARD J.
BLDG. 220, RM B344
NBS WASH. DC 20234

VERDEYEN, JOSEPH T.
DEPT E.E UNIV ILL AT URBANA
CHAMPAIGN, IL 61820

VICHARELLI, PABLO A.
JILA. UNIV COLORADO, BOULDER
BOULDER, CO 80302

VILLA, F.
S.L.A.C., BOX 4349
STANFORD, CA 94305

WADEHRA, J.M.
WAYNE STATE UNIV.
DETROIT, MI 48202

WALKER, KEITH G.
BETHANY NAZARENE COLLEGE
BETHANY, OK 73008

WALTER, ROBERT F.
9707 LONA LANE NE
ALBUQUERQUE, NM, 87111

WARNER, BRUCE E.
LLL BOX 808, L-467
LIVERMORE, CA 94550

WELLS, WILLIAM E.
MIAMI UNIV.
OXFORD, OH 45056

WHITE, MICHAEL G.
TEXAS TECH UNIV.
LUBBOCK, TX 79401

WHITTEN, BARBARA L.
LLL BOX 808, L-355
LIVERMORE, CA 94566

WILLIAMS, FRAZER W.
DEPT. ELEC. ENG. TEXAS TECH.
LUBBOCK, TX 79405

WILSON, WILLIAM L.
RICE UNIV.
HOUSTON, TX 77251

WOO, SHIEN-BIAU
PHYS. DEPT. UNIV DELAWARE
NEWARK, DE 19711

WU, RICHARD L.C.
BREHM LAB. WRIGHT ST. UNIV.
DAYTON, OH 45435

YE, XUE MIN
UNIV. ARKANSAS
FAYETTEVILLE, AR 72201

YORK, GEORGE
LOS ALAMOS NATL. LAB.
LOS ALAMOS, NM 87544

YOUNG, CHRIS
TEXAS TECH. UNIV
LUBBOCK, TX 79424

YU, SIMON S.
LLL PO BOX 808, L-321
LIVERMORE, CA 94550

ZAPATA, LUIS E.
7 WILLOWOOD DR. #104
HAMPTON, VA 23666

ZNOTINS, THOMAS
MSNW, 2735 NORHTUP WAY
BELLEVUE, WA 98004

ZOLLWEG, ROBERT J.
WESTINGHOUSE R&D
PITTSBURGH, PA 15235